KAPOSI SARCOMA ASSOCIATED HERPESVIRUS AND HEME OXYGENASE-1: THE BIDIRECTIONAL RELATIONSHIP BETWEEN VIRUS AND HOST

By Sara Botto

A DISSERTATION

Presented to the Department of Molecular Microbiology and Immunology and the Oregon Health & Science University School of Medicine in partial fulfillment of the requirements for the degree of

Doctor of Philosophy

February 2016

ABSTRACT

Kaposi sarcoma (KS) is an angioproliferative tumor with infectious etiology, driven by viral infection of endothelial cells (EC) by Kaposi sarcoma herpesvirus (KSHV/HHV8). KS is the most common AIDS-associated malignancy, resulting in significant morbidity and mortality in the absence of immune-reconstitution. While KS incidence has decreased substantially in the post-HAART era, there is an ongoing need for affordable and effective therapies that specifically target KS/KSHV, particularly in resource-limited areas where KS is endemic and KSHV/HIV co-infection rates are high.

Dr. Moses' group previously showed that the host gene heme oxygenase-1 (HO-1) is upregulated by KSHV infection of EC *in vitro*, as well as in spindle (tumor) cells in KS biopsies, and plays a key role in the growth and survival of infected EC. HO-1, the rate-limiting enzyme for heme catabolism, is strongly induced as a protective response to cell stress and is highly expressed in several types of cancer. The pro-survival effect of HO-1 is primarily the result of the degradation of heme, a potentially toxic molecule, into metabolites with antioxidant, pro-angiogenic and pro-survival activities. Thus, studying HO-1 in the KS model will not only be of specific importance to KS research and treatment, but will have broader benefits for understanding the role of this enzyme in cancer biology.

In my dissertation, I aim to provide an in-depth review of the research to date on KSHV with a focus on how host genes, such as HO-1, can

modulate KSHV infection and tumorigenesis. To this end, I have made the novel discovery that KSHV infection of EC induces HO-1 in a biphasic manner, characterized by a transient induction peak upon initial infection and a sustained upregulation co-incident with the establishment of latency. These two phases of HO-1 induction are independently regulated, suggesting distinct roles in the virus life cycle. A virally encoded microRNA, miR-K12-11, is partially responsible for induction of HO-1 during KSHV latency, but not at early times post infection. The first peak of HO-1 induction is independent from *de novo* viral gene expression and described by Dr. Bala Chandran's group as the consequence of reactive oxygen species (ROS) production and activation of HO-1 transcription.

A second novel and important discovery that I have made is that HO-1 induction plays a critical role in KSHV life cycle through inhibition of TLR4 signaling. HO-1 metabolite carbon monoxide is responsible for preventing TLR4 interaction with its adaptor proteins, thus blocking signaling and transcription of type I interferon (IFN) and inflammatory cytokines. In addition, inhibition of HO-1 activity prior to infection results in lower infection rate and higher levels of inflammatory cytokines and IFN. Suggesting that HO-1 may represent a novel innate immune evasion factor in KSHV infected cells.

In conclusion, in this dissertation I show that HO-1 induction by KSHV is not only beneficial for KS tumorigenesis, but is also important for attenuating anti-viral innate immune responses, thus enhancing HO-1's importance as a therapeutic target for KS.

ACKNOWLEDGMENTS

Firstly, I would like to express my sincere gratitude to my advisor **Dr. Ashlee V. Moses** for the continuous support of my PhD study and related research, for her patience, motivation, and immense knowledge. Her guidance helped me in all the time of research and writing of this thesis. I could not have imagined having a better advisor and mentor for my graduate career.

Besides my advisor, I would like to thank the rest of my thesis committee: **Dr. Scott Wong, Dr. Daniel Streblow, Dr. Victor Defilippis** and **Dr. Owen McCarty** for their insightful comments and encouragement, but also for the difficult questions which incented me to widen my research from various perspectives.

Also I thank my labmates, classmates, friends at OHSU and VGTI for their moral support and their help throughout these five years and especially during the writing of my thesis.

Last but not the least, I would like to thank my family: my husband, **Djamil Legato**, who stayed beside me throughout my Bachelor degree, my Master degree and also my PhD. Thank you for the patience and the support you always showed me. To my parents, my mother-in-law, my best friend, which I consider sister, **Sara Astegiano,** and my kitty, **Pixel,** for supporting me however they can, morally and virtually, throughout all these years of graduate school and my life in general.

SELECTED ABBREVIATIONS

BAC: Bacterial Artificial Chromosome

BACH1: BTB And CNC Homology 1

DMVEC: Dermal Microvascular Endothelial Cells

E: Early

EC: Endothelial Cells

EBV: Epstein Barr Virus

EIF2α: Eukaryotic Translation Initiation Factor 2A

γ: Gamma

HBV: Human Hepatitis Virus B

HCV: Human Hepatitis Virus C

HCMV: Human Cytomegalovirus

HHV: Human Herpesvirus

HO-1: Heme Oxygenase-1

HPV: Human Papilloma Virus

HSV: Herpes Simplex Virus

HTLV-1: Human T Cell Lymphotropic Virus 1

IE: Immediate Early

IFN: Interferon

IκBα: Inhibitor Of Kappa B Alpha

IKK: Iκb Kinase

iLEC: Immortalized Lymphatic Endothelial Cells

IRF: Interferon Regulatory Factor

ISG: Interferon-Stimulated Genes

KLAR: KSHV Latency Associated Region

KS: Kaposi Sarcoma

KSHV: Kaposi Sarcoma Associated Herpesvirus

L: Late

LPS: Lipopolysaccharide IV

MCD: Multicentric Castleman Disease

MCV: Merkel Cell Polyomavirus

MHV-68: Murine Herpesvirus 68

miRNA: microRNA

MyD88: Myeloid Differentiation Primary Response Gene 88

NFκB: Nuclear Factor Kappa-Light-Chain-Enhancer Of Activated B Cells

NHP: Non-Human Primate

NLR: NOD-Like Receptors

NRF2: nuclear factor erythroid 2-related factor 2

ORF: Open Reading Frame

PAMP: Pathogen Associated Molecular Patterns

PEL: Primary Effusion Lymphoma

PKR: Protein Kinase-R

PRR: Pattern Recognition Receptors

RLR: RIG-I-Like Receptors

RM: Rhesus Macaques

ROS: Reactive Oxygen Species

RRV: Rhesus Rhadinovirus

TIR: Toll/Interleukin-1 Receptor

TLR: Toll-Like Receptors

TRIF: TIR-Domain-Containing Adapter-Inducing Interferon-B

VZV: Varicella Zoster Virus

WT: Wild Type

Table of Contents

CHAPTER 1

INTRODUCTION

1.1 Human Herpesviruses

1.1.1 Classification

Herpesviruses are ubiquitous and highly species-specific viruses. To date, eight human herpesviruses have been identified: herpes simplex virus 1 (HSV-1), herpes simplex virus 2 (HSV-2), varicella-zoster virus (VZV, HHV-3), Epstein-Barr virus (EBV, HHV-4), human cytomegalovirus (HCMV, HHV-5), human herpesvirus 6 (HHV-6), human herpesvirus 7 (HHV-7) and Kaposi sarcoma associated herpesvirus (KSHV, HHV-8). The *Herpesviridae* family was first classified based on the structure of the virus particle. The virion is composed of a linear double-stranded DNA genome that is surrounded by an icosahedral capsid, an amorphous component called tegument, and an envelope (Figure 1.1) (1,2). Additionally, herpesviruses share several important biological properties such as nuclear viral DNA replication, destruction of infected cells during productive replication and establishment of latency in the infected host. In contrast, herpesviruses differ with respect to key features of host cell tropism, duration of the lytic replication cycle, and the cellular reservoir of latent infection (1).

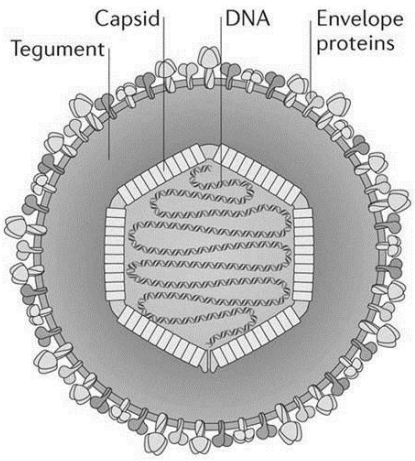

Figure 1.1 Herpesvirus virion structure

With permission from Zerboni L, et al. Nature Reviews Microbiology, 2014.

Members of the *Herpesviridae* family are categorized into three subfamilies: *Alphaherpesvirinae, Betaherpesvirinae,* and *Gammaherpesvirinae* (1). This classification is based on distinct biological properties: for example, alphaherpesviruses are characterized by a broad cell tropism and a short replication cycle. These viruses spread quickly in cell culture and efficiently destroy the infected cells. Additionally, members of this subfamily establish latency in sensory ganglia. Examples of human alphaherpesviruses are the simplex viruses HSV-1 and -2 and the varicellovirus VSV (2).

Viruses within the *Betaherpesvirinae* subfamily exhibit strict species-specificity and have a relatively long reproductive cycle, resulting in slow spread in culture. These viruses become latent in secretory glands, lymphoreticular cells, T-cells, and monocytes. Included in this subfamily are HCMV, HHV-6 and HHV-7 (2).

Gammaherpesvirinae infect a narrow host cell type range, typically B- or T-cells, and are able to replicate in lymphoblastoid cells *in vitro*. Viruses of this subfamily become latent in lymphoid tissues of an infected host. These viruses are further divided into *gamma-1 lymphocryptoviruses* and *gamma-2 rhadinoviruses*. EBV is a human

gamma-1 herpesvirus, while human gamma-2 herpesvirus is represented by KSHV (2).

1.1.2 Human Herpesvirus Pathogenesis

Herpesvirus infection remains fairly asymptomatic in the context of immunocompetent hosts. However, clinical manifestations and complications can occur in immunocompromised hosts.

Primary infection by the alphaherpesviruses **HSV-1** and **HSV-2** occurs through contact with infected individuals shedding the virus. Both viruses target the mucosal epithelium, causing skin vesicles or mucosal ulcers in the mouth or genitals of the infected host. Herpes simplex viruses are neurotropic as they establish latency in the dorsal root ganglia. Reactivation of the virus can occur through induction of physical or emotional stress, or immune suppression. Viral replication can lead to disease, but it is rarely life threatening (encephalopathy) (3,4).

VZV, another alphaherpesvirus, causes varicella (chickenpox) upon primary infection and it can later reactivate resulting in herpes zoster (shingles). Infection of naïve hosts occurs via aerosolized virus particles that contact the mucosal epithelium within the upper respiratory tract. The typical skin lesions caused by VZV are due to the presence of infected T cells. Like HSV-1 and HSV-2, VZV also establishes latency in the dorsal root ganglia (4). VZV is T-cell tropic and T-cells provide a means of spreading the virus from the initial site of infection to the skin for further dissemination. Reactivation of VZV results in herpes zoster (shingles), which is characterized by an extremely painful eruption of vesicles on specific areas of the skin supplied by a single nerve ganglion. Like varicella, herpes zoster lesions clear in a week, however pain can last for several weeks with over 30% of the patients

developing chronic pain and postherpetic neuralgia. In 2006, a live attenuated vaccine against VZV was licensed in the USA and has been proven to be effective in changing the epidemiology of VZV in the United States (5,6).

HCMV is a betaherpesvirus and, while primary infection is largely asymptomatic in immunocompetent individuals, it can cause significant morbidity and mortality in immunocompromised patients as an opportunistic infection. Some important groups at risk for CMV-associated diseases include organ transplant recipients, fetuses and newborn babies, and AIDS-patients. Congenital infection occurs upon primary infection or reactivation of CMV within the mother, leading to damage of the fetal central nervous system (CNS), hearing impairment and mental retardation. CMV-associated diseases and complications in immunocompromised patients are usually the result of CMV reactivation and can be potentially life threatening (i.e. rejection of the transplant, secondary infections) (7).

HHV-6 and **HHV-7**, also betaherpesviruses, are known as Roseoloviruses. Both viruses are ubiquitous and primary infection typically occurs in infants. The disease associated with Roseoloviruses, exanthema subitum (ES), is characterized by sudden high fever and a red rash on the trunk, legs and face of infected individuals. The rapid onset of fever can sometimes lead to febrile seizures and, in rare cases, liver dysfunction can occur (8).

EBV and **KSHV**, both gammaherpesviruses, are classified as oncogenic viruses. They both are lymphotropic and capable of establishing latency in B-cells. **EBV** is nearly ubiquitous, with approximately 90% of the adult population being seropositive. Transmission of the virus mainly occurs via oral contact ("kissing disease"), but can also occur through genital sexual contact, blood transfusion or organ transplantation. Although primary infection is generally asymptomatic, it can be associated with infectious mononucleosis, which is characterized by fever, malaise

and fatigue that can last weeks to months. EBV has been identified as the causative agent for several cancers, including Hodgkin lymphoma, Burkitt lymphoma, T and NK cells lymphomas, AIDS lymphomas, and nasopharyngeal and gastric carcinoma (7). The reader is referred to section 1.2.1.1 “Oncogenic viruses” for further details on EBV pathogenesis. **KSHV**, formally known as HHV-8, is the most recently identified human herpesvirus and is the subject of this thesis. KSHV is the etiological agent of Kaposi’s sarcoma and two B-cell malignancies (9). Aspects of KSHV biology and pathogenesis will be discussed in detail in section 1.3: Kaposi Sarcoma and KSHV.

1.2 Human Oncogenic Viruses

1.2.1 Introduction

Human oncogenic viruses account for more than 10% of human cancers worldwide. Human viral oncogenesis has been the subject of numerous studies. However, the limited availability of animal models, the high diversity among the cancers, and the extreme complexity of virus-host interactions render difficult both the understanding and management of these diseases (10,11,12).

Human viral-induced oncogeneses all share the same characteristics: oncoviruses are necessary but not sufficient for cancer development, so that only a small percentage of the infected individuals develop cancer; viral cancers appear in the context of persistent infections and can occur many years to decade after the primary infection; the role of the immune system can be either harmful or protective against the viruses and virus-associated cancers, depending on the type of cancer (12,10).

Human viral oncogenesis (Figure 1.2) shares the hallmarks of cancer described by Weinberg and Hanaha in “The Hallmarks of Cancer” (13,14), which outlines the development of cancer as a progressive acquisition of cellular mutations that produce a malignant phenotype (15). As previously stated, oncogenic viruses are necessary but not sufficient for the development of the associated cancer. Therefore, additional factors such as host genetics, immunosuppression, chronic inflammation, environmental mutagenesis, and gene mutation are generally necessary for cancer development (12,16).

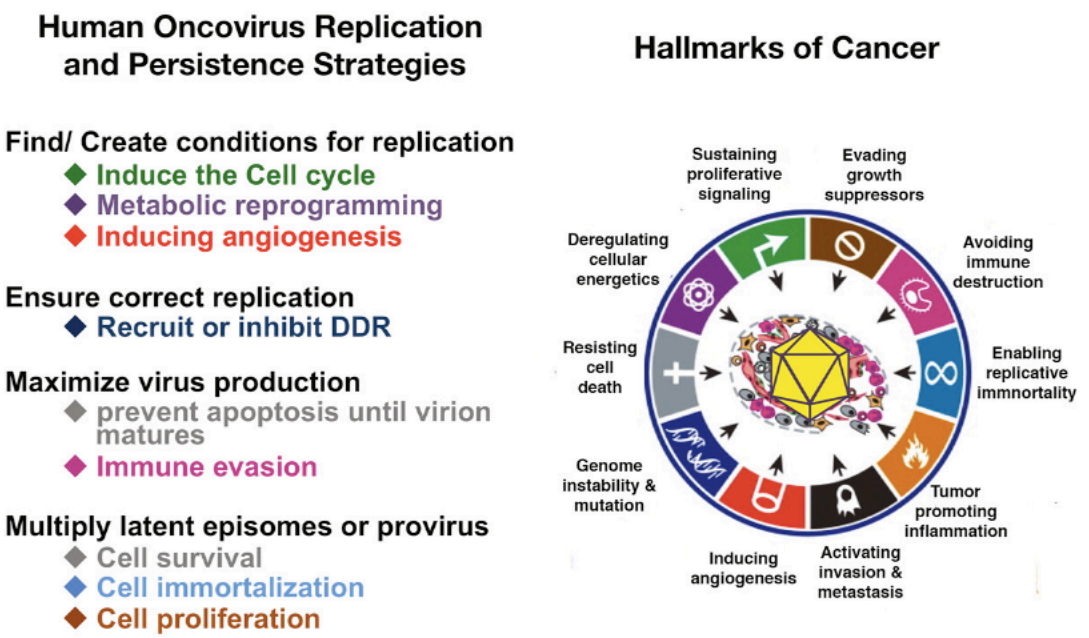

FIGURE 1.2 Virus oncogenesis

With permission from Mesri EA. et al. Cell Host & Microbe, 2014

To ensure replication and persistence in their hosts, human oncogenic viruses employ different strategies to hijack the host signaling machinery (15). There are several underlying mechanisms whereby a virus can promote anti-apoptotic and proliferative programs. For example: (i) Signaling mimicry, in which viruses encode proteins able to take over host-signaling mechanisms involved in growth and survival (12). (ii) An effect on the DNA damage response (DDR), which is often advantageous to virus replication, but deleterious to the host cells because it increases mutations and potential oncogenic alterations (17). (iii) Chronic inflammatory responses to persistent viral infection, which drive production of reactive oxygen species (ROS) that also promote acquisition of mutations (18,19).

Broadly-speaking, both DNA and RNA viruses have been identified as human oncogenic viruses (Figure 1.3). Human viruses are categorized as group I biological carcinogenic agents and include Hepatitis B virus (HBV), Hepatitis C virus (HCV),

EBV, high-risk sub-types of human papillomavirus (HPV), human T cell lymphotropic virus-1 (HTLV-1), KSHV, and Merkel cell polyomavirus (MCV) (10,20).

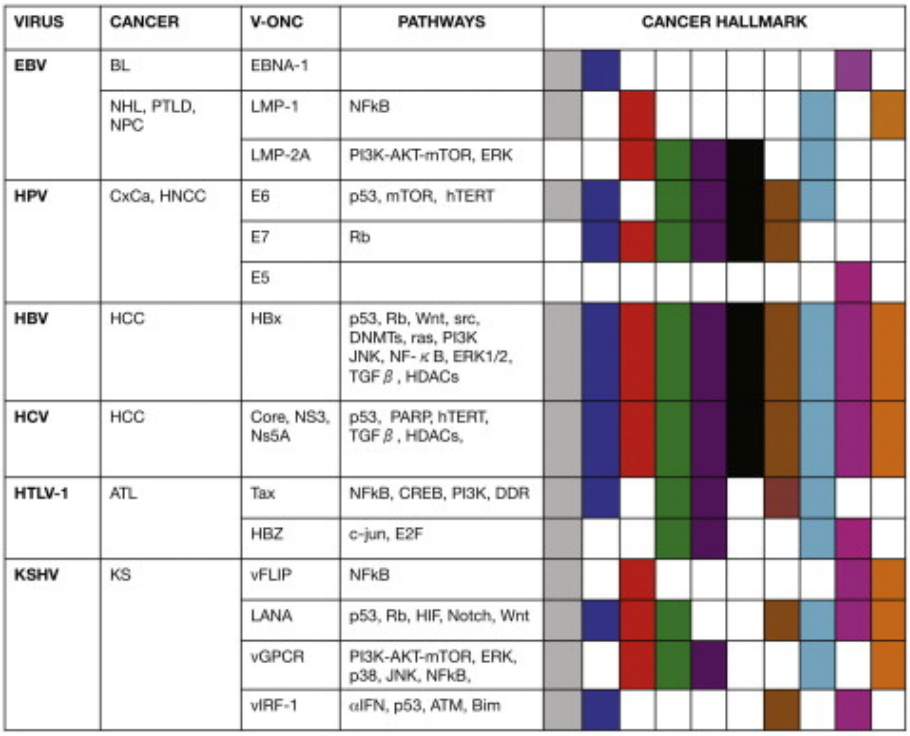

VIRUS	CANCER	V-ONC	PATHWAYS	CANCER HALLMARK
EBV	BL	EBNA-1		
	NHL, PTLD, NPC	LMP-1	NFkB	
		LMP-2A	PI3K-AKT-mTOR, ERK	
HPV	CxCa, HNCC	E6	p53, mTOR, hTERT	
		E7	Rb	
		E5		
HBV	HCC	HBx	p53, Rb, Wnt, src, DNMTs, ras, PI3K JNK, NF-κB, ERK1/2, TGFβ, HDACs	
HCV	HCC	Core, NS3, Ns5A	p53, PARP, hTERT, TGFβ, HDACs,	
HTLV-1	ATL	Tax	NFkB, CREB, PI3K, DDR	
		HBZ	c-jun, E2F	
KSHV	KS	vFLIP	NFkB	
		LANA	p53, Rb, HIF, Notch, Wnt	
		vGPCR	PI3K-AKT-mTOR, ERK, p38, JNK, NFkB,	
		vIRF-1	αIFN, p53, ATM, Bim	

Figure 1.3 Oncogenic viruses

With permission from Mesri EA. et al. Cell Host & Microbe, 2014.

1.2.2 Human T Cell Lymphotropic Virus-1 (HTLV-1)

HTLV-1 was the first described human lymphotropic retrovirus (21). The most important routes of HTLV-1 transmission occur from sexual intercourse, from mother to child predominantly through breastfeeding, and through blood contact, including transfusion of infected cellular products and/or sharing of needles and syringes. Like HIV, the reversed transcribed HTLV-1 genome integrates into the host cell DNA. Once integrated, HTLV-1 continues to exist only as a provirus, which can spread from cell to cell through viral synapses. The route of infection has been shown to determine the development of a specific type of HTLV-1-associated disease. For example, adult T-cell leukemia/lymphoma (ATL) has been associated with

breastfeeding, while HTLV-1-associated myelopathy/tropical spastic paraparesis (HAM/TSP) has been associated with blood transfusion (22).

Two steps characterize HTLV-1 oncogenesis: the first stage is Tax-dependent and the second Tax-independent. During the first step, the Tax transactivator induces T cell proliferation and survival. During the second step, while Tax is inhibited, HTLV-1 b-Zip (HBZ) protein and its RNA drive the oncogenic process (22). Despite several advances supporting the development of novel treatment agents, the prognosis for ATL remains poor. The variety of therapeutic approaches tested over the past 2 decades has been immense. Patients with aggressive ATL have a poor prognosis because of the multidrug resistance of malignant cells, the large tumor burden with multiorgan failure, hypercalcemia, and/or frequent infectious complications as a result of a profound T-cell immunodeficiency. Thus, there is an ongoing need for a vaccine against HTLV-1 (20).

1.2.3 Hepatitis B Virus (HBV) and Hepatitis C Virus (HCV)

HBV and HCV are the major etiological causes of hepatocellular carcinoma (HCC) worldwide. HCC is the fifth most prevalent tumor type and the third leading cause of all cancer deaths (11). Both viruses infect hepatocytes and establish chronic infection with inflammation of the liver (hepatitis), which leads to degradation of the liver tissue (fibrosis) and ultimately results in cirrhosis and development of HCC (23). During viral infection, the HBV-encoded X antigen (HBx) and HCV-encoded core, non-structural protein 5A (NS5A) and NS3 directly promote HCC by altering host gene expression and signaling. HBx has a role in both the early and late stages of HCC with deregulation of signaling pathways and induction of ROS and “stemness” (cancer stem cell-like phenotype) (23). HCV core proteins also affect early and late

stages of liver cancer by promoting survival, proliferation, ROS production and "stemness" (23). Both HBV and HCV promote proliferative signaling that contributes to virus replication. They both evade growth suppression and immune destruction by blocking apoptosis as well as by promoting invasion and metastasis (24,25).

Two different therapeutic treatments for hepatitis B patients are available: immune modulation and viral suppression (26). Interferon is the only example of immune modulatory HBV therapy, while nucleoside or nucleotide analogues are used in the antiviral approach. Vaccination for hepatitis B has been available since 1982, and has effectively reduced the incidence of acute viral hepatitis B. Prevention through worldwide vaccination and screening for HBV in individuals at risk are the public health strategies adopted by many countries.

Until 2011, the combination of PegIFNα and ribavirin was the standard treatment for HCV infection. After 2011, new oral effective drugs have been introduced in the treatment of chronic HCV infection with the cure rate about 90% (i.e. ledipasvir/sofosbuvir) (27,28), suggesting that it might soon be possible to cure all patients with HCV.

1.2.4 Human Papillomaviruses (HPVs)

Papillomaviruses are epitheliotropic non-enveloped viruses with a double-stranded DNA genome of ~8Kbp. Among these, only the high-risk HPVs cause cervical carcinoma, which is one of the leading causes of cancer death in women. By contrast, the low-risk HPVs cause benign warts. HPV-16 and -18 are the most abundant high-risk HPVs, while HPV-6 and -11 are the most frequent low-risk HPVs (29,30). HPVs infect basal epithelial cells where the viral genome is maintained as a low-copy episome. HPV multistep tumorigenesis is characterized by tightly controlled expression of the viral oncoproteins during HPV infection of epithelial cells. Viral

genome replication, gene expression and production of viral particles occur only in the terminally differentiated layers of the epithelium. HPV-associated cancers are generally characterized by nonproductive infections, where only a subset of proteins is expressed, but no viral progeny is produced. Additionally, certain viral genome sequences such as E6 and E7 have the ability to integrate into the human genome, an action which itself constitutes an additional mechanism of carcinogenesis. HPV E6 and E7 are potent oncoproteins (31): E7 targets the retinoblastoma tumor suppressor pRb for proteosomal degradation, leading to sustained proliferative signaling (32). HPV E6 targets the cellular proapoptotic transcription factor p53 for degradation and stimulates telomerase expression and activity (33). Together with E5, E6 and E7 exploit other pro-oncogenic activities including promotion of immune evasion, induction of abnormal angiogenesis and deregulation of cellular metabolism (i.e. Warburg effect) (34).

FDA-approved HPV vaccines are able to prevent infections by certain types of human papillomavirus associated with the development of cervical cancer, genital warts, and other cancers. The World Health Organization (WHO), as well as public health officials in Australia, Canada, Europe, and the United States recommend vaccination of young people of both genders against HPV (35). Two vaccines have market approval in many countries as of 2014; Gardasil and Cervarix in the US. Both vaccines protect against the two HPV types (HPV-16 and HPV-18) that cause 70% of cervical cancers, 80% of anal cancers, 60% of vaginal cancers, and 40% of vulvar cancers (36,37). Despite the existence of vaccines, HPV constitutes the most common sexually transmitted infection in adults worldwide. Thus, the need to promote prevention and vaccination programs remains.

1.2.5 Merkel Cell Polyomavirus (MCV)

Merkel cell polyomavirus (MCV) is a newly discovered human polyomavirus thought to be associated with Merkel cell carcinoma (MCC), an aggressive skin cancer associated with immunosuppression (38). MCV infection is common in the general population and is acquired early in childhood (39). In the setting of a compromised immune system, MCV can reactivate and the burst of virus production can facilitate viral integration in susceptible Merkel cells. Currently little is known about MCV biology. Similarly to SV40, MCV is able to integrate in the human genome and expression of a full-length large T (LT) protein leads to unregulated DNA replication causing DNA-strand breakage. MCV LT has protein motifs similar to those found in SV40 LT, and can bind to pRB and other proteins promoting proliferation (40). Similarly to SV40, MCV also encodes small T (sT) proteins. MCV sT inhibits the tumor suppressor PP2A promoting proliferation. Unique to MCV sT is the manipulation of the Akt-mTOR pathway enhancing cell transformation (41,42).

Immunosuppression is recognized as risk factor for MCC. Indeed, patients with AIDS have a 13-fold increased risk for developing MCC compared to the general population. Similarly to Kaposi sarcoma, MCC targets (in additional to AIDS-patients) elderly and transplant recipients, reinforcing the role of the immune system in maintaining viral infection under surveillance (43). Similar to other human oncogenic viruses, MCV infection alone is not sufficient for tumor development. In fact, MCC tumors require specific mutations (both T antigen truncation and genomic integration) and possibly additional cellular changes or mutations, likely in the setting of immunosuppression, that favor the establishment of the tumor (43,44).

1.2.6 Epstein-Barr Virus (EBV)

As introduced in Section 1.1, EBV is an oncogenic gamma-1 herpesvirus implicated in several lymphoid malignancies, such as Burkitt lymphoma, Hodgkin disease and non-Hodgkin lymphoma, post-transplant lymphoproliferative disorder and nasopharyngeal carcinoma (45,46). EBV infects B-cells and adopts different transcription programs to persist in the host (47). When EBV infects naïve B-cells, it establishes a Latency III program, also called "growth program", in which EBV expresses proteins (EBNA-2,3, LMP-1,2) with sufficient oncogenic potential to cause immortalization in tissue culture and *in vivo*. EBV lymphomas with a latency III program develop only in immunocompromised individuals (HIV patients, post-transplant recipients), while other lymphomas and cancers in immunocompetent hosts will display Latency I or II patterns, expressing only EBNA-1 and LMPs with low immunogenicity. EBNA-1 expression alone (Latency I) allows the EBV genome to be maintained as an episome and segregate in dividing cells (45,48).

Although increasing evidence has demonstrated a potential role for EBV in EBV-associated lymphoproliferative disorders (LPDs), no unified targeted therapeutic strategies have been established. Antivirals in clinical use are mainly broad-spectrum anti-herpesvirus agents with a variable anti-EBV effect, e.g., acyclovir, ganciclovir, and valacyclovir. Approaches targeting oncogenic pathways have been intensively studied based on the altered pathways detected in EBV-associated LPDs (49). The current understanding of EBV pathogenesis has revealed the role of the virus in the initiation, acceleration or maintenance of EBV-associated LPDs. The mechanisms whereby EBV maintains its latent infection and contributes to a spectrum of lymphoid malignancies still remain to be elucidated. Further experimental and clinical studies are needed to improve therapeutic strategies for EBV-associated disorders.

1.2.7 Kaposi Sarcoma Herpesvirus (KSHV)

KSHV or human herpesvirus 8 (HHV-8) is a gamma-2 herpesvirus that is causally associated with the angioproliferative tumor Kaposi sarcoma (KS) and B cell lymphoproliferative disorders (9,50).

1.3 KSHV and Kaposi's Sarcoma

1.3.1 Introduction and Classification of KS

In 1872, Moritz Kaposi, a dermatologist at the University of Vienna, was the first to describe five cases of middle aged and elderly men who presented with a multiple idiopathic pigmented sarcoma of the skin. The disease was named Kaposi sarcoma (KS) few years later (51,52). In 1994, Yuan Chang's group identified KSHV DNA sequences in cutaneous KS tissue. Since then KSHV has been associated not only with with KS, but also with rare lymphoproliferative disorders including multicentric Castleman disease (MCD) and primary effusion lymphoma (PEL) (51,52).

KS is classified into four distinct epidemiological forms; classic KS, a relatively indolent variant first described in elderly Mediterranean men; endemic KS, an aggressive variant common in sub-Saharan Africa; AIDS-KS, the most common AIDS-associated cancer, is a severe and often fatal form of KS; and iatrogenic KS, which is typically associated with organ transplantation (53). All of these forms share the same KS characteristics in which the neoplasm presents as multiple violaceous dermal and/or mucosal lesions. As the tumor progresses, the patch lesions become plaque lesions and ultimately they reach the nodular stage and, sometimes, even ulcerate (54). In some cases, dissemination to the visceral organs can occur, an event that is usually associated with a poor prognosis (51,52). The four different forms of KS are histologically indistinguishable with disorganized networks of abnormal microvasculature composed of elongated endothelial cells, called "spindle cells". Spindle cells do not preserve the integrity of the endothelium, thus allowing fluids and cells to extravasate, causing lymphedema and accumulation of inflammatory cells and erythrocytes in the surrounding tissue (52,55-57). Spindle

cells are thought to be of endothelial lineage and become the most predominant cell type in KS during the plaque and nodular stages. Patch lesions are typically polyclonal, but oligoclonal and monoclonal lesions have been described in later stages. All KS stages and forms are associated with the presence of KSHV DNA in the tissue (58,59).

1.3.2 Lymphoproliferative disorders associated with KSHV

a) Multicentric Castleman Disease (MCD)

MCD is also known as “angiofollicular hyperplasia” and it is most commonly observed in HIV+ patients and transplant recipients. Interestingly, MCD has also been described in HIV-negative patients and occasionally in KSHV-negative patients (60,61). Most MCD patients have lymphoadenopathy, fever and hepatosplenomegaly, with KS co-present in up to 70% of the individuals. MCD is characterized by hyperplastic follicles with indistinct borders and interfollicular zones with plasma cells and vascular hyperplasia. These tumors are often polyclonal, but sometimes progress into monoclonal lymphomas (62,63).

b) Primary Effusion Lymphoma (PEL)

PEL is an aggressive lymphoma characterized by pleural, pericardial or peritoneal effusions, even at early stages. Cells are of B-cell origin and they all present KSHV positivity (60,64). Despite the fact that some PEL patients show EBV co-infection, KSHV is thought to be the major driver of disease. Cases have also been observed in HIV-negative patients and occasionally in other immunocompromised individuals, such as transplant recipients and the elderly (65).

1.3.3 Therapy in KS

The incidence of AIDS-associated KS has decreased dramatically since the introduction of combination antiretroviral therapy (cART) in 1996, however KS still remains the most common neoplasm in HIV-seropositive patients (66,67). Moreover, endemic and classical KS remains a significant problem, especially in the Sub-Saharan areas (http://globocan.iarc). For patients with more advanced and symptomatic KS systemic chemotherapy is used, typically doxorubicin (67) or imatinib (68). Inhibitors of viral DNA polymerases, such as the herpesvirus inhibitors cidofovir and foscarnet, have been employed to prophylactically treat patients, but such drugs have limited efficacy in individuals with established KS. Other non-viral proteins have been the target of more recently developed drugs, such as inhibitors of tyrosine kinases (Abl, c-kit and PDGFR) (53,69). Despite the encouraging results from the use of the aforementioned drugs, there is a strong demand for the development of vaccines or novel therapeutic agents that are also affordable in resource-limited areas (i.e. sub-Saharan Africa).

1.3.4 KSHV genome

The structure of the KSHV genome is similar to HSV, having a long unique region (LUR) flanked by terminal repeat (TR) units. The ~140 Kbp LUR sequence has 53.5% G+C content and includes about 87 identified KSHV ORFs. TR regions consist of multiple 800 bp direct repeat units having 84.5% G+C content with potential packaging and cleavage sites (8,70). TR sequences are required for the maintenance of the episomal DNA in latently infected cells (Figure 1.4). During the lytic cycle, initiation of viral DNA replication is dependent on another site on the genome, called *OriLyt*, which have been identified in all herpesviruses (71,72).

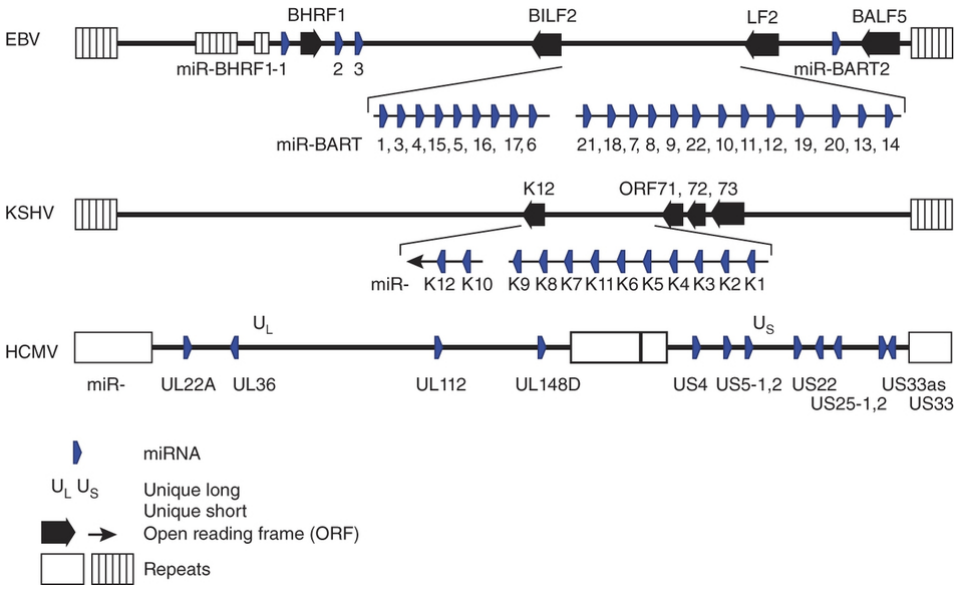

Figure 1.4 KSHV genome structure

With permission from Cullen B. Nature Immunology, 2013.

1.3.5 KSHV life cycle

KSHV infection is a complex multistep process involving the regulation of several different cellular pathways. A productive KSHV primary infection in adherent cells involves an initial lytic phase (2hpi), followed by a latent phase (24hpi) coincident with a decline of the lytic phase. KSHV typically establishes latency starting at 24 hours post infection (73). The initial lytic phase is critical to ensure both the spread of the virus and the establishment of a persistent latent infection in target cells.

KSHV infects a variety of cell types *in vivo* including endothelial cells, B cells, monocytes and epithelial cells. *In vitro*, KSHV has been shown to infect human B cells, endothelial cells, epithelial cells, fibroblasts, monocytes and stem cell precursors of dendritic cells (DC). Additionally, KSHV is able to infect monkey kidney cells, BHK-21 cells, CHO cells and mouse fibroblasts (73).

Several studies have been conducted to investigate the life cycle of KSHV in different cell types (Figure 1.5). As of today, several binding receptors have been identified, the most well-known being the ubiquitous cell surface heparan sulfate proteoglycan (74). DC-SIGN has also been documented as a KSHV binding receptor for human B cells, macrophages and DC (75). Several integrins have been proposed as entry receptors for KSHV in a variety of cells; the viral envelope protein gB is responsible the interaction with integrins and the subsequent endocytosis of the virus into the cells (76,77). Another entry receptor shared by different cell types is the glutamate/cysteine exchange transporter protein xCT (78), although the KSHV envelope protein/s responsible for the interaction with xCT has yet to be identified.

Endocytosis is the predominant mechanism of KSHV entry into endothelial cells, B cells, fibroblasts, monocytes and epithelial cells. However, actin-dependent macropinocytosis has also been observed in endothelial cells (73). After entry and fusion of the virus particles with the plasma membrane, KSHV capsids are released into the cytoplasm of the infected cells where they travel on microtubules towards the nucleus. When capsids reach the nuclear pores, viral DNA is released into the nucleus where genome replication and transcription occur (73). As per all herpesviruses, KSHV gene expression is a tightly temporally-regulated process that is initiated and controlled by a viral transactivator delivered into the cells as a component of the tegument. Viral transcripts can be subdivided into three temporal groups: immediate-early (IE), early (E) and late (L) transcripts (Figure 1.5) (79).

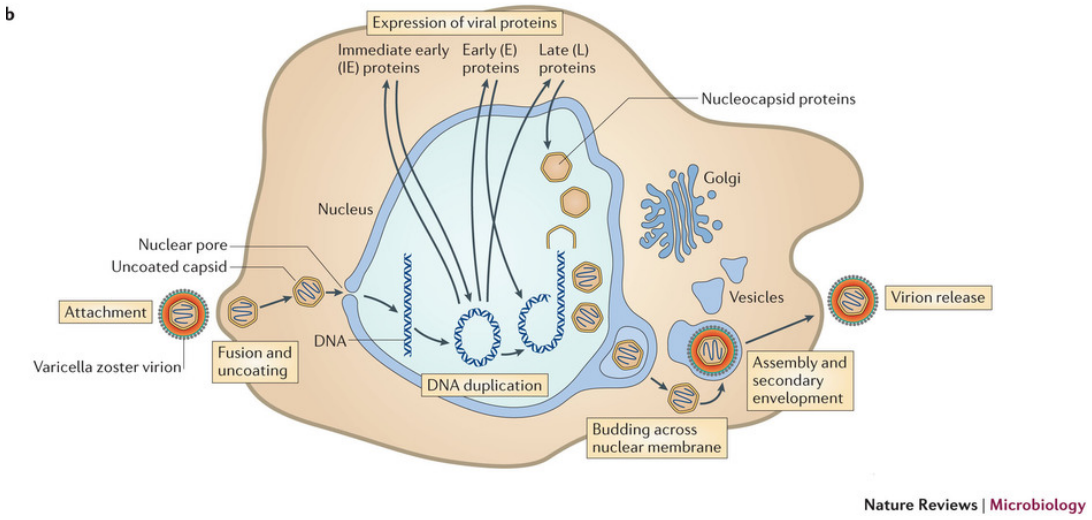

Figure 1.5 Herpesvirus life cycle

With Permission from Zerboni L., et al. Nature Reviews Microbiology, 2014

These groups can be further characterized by their sensitivity to cyclohexamide (CHX, a translation inhibitor) and phosphonoacetic acid (PAA, a DNA synthesis inhibitor). IE transcripts are insensitive to CHX and are not dependent on newly expressed viral proteins. IE genes encode proteins that play an important role in the regulation of E and L gene expression as well as in evasion of the host innate immune response. Unlike IE genes, E genes are sensitive to CHX, as they require expression of IE proteins. Conversely, E genes are insensitive to PAA treatment due to their independence from viral DNA synthesis. The L genes encode structural proteins and proteins important for virion assembly. L genes are dependent on viral DNA replication and are therefore sensitive to PAA treatment (79). Shortly after release into the nucleus and circularization, the viral genome is competent for replication cycle, which initiates at the *OriLyt* sites in the genome. Initially replication occurs by a theta-type (θ) mechanism and proceeds in a rolling circle mechanism, characterized by long head-to-tail genomes (concatemers) (79). Concatemers are then resolved into units of full-length genome, which are packaged into pre-

assembled capsids. Capsids acquire both the genome and first layer of tegument in the nucleus of the infected cells. Nuclear egress and acquisition of tegument and envelope have long been subjects of controversy, but it is now well accepted that virion assembly occurs through a process of envelopment-de-envelopment-re-envelopment (80). The model suggests that capsids acquire a first envelope by budding out of the nucleus. The capsids then lose their envelope by fusing with the outer nuclear membrane. Subsequently, naked capsids are released in the cytoplasm where they travel through the TGN and ER and acquire the tegument layer and final envelope. The mature virions are then ready to be released from the cell (81).

A recent RNA-seq analysis on KSHV-infected cells observed transcription of genes involved in viral DNA replication as early as 4 hpi. These transcripts include ORF59 (processivity factor), ORF9 (DNA polymerase), ORF6 (single-stranded DNA binding protein), ORF56 (DNA replication protein), ORF40 (primase-associated factor), and ORF54 (dUTPase), along with ORF60, ORF61, ORF70 and ORF37. Apart from these transcripts, several other transcripts, encoding the viral structural proteins ORF8 (glycoprotein B), ORFK8.1 (glycoprotein), and the tegument proteins ORF64 and ORF75, were also detected. Additionally, early lytic genes involved in immune-modulation (ORF50 RTA, K5, vIRF2, ORF54, ORF74 vGPCR), and prevention of apoptosis (K4 vMIP-II, K6 vMIP-I, K2 vIL-6) were observed. Surprisingly, transcripts for the latent gene ORF73 (LANA-1) can also be detected very early after infection, potentially indicating a critical role for this viral factor in the productive KSHV life cycle (82). Additionally, many of the noncoding RNAs including PAN RNA, T0.7, and T1.5 (OriLyt transcript) were abundantly detected in the RNA-seq analysis.

Similar to the transcription of viral genes, KSHV DNA replication also can be detected as early as 4 hpi, increasing exponentially up to 48 hpi and then decreasing with time after establishment of latency (83). The viral episome is tethered to the host genome through the interaction of LANA-1 with the host chromatin. Like the cellular genome, the viral episome is also packaged into chromatin-like structures, protected from DNA damage and tightly regulated for gene expression (84). During latency, KSHV promotes expression of a small subset of genes encoded in the KSHV latency associated region (KLAR). These genes include LANA-1 (ORF73) and -2 (vIRF3), v-cyclin (ORF72), Kaposin-A and –B (ORFK12), vFLIP (ORF71), and the viral microRNAs (72). The genes encoded by the KLAR ensure viral persistence play an important role in the development of KS by promoting evasion of host antiviral immune responses and survival of infected cells (85).

1.3.6 Mechanisms of KSHV pathogenesis

KSHV infection of endothelial cells leads to reprogramming of cellular signaling pathways involved in proliferation, inflammation and angiogenesis. KS tumor progression is ensured not only by virtue of the effect of viral proteins and viral miRNAs, but also indirectly by the paracrine effect of cellular and/or viral cytokines released from the infected cells (Figure 1.6) (54). An overview of the different mechanisms of KSHV pathogenesis follows.

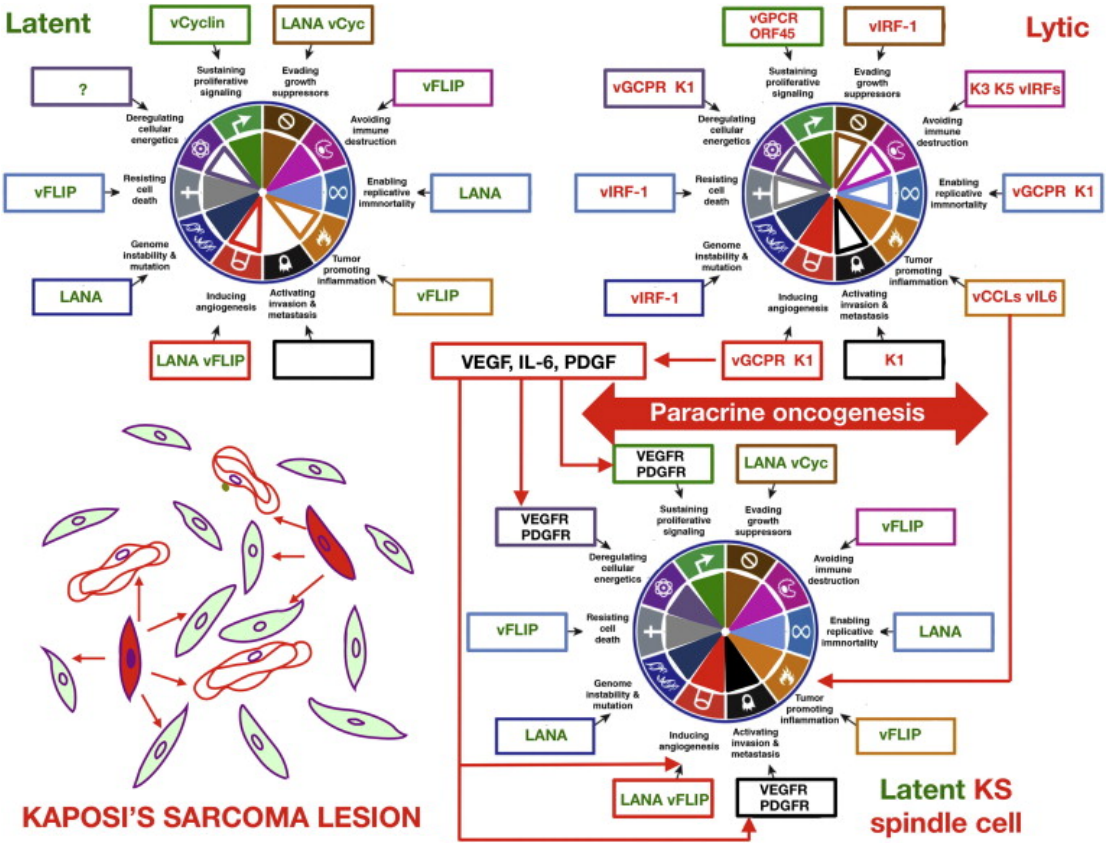

Figure 1.6 KSHV tumorigenesis

With permission from Mesri EA. et al. Cell Host & Microbe, 2014.

1.3.6.1 Proliferation

Several viral factors are involved in the deregulation of the cell cycle and inhibition of apoptosis in KSHV latently infected endothelial cells. Nuclear latency protein LANA-1 is strongly expressed during KSHV latency as well as during lytic replication. LANA-1 ensures the segregation and maintenance of the viral genome throughout cellular replication (86). Additionally, LANA-1 modulates the activity of several cellular transcription factors by inhibiting p53 ability to induce apoptosis. It targets the pRB and GSKB3 proteins, which modulate the cell cycle, and has also been shown to increase the stability of the cellular oncogene c-MYC (87-90).

The viral homologue of cellular cyclin D (vCyc) and the viral FLICE-like inhibitory protein (vFLIP) also contribute to KSHV pathogenesis (91,92). Both vCYC and vFLIP are expressed from the KLAR during latency, from a bicistronic mRNA. vCYC increases DNA synthesis, shifting the cell cycle toward the S phase by phosphorylating several substrates, such as Cdc6 and Rb (93,94). vFLIP is able to block the oncogene-induce senescence caused by vCYC and prevent autophagy of infected cells (95,96).

1.3.6.2 Inflammation

KS lesions are characterized by the presence of numerous inflammatory cells including monocytes, plasma cells and eosinophils. Chronic immune activation and inflammation promote the development of KS in infected individuals (55). KSHV encodes cytokines, homologous to cellular proteins that can trigger an inflammatory response; these include vCCL1 (K6), vCCL2 (K4), vCCL3 (K4.1), which are homologues of MIP1α, MIP1β and CCL2, respectively (97,98). These viral cytokines are able to elicit an inflammatory response by acting as ligands to chemokine receptors CCR4 and CCR8 expressed on Th2 cells. vFLIP and K15 are able to induce COX2 expression, which is an inducible form of cyclooxygenase involved in the production of proinflammatory mediators such as prostaglandins (57). Induction of COX2 leads to secretion of pro-inflammatory (RANTES, MCP2, MIP1α) and pro-angiogenic factors (IGF1, PDGF, MCSF, VEGF-A and VEGF-C). COX2 also increases the secretion of matrix metalloproteinases (MMPs) promoting invasion of infected cells (55).

1.3.6.3 Angiogenesis, invasion and migration

KSHV-infected endothelial cells have the ability to form tubule-like networks *in vitro* even in the absence of exogenous growth factors. Both lytic and latent viral-encoded proteins and miRNAs contribute to this angiogenic effect. The viral homologue of IL-6 (vIL-6) has angiogenic, anti-apoptotic and mitogenic properties: vIL-6 modulates the MAPK pathway resulting in expression of angiogenic (VEGFR2, bFGF, cyclin D and cIL-6) and inflammatory factors (PTX3) (99) .

The viral G-protein-coupled receptor (vGPCR, ORF74) is a ligand-independent, constitutively active IL-8 receptor. vGPCR is expressed during early lytic cycle and activates the NF-*k*B pathway and AP1/NFAT networks, promoting secretion of several angiogenic factors (i.e. VEGF, bFGF, IL-2, IL-4, IL-6, IL-8, and TNFα) (100).

The non-structural proteins K1 and K15 also show promotion of angiogenic factors and inflammatory cytokines. For example, K1 increases VEGF secretion and induces secretion of IL-1α, IL-1β, IL-8, IL-10 and RANTES. Furthermore, K1 leads to activation of the Akt-PI3K pathway, modulating proteins such as PTEN and mTOR, thus promoting cellular survival. K15 activates PLCγ1, leading to tubule formation in *in vitro* angiogenesis assays. Additionally, K15 interacts with Src kinases and promotes *cox2*, *nfat* and *dscr1* transcription (101).

The major latency protein LANA-1 also has a role in promoting angiogenesis and invasion in KSHV-infected cells. For example, LANA-1 induces expression of the protein emmprin, known to be a prometastatic and proangiogenic factor in cancer. As result of emmprin induction, cells induce secretion of angiogenic factors (IL-6 and VEGF) and MMPs contributing to metastasis (102).

1.3.7 Models of KSHV Pathogenesis

1.3.7.1 *In vitro* models

Dr. Ashlee Moses' research group was one of the first to establish an *in vitro* model of KSHV infection in endothelial cells (103). Her group was able to immortalize dermal microvascular endothelial cells (DMVEC) via transduction of HPV16 E6 and E7 genes. Although several additional groups have been able to infect primary DMVEC with KSHV (reviewed in (104)), the percentage of infected cells is low, latency is poorly maintained and the virus does not spread well in such cultures. The inability to establish a significant productive infection in primary DMVEC may be attributed to their naturally limited life span in culture. Immortalized DMVEC retain the essential *in vitro* features of primary cells, but their extended life span facilitates the establishment of infection. Morever, the use of immortalized DMVEC enables the long-term maintenance of age and passage-matched mock-infected control cells in parallel with KSHV-infected cultures for identification of KSHV-specific phenotypic changes. For example, following KSHV infection, DMVEC shape changes from a classical cobblestone-like to a spindle-like morphology. Importantly, infected DMVEC also acquired features characteristic of transformed cells including loss of contact inhibition and the acquisition of anchorage-independent growth (104). It is noteworthy that the altered phenotype of *in vitro* infected DMEC resembles that of KS spindle cells *in vivo* and supports the hypothesis that KSHV-infected endothelial cells are the precursors of KS spindle cells (105),(106). Interestingly, despite the fact that oncoproteins E6 and E7 target several cellular proteins including Rb and p53, their expression does not result in transformation of DMVEC (i.e. contact inhibition is still observed and colony growth in soft agar does not occur). Because KSHV LANA-1 also targets Rb and p53, it is important to take into consideration effects

attributable to both KSHV and the HPV E6/E7 proteins when interpreting phenotypes observed with HPV-immortalized DMVEC (104).

Another efficient *in vitro* model for KSHV infection is represented by telomerase-immortalized microvascular EC, also called TIME cells (107). In order to obtain TIME cells, DMVEC are transduced with a retroviral vector expressing the telomerase reverse transcriptase subunit (hTERT). Similarly to E6/E7 DMVEC, TIME cells can be used for studies of early events in *de novo* infection (107). However, TIME cells are not as efficient as E6/E7 DMVEC in maintaining the viral episome throughout multiple cellular passages (104), thus posing some limitations to latency studies.

1.3.7.2 Humanized BLT mice

The generation of a new humanized mouse, called the BLT (bone marrow, liver, and thymus) mouse (hu-BLT) generated from a NOD/SCID/IL2rγ (NSG) mouse, has been shown to be an excellent model for studying human viral infection (108). This model is able to sustain high levels of transplanted human immune cells and is the only one that can generate a human mucosal immune system. Dr. Charles Wood's research group recently reported that the humanized BLT mouse model is able to support robust KSHV latent and lytic infection, via routes of transmission that are natural in humans (109). Their data showed that latent and lytic viral transcripts and viral protein expression were detectable in various tissues, including spleen and skin tissues. Interestingly, these mice could be infected via several routes, including the oral mucosa. Furthermore, this group was able to show KSHV-establishment of latency in human B cells and macrophages (109). The humanized BLT mouse model will be potentially useful not only for studying KSHV pathogenesis *in vivo* but also for

studying spread of the virus in the infected host.

Due to the species-specificity of the herpesviruses, it has been challenging to develop animal models for KS using KSHV. Thus, researchers have utilized other members of the gammaherpesvirus family to better understand KSHV infection and pathogenesis. The main two KSHV models in use are represented by the Rhesus macaque rhadinovirus (RRV) and the Murine gammaherpesvirus 68 (MHV-68).

1.3.7.3 Rhesus Rhadinovirus (RRV)

RRV is a gamma-2 herpesvirus that is genetically similar to KSHV but is a natural pathogen of rhesus macaques (110). Two different strains of RRV have been isolated: strain H26-95 was isolated and identified at the New England Primate Research Center (111), while another strain, RRV_{17577}, was isolated at the Oregon National Primate Research Center (112). RRV_{17577} was identified in simian immunodeficiency virus (SIV) infected rhesus monkeys, which developed an angiofollicular lymphadenopathy resembling the MCD seen in humans (112). While the two RRV strains are genetically very similar, only RRV_{17577} is used as a model for KSHV infection and pathogenesis in Old World Monkeys (112).

The RRV_{17577} genome is co-linear with KSHV genome, sharing a high percentage of ORF similarity. In general, the organization of RRV_{17577} is similar to that of other gammaherpesviruses, with a unique long sequence of ± 130kb interspersed with internal repeat regions and terminal repeats at both ends.

Despite the prevalence of RRV in Rhesus macaque colonies in captivity, only a small number of macaques develop RRV-associated disease (110). Reminiscent of KSHV in HIV-positive patients, RRV disease is seen only in immunocompromised macaques (typically following SIV infection). RRV infection has been linked not only

to MCD-like disease, but also to the development of mesenchymal cell proliferative lesions similar to those seen in KS (called retroperitoneal fibromatosis) (113) and non-Hodgkin lymphoma (114).

Many of the KSHV ORFs involved in pathogenesis, including several implicated in cell proliferation, inhibition of apoptosis and immune evasion, are conserved in RRV, reinforcing the use of RRV as model for KSHV. A summary of the principle RRV factors involved in infection follows: vIL-6, a viral homologue of IL-6, promotes B cell proliferation (114,115); the vGPCR ORF74 is involved in oncogenesis (116); viral interferon regulatory factors (vIRFs, 8 of which are encoded by RRV) have homology to cellular IRFs directly involved in the regulation of IFN expression (117,118); viral CD200, an homologue of cellular CD200, inhibits the activation of myeloid cells and the production of inflammatory cytokines (119,120). In addition, RRV microRNAs have been shown to play a role in RRV pathogenesis, although the full influence of these genetic elements remains to be elucidated (121).

RRV has become a commonly used model for the study of KSHV pathogenesis *in vivo*. As previously mentioned, RRV shares a high degree of sequence homology with KSHV and induces similar pathogenesis in infected rhesus macaques. Furthermore, the availability of recombinant forms of RRV with mutated or deleted ORFs allows for the investigation of specific viral ORFs with respect to their role in viral pathogenesis (122).

The RRV model in Rhesus macaques provides a unique insight into the mechanisms of KSHV disease development, and allows for the study and development of novel anti-viral therapies that may also prevent KSHV-associated diseases in humans.

1.3.7.4 Murine Herpesvirus-68 (MHV-68)

MHV-68 is a member of the gamma-2 herpesvirus family first isolated from bank voles. The genome encodes for 80 genes products, 63 of which are co-linear and homologous to KSHV. The genomic organization of MHV-68 consists of 118kb of a unique long sequence of DNA, flanked by terminal repeats, a structure that is characteristic of the gamma-2 herpesviruses, including KSHV (123).

MHV-68 is able to infect mice and establish latency in lymphoid tissues and, like KSHV, can induce the development of lymphoproliferative diseases and lymphomas following long-term infection (123). Notably, such disorders are only observed in a small percentage of MHV-68-infected mice. MHV-68, like KSHV and RRV, encodes a series of viral proteins recognizable as cellular homologues. These proteins have been shown to play an important role in the viral pathogenesis by regulating apoptosis, immune responses and cell cycle (124). For example, the MHV-68 vGPCR, like the KSHV vGPCR, plays a role in angiogenesis and tumor formation (125), while the viral Bcl-2 (vBcl-2) homologue inhibits cellular apoptosis and promotes survival of the infected cells (126). Due to the ability to induce infectious mononucleosis, MHV-68 is not only used as a model for KSHV, but has become a suitable model for studying EBV-induced mononucleosis (123,127,128).

1.4 KSHV MicroRNAs

1.4.1 Expression and regulation

MicroRNAs (miRNAs) are small, noncoding RNA molecules that range from 19 to 24 nucleotides in length. miRNAs bind to their complementary message RNAs (mRNAs) to regulate gene expression at a post-transcriptional level. miRNAs have been identified and isolated in both plant and animal cells. Most animal miRNAs have incomplete complementarity to the 3' untranslated region (UTR) of a target gene and modulate gene translation either by degrading the mRNA or by post-transcriptional modifications (129,130). Recently, several DNA viruses, including herpesviruses, have been shown to encode miRNAs (131-136).

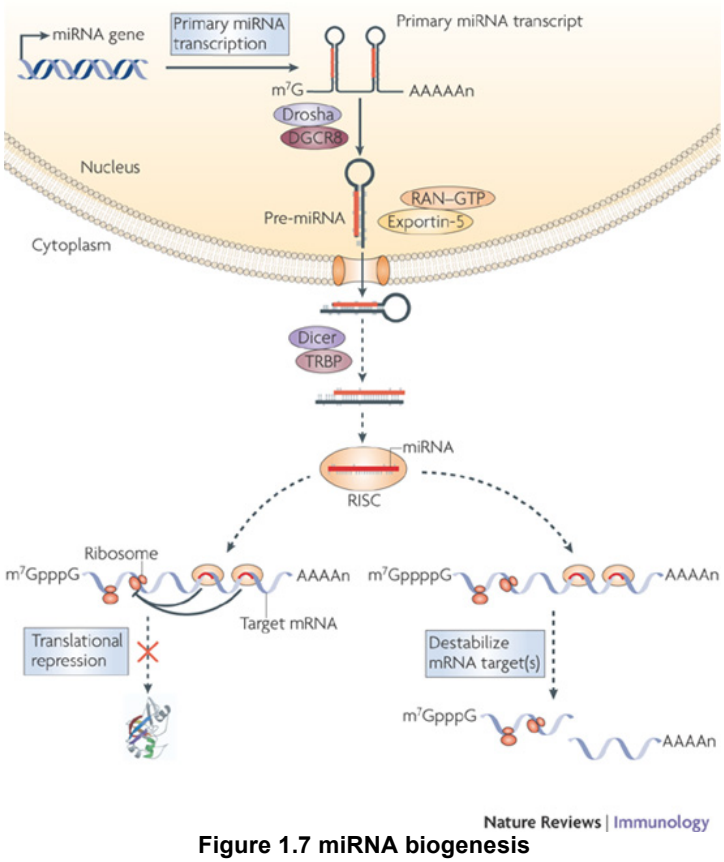

Figure 1.7 miRNA biogenesis

With permission from Lodish HF, et al. Nature Review Immunology, 2008.

The biogenesis of miRNAs begins with the transcription of a long capped, polyadenylated transcript by RNA polymerase II; this transcript is known as the primary miRNA (pri-miRNA). Subsequently, the pri-miRNA is processed by the RNase III enzyme Drosha and its cofactor DGCR8, generating a precursor miRNA (pre-miRNA) (137). The resultant pre-miRNA hairpin is exported to the cytoplasm by the nuclear export factor exportin 5, where it interacts with a second RNase III enzyme called Dicer. Dicer, together with its cofactor TRBP, removes the terminal loop of the pre-miRNA hairpin to generate a 22nt miRNA duplex intermediate. One strand of the miRNA is incorporated into the RNA-induce silencing complex (RISC), where it acts as a guide to direct RISC to complementary mRNA targets (Figure 1.7) (138,139).

As previously mentioned, the KLAR encodes 12 pre-miRNAs, which are responsible for the expression of at least 18 mature miRNAs. The mature KSHV miRNAs are named miR-K12-1 to miR-K12-12, based on their proximity to Kaposin (K12); 10 of the 12 miRNAs are located within the intron of K12, while miR-K12-10 is located within the Kaposi A ORF and the 3'UTR of Kaposin B, and miR-K12-12 is located within the 3'UTR of K12 (140,141). The KSHV miRNAs are constitutively expressed during latency and their expression is maintained during lytic replication. The miRNAs promoters with start sites at 127880/86 and 123751/60 are active during latency and the resulting pri-miRNAs contain miR-K1-K9 and miR-K11 within a ~4.8-kb intron and miR-K10/miR-K12 in their 3'-terminal exon (142). The latency promoters also drive the expression of mRNAs encoding LANA, v-Cyclin, and vFLIP. In addition, a predominantly lytic promoter gives rise to an unspliced ~1.3 kb transcript that was shown to minimally express Kaposin B and also contains the miR-

K12-10 and miR-K12-12 stem-loops, resulting in increased levels of miR-K12-10 and miR-K12-12 expression during lytic replication.

Some KSHV miRNAs are highly conserved between KSHV strains (such as miR-K12-1, -3, -8, -10, -11, 12), while others exhibit sequence alterations (miR-K12-2, -4, -5, -6, -7, -9), likely affecting their function. Interestingly, individual KSHV miRNAs are expressed at very different copy numbers in infected cells. Some of them (including miR-K12-1, -3, -4, -6, -11) are always detectable, while others are not very abundant (140,141,143). Because a common promoter regulates their transcription, their different expression could be attributable to post-transcriptional modifications and processing.

With the exception of KSHV miR-K12-10 and RRV miR-rR1-15, KSHV miRNA seed sequences are not conserved between KSHV and other herpesviruses (143).

1.4.2 KSHV miRNAs targetome

KSHV miRNAs target a variety of cellular mRNAs involved in diverse aspects of KSHV infection. As shown in the table above, several different miRNAs share the same target and/or pathway. Some of the functions of KSHV miRNAs include regulation of virus entry (miR-K12-1, -9, -11), viral gene expression (miR-K12-7, -9, -4, -1, -3, -5, -11, -10 and -12), cell survival (miR-K12-10, -1), immune evasion (miR-K12-7), cytokine secretion (miR-K12-3, -7, -11, -10) and aerobic glycolysis (140,144-146). In a recent publication, it was shown that KSHV miRNAs are loaded into microvesicles (exosomes) and can be transported in the bloodstream or in other bodily fluids. Exosome delivery constitutes an important form of cellular communication between infected/cancerous cells (paracrine signaling) and to

uninfected cells (146). Because of their importance in KSHV infection, a successful therapeutic approach against viral malignancies could potentially be achieved by combining drugs targeting miRNA with existing therapies.

1.4.3 KSHV miR-K12-11

KSHV miRNAs target host and viral mRNAs. Interestingly, KSHV encodes miRNAs that are viral orthologs of cellular miRNAs (141,143,144).

For example, two independent studies reported that miR-K12-11 is the ortholog of host hsa-miR-155, through sharing of the identical seed sequence (Figure 1.8) (147,148).

miR-155 is a multifunctional miRNA that is important in immunity, hematopoiesis, inflammation, and oncogenesis (149). Of note, miR-M4, a miRNA encoded by the highly oncogenic Marek's disease virus, is also a functional ortholog of hsa-miR-155 (150). EBV does not encode a miR-155 ortholog, but induces miR-155 expression through expression of the viral oncoprotein LMP1 (151,152).

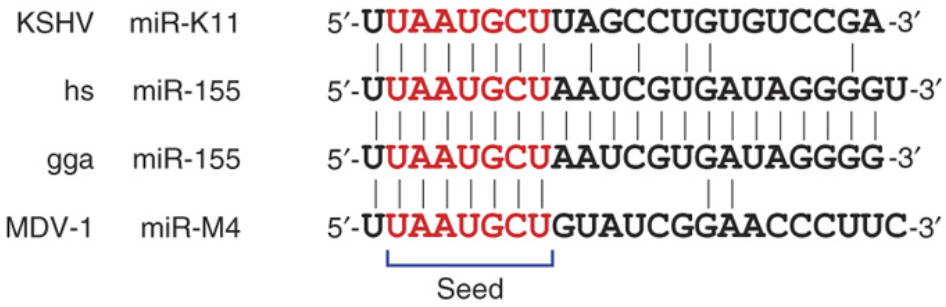

Figure 1.8 KSHV miR-K11 homology to human miR-k155

With permission from Cullen B. Nature Immunology Review. 2013

Because miR-K12-11 shares the same seed sequence as hsa-miR-155, these two miRNAs may have similar functions and targets. Expression of miR-K12-11 or hsa-miR-155 results in the downregulation of an extensive set of mRNA

targets, including the transcriptional regulator BACH1. BACH1 is involved in transcriptional regulation of several cellular genes including xCT and HO-1, both of which play an important role in KSHV infection and pathogenesis (78,153,154). Additionally, ectopic expression of miR-K12-11 or miR-155 targets C/EBPβ, which leads to a significant expansion of the CD19 (+) B-cell population (155). Further studies have indicated that miR-K12-11 is involved in attenuating interferon signaling and contributing to KSHV latency maintenance through targeting of I-kappa-B kinase epsilon (IKKε) (156). Moreover, ectopic expression of miR-K12-11 downregulates TGF-β signaling and facilitates cell proliferation by directly targeting SMAD5 (157).

1.5 Innate Immunity in KSHV infection

The immune system protects organisms from infection with layered defenses of increasing specificity. The innate immune system provides the first line of immune response, which is immediate but non-specific. Innate immune systems are found in all plants and animals (158,159). If pathogens successfully evade the first line of defense, vertebrates exhibit a second layer of protection represented by the adaptive immune response, which is activated by the innate response. Here, the immune system alters its response during an infection to improve its recognition of the pathogen. This immune response can be retained after the pathogen has been eliminated in the form of an immunological memory and allows the adaptive immune system to react faster and stronger each time the same pathogen is encountered (159,160).

1.5.1 Intrinsic Antiviral Immunity

Intrinsic antiviral immunity refers to a form of immunity that directly restricts viral replication and assembly, thereby rendering a cell non-permissive to a specific virus. Intrinsic immunity is conferred by restriction factors that are mostly constitutive in certain cell types (161).

Despite the fact that intrinsic antiviral factors pre-exist in certain cells, their expression can be further induced by interferon. Many intrinsic antiviral factors have evolved under strong positive selection through co-evolution with the virus (159). Studies on intrinsic antiviral factors have been critical to understand permissiveness of a cell type to a specific virus and to investigate the mechanisms by which viruses have coevolved with their hosts to counteract these factors.

Mechanisms of intrinsic immunity include apoptosis, autophagy, RNA interference and antiviral factors (161).

1.5.1.1 Evasion of intrinsic immune response by KSHV

During KSHV infection, processes related to viral replication frequently induce stress responses that perturb cellular homeostasis, including apoptosis and autophagy. KSHV has evolved to evade cell apoptosis by expressing two human homologues: vFLIP and vBcl-2. vFLIP interferes with the formation of the death-inducing signal complex (DISC), a component of the death receptor-mediated apoptosis pathway (162). vBcl-2 has lost the inhibitory group present in cellular Bcl-2, which converts cellular anti-apoptotic pathways into pro-apoptotic ones (163). Additionally, LANA and vIRF4 both target p53 for degradation, while K1, miR-K10a and vIAP also contribute to preventing apoptosis. Another intrinsic immune

mechanism of response is represented by autophagy. Autophagy is a homeostatic process through which the cell self-engulfs and auto-digests cytoplasmic constituents in order to balance sources of energy at critical times such as stress or nutrient starvation. In additional to influencing cellular proliferation, both vFLIP and vBcl-2 can inhibit autophagy by targeting ATG3 and Beclin-1, respectively (164).

1.5.2 Role of Pattern-recognition Receptors in innate immunity

The most important role undertaken by the immune system is the detection of microbial components. Appropriate recognition of invasive microbes is critical for establishment of an effective immune response. Pathogen detection by the innate immune system is carried out by a class of immune sensors called pattern recognition receptors (PRR). The Toll-like receptors (TLRs) are a class of PRRs that detect a broad range of molecular patterns. They were initially identified based on homology with the Toll receptor in *Drosophila* (165). The fly Toll is essential for recognition of fungal pathogens, as well for fly development. TLRs are type I transmembrane proteins with ectodomains containing leucine-rich repeats that mediate recognition of pathogen-associated molecular patterns (PAMPs) (165). The intracellular Toll-interleukin 1 receptor (TIR) domain is required for downstream signal transduction. So far, 10 functional TLRs have been identified in humans (12 in mice). PAMPs recognized by TLRs include lipids, lipoproteins, proteins and microbial nucleic acids. The recognition of PAMPs by TLRs can occur in various cellular compartments, such as the plasma membrane and intracellular vesicles. After the discovery of TLRs, several classes of cytosolic PRR, including RIG-I like receptors (RLRs) and Nod-like receptors (NRLs) were identified. The RLR family consists of three members: RIG-I, MDA5 and LPG2, which detect virus-associated dsRNA. The NRL family consists of more than 20 members, several responding to PAMPs and

other detecting cell stresses and non-PAMP particles. The primary consequence of TLR signaling activation is the induction of NF-*k*B pathways, IRF-3, cytokine secretion and expression of co-stimulatory molecules important for immunological processes that aim to control and clear pathogens (166).

TLR responses are initiated by ligand-induced multimerization leading to recruitment of different primary adaptor molecules. The majority of the adaptor molecules contains a TIR domain and this family includes MyD88, TIRAP (Mal), TRIF and TRAM. MyD88, the first identified member of the TIR family, is universally used by all TLRs except for TLR3 and activates NF-kB and MAPKs to induce inflammatory cytokine transcription. By contrast, TRIF is used by both TLR3 and TLR4 and induces alternative pathways leading to the activation of the transcription factor IRF3 and the consequent induction of type I interferon and inflammatory cytokines (166,167).

TLRs are subdivided into two main groups, depending on their cellular localization and PAMP ligands. One group is localized on the cell surface and recognizes mainly microbial membrane components, such as lipids, lipoproteins, and glycoproteins. This group consists of TLR1, TLR2, TLR4, TLR5, TLR6, and TLR11. The second group of TLRs is found in intracellular vesicles and recognizes microbial nucleic acids. Members of this group include TLR3 (dsRNA), TLR7 (ssRNA), TLR8 (ssRNA) and TLR9 (CpG DNA (Figure 1.9) (167).

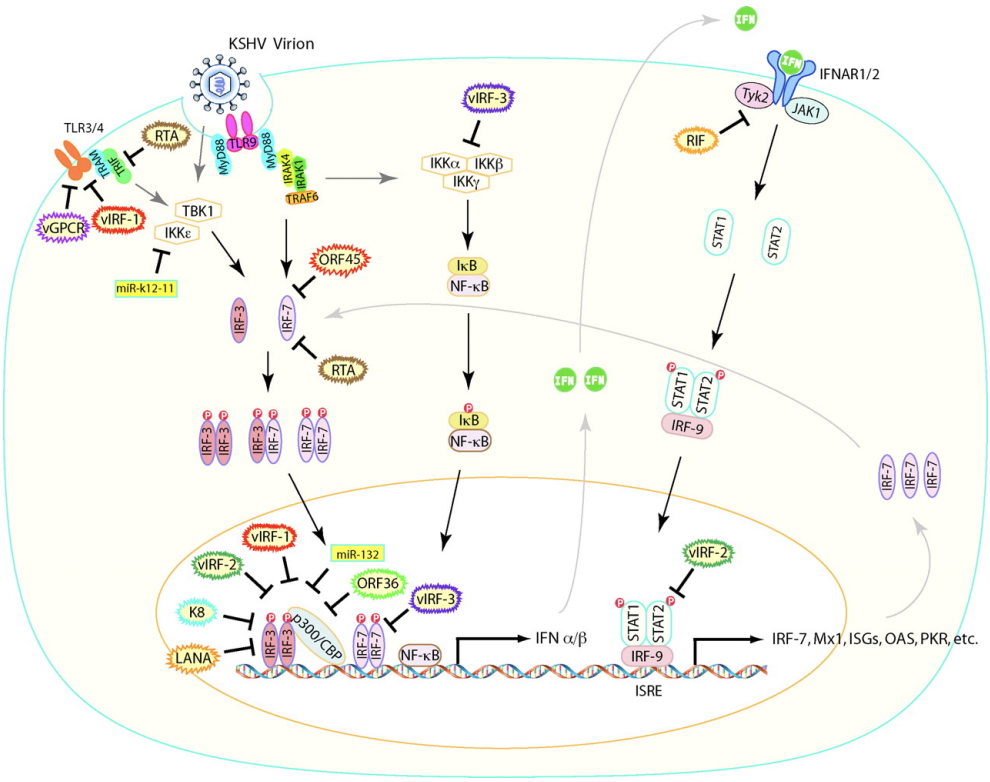

Figure 1.9 PRRs in KSHV infection

With permission from Sathish N, and Yuan Y. Journal of Virology Minireview, 2011

1.5.2.1 Nucleic acids sensors

Foreign or mislocalized DNA and RNA molecules are potent triggers of type I IFN and pro-inflammatory cytokines. Viral DNA recognition can occur in different cellular compartments such as the cytosol, endosomes and nucleus. Several DNA sensors have been described including IFNγ-inducible (IFI16), cGAMP synthetase (cGAS), helicase DDX41, and cytosolic sensor DAI/ZBP1 (168,169).

IFI16 is distinguished from other known DNA sensors by its ability to shuttle between the cytosol and the nucleus (168,170). Although originally shown to sense HSV-1 DNA in the cytosol (171), accumulating evidence suggests that IFI16 may function primarily in the nucleus (172,173). As early as 2 hours after *de novo* infection of primary endothelial cells, KSHV genomic DNA is evident within IFI16-

containing nuclear bodies. This phenotype is accompanied by IFI16-dependent inflammasome formation and caspase-1-mediated secretion of IL-1β (172).

TLR9 is an endosomal TLR that can sense virion-associated nucleic acids or replication intermediates. TLR9 is mainly expressed in B cells and plasmacytoid dendritic cells (pDCs), where it triggers IRF7-dependent activation of type I IFNs, in particular IFNα (166). *De novo* infection of pDCs by KSHV results in induction of IFNα and this phenotype is at least partially dependent on TLR9. Although other TLR9 ligands have been proposed, unmethylated CpG motifs of double-stranded DNA (dsDNA) constitute the best characterized TLR9 agonist. Interestingly, the KSHV genome has a normal CpG abundance, suggesting that the viral genome itself is not under selective pressure to avoid TLR9 stimulation (reviewed in 174).

TLR3 senses viral replication intermediates, including dsRNA, leading to TRIF-dependent induction of inflammatory cytokines and type I IFN (166). While the TLR3 pathway is clearly affected by KSHV, it is not known whether this involves direct stimulation of TLR3 by a KSHV PAMP. KSHV infection does not appear to upregulate TLR3 expression in lymphatic endothelial cells (LEC) (175). To date, the role of TLR3 in KSHV antiviral defense remains unclear.

RIG-I, a cytosolic RNA sensor, can recognize 5'-triphosphate RNA of both RNA and DNA viruses (166) and requires TRIM25-mediated ubiquitination for its signaling activity (176). Upon KSHV infection, RIG-I contributes to IFNβ production and suppression of viral gene expression (177,178). RNA purified from KSHV-infected cells undergoing lytic replication is sufficient to activate RIG-I signaling upon delivery by transfection (178). Although PAN RNA accounts for ~80% of polyadenylated KSHV RNA, it does not appear to play a role in RIG-I activation.

Nevertheless, the identity of the RNA PAMP(s) involved in RIG-I activation remains unknown (178).The same study demonstrated that expression of ORF64, a conserved herpesviral tegument protein, results in reduced TRIM25-dependent ubiquitination of RIG-I and IFNβ promoter activity.

1.5.2.2 Additional sensors with relevance to KSHV

TLR4 recognizes LPS from bacteria and viral glycoproteins. TLR4 forms a complex with MD2 on the cell surface and together they bind to LPS. The multimerization of two TLR4-MD2 complexes upon LPS binding initiates signal transduction by recruiting intracellular adaptor molecules. The respiratory syncytial virus (RSV) F protein is a known trigger of TLR4 and TLR4 has a protective role against RSV infection in mice (179) and humans (180). KSHV infection of LECs downregulated for TLR4 showed increased levels of LANA message and reduction in inflammatory cytokines (TNFα, IL-1β, IL-6) and type I IFN (IFNβ) (175). Although still unknown is how KSHV triggers a TLR4-dependent response, there is evidence showing that UV-inactivated KSHV retains the ability to induce TLR4 signaling, suggesting that one or more glycoproteins may act as agonists (175). In particular, treatment of fibroblasts with a purified soluble version of KSHV glycoprotein K8.1 is sufficient to induce IFNβ and ISG production (181,182). Therefore, TLR4 appears to contribute to innate immunity against KSHV by recognizing glycoproteins on the KSHV envelope. The significance of TLR4 in the regulation of KSHV is further highlighted by the evidence that vIRF-1 and vGPCR are able to suppress TLR4 (175). Moreover, KSHV encodes proteins and miRNAs able to block the TLR4 adaptor proteins MyD88 and TRIF. For example, RTA is able to degrade TRIF, while viral miR-K9 downregulates MyD88 and also targets IRAK1, another protein in the same pathway.

NLRP1 is currently the only NLRP family member implicated in the sensing of KSHV (183). It is one of the many cytosolic proteins known to take part in the inflammasome complex (184). The major outcome of inflammasome activation is the maturation and release of IL-1β and IL18, and induction of pyroptosis (185). Inflammasome activation is initiated by the NLRs, in response to a variety of stimuli (184). Expression of ORF63, a large tegument protein encoded by KSHV, prevents inflammasome formation by blocking the oligomerization of NLRP1 as well as the interaction between NLRP1 and pro-caspase-1. Knockdown of NLRP1 results in more efficient TPA-induced lytic replication of KSHV in BCBL-1 cells, a PEL cell line (183). Thus, inflammasomes appear to be important for curbing lytic replication. Future studies are needed to determine how KSHV infection triggers an NLRP1-dependent response.

1.5.3 IFN production and its evasion by KSHV

Type I IFN and a family of IFN-stimulated genes (ISGs) provide the first line of defense against viral infection. Virus-infected cells secrete IFN upon recognition of specific PAMPs by PRRs, while activation of TLR pathways (and other pathways) leads to activation of a family of transcription factors, called IFN regulatory factors (IRFs), which initiate transcription of Type I IFN genes. Secreted IFN binds to the type I IFN receptor (IFNAR) triggering ISG expression. KSHV interferes with the IFN pathway at different levels, antagonizing both the expression and function of several components of the IRF pathway. KSHV encodes four homologs of cellular IRFs (vIRFs), which interfere with the activity of specific IRFs (97,117,186). vIRF-1 binds to host IRF-1 or CBP/300 to block transcriptional activation. vIRF-2 degrades IRF-3 via caspase-3 dependent pathway and binds to IRF1. Additionally, vIRF-2 interacts with protein kinase R (PKR), inhibiting its antiviral function. vIRF-3 antagonizes IRF-5

and IRF-7 via direct inhibitory interactions. vIRF-4 degrades p53, but has no apparent activity in antagonizing IFN-mediated signaling. KSHV has additional mechanisms to target IRFs: for example, LANA-1 and K-bZIP (K8) bind to the IFN-β promoter preventing its induction during latency and virus activation (97,187). Another example is ORF45, a conserved tegument protein, which binds to IRF7 preventing its activation and translocation (182,188-190).

1.6 Oxidative Stress and Heme Oxygenase 1

1.6.1 Oxidative stress in viral infection

Accumulating evidence has suggested an important role for ROS and oxidative stress during viral infection (191). It has been shown that Adenovirus 5 (Ad5) infection leads to a rapid increase of ROS production after lysosomal rupture (192). Additionally, the enterovirus 71 (E71) is also able to induce ROS shortly after infection (193). ROS were also found to be induced by several member of the herpesvirus family. In particular, HSV-1 entry and replication induces ROS for a long period of time after infection, and its induction is dependent on NAPDH oxidase activity (194,195). HSV-2 also induces oxidative stress during early stages of infection (196). Similarly, EBV promotes ROS production early after infection of B-cells and epithelial cells (197). Interestingly, KSHV infection of endothelial cells sustains induction of ROS at early times post infection and during latency. Several studies support the notion that ROS can play a role in tumorigenesis, such as through the promotion of metastasis and genome instability. In addition, ROS can play and important role in facilitating viral infection. In fact, several studies suggest that RNA and DNA viruses use oxidative stress to regulate their life cycle. Indeed, treatment with anti-oxidant compounds has been shown to inhibit HSV-1, influenza, enteroviruses and HIV replication. Interestingly, antioxidant treatment in endothelial cells results in inhibition of KSHV entry. By contrast, induction of oxidative stress can lead to reactivation of latently KSHV-infected endothelial cells, suggesting an important role of ROS in the regulation of viral gene expression (198).

Because of the important role of oxidative stress and ROS production during KSHV infection and tumorigenesis, these pathways have become attractive targets for therapeutic drugs controlling both KSHV infection and KS.

1.6.2 Heme oxygenase 1 (HO-1)

Heme oxygenases (HO) are enzymes involved in the degradation of heme, a component of hemoglobin. Interest in these proteins has increased among researchers from many disciplines, due to their involvement in several physiological and pathological aspects of human biology. HO catalyze the rate-limiting step in the oxidative catabolism of heme, in a reaction that generates carbon monoxide (CO), ferrous iron, and biliverdin-IXa (BV). BV is then converted into bilirubin-IXa (BR) by biliverdin reductase (199).

Heme is both a substrate and enzyme cofactor for HO. Heme is also a key mediator of many vital biological processes including oxygen transport, peroxide metabolism, cell signaling, xenobiotic detoxification, and mitochondrial bioenergetics (200). Two genetically distinct isozymes of HO have been characterized: an inducible form, heme oxygenase-1 (HO-1), and a constitutively expressed form, heme oxygenase-2 (HO-2). HO-1 and HO-2 represent the products of distinct genes and differ in primary amino acid sequence and biochemical and biophysical properties. HO-1 and HO-2 share a highly conserved heme catalytic domain and hydrophobic regions at the carboxyl terminus (200). HO-1 is potently upregulated in mammalian cells during cellular stress and is strongly-expressed in several cancers (201). The protein typically localizes to the smooth endoplasmic reticulum (ER), although recent evidence suggests an association with other intracellular membranes, including the inner mitochondrial membrane and plasma membrane caveolae (201,202). HO-1 has also been found in the nucleus, although its functional activity in this compartment is incompletely understood.

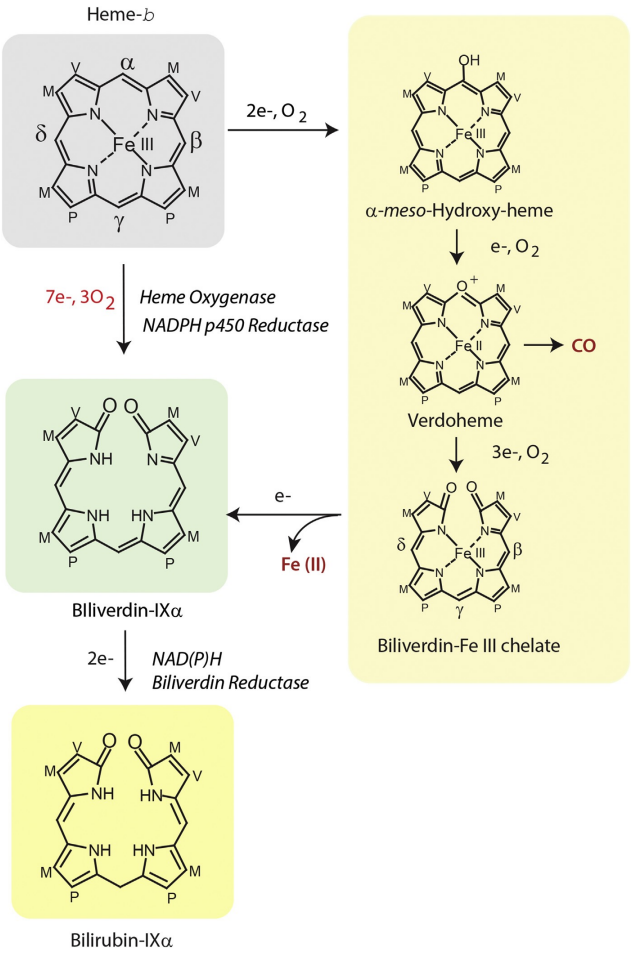

Figure 1.10 Heme degradation

With permission from Ryter SW and Choi MK. Translational Research, 2015.

The gene that encodes HO-1 (HMOX1 in humans) is highly transcriptionally regulated by stress stimuli. In addition to heme, oxidizing stressors such as UV-A radiation, hydrogen peroxide and redox compounds are powerful HO-1 inducers. Furthermore, HO-1 can be induced by a multiplicity of chemical and physical agents including fluctuation in oxygen tension, nitric oxide, heavy metals, and cytokines (201,202).

1.6.2.1 Regulation of HO-1 expression

HO-1 transcriptional expression has been extensively studied. Studies of the mouse Hmox1 gene promoter have revealed 2 major regulatory enhancer regions located at -4 and -10 Kb upstream of the transcriptional start site. Both enhancer regions contain tandem repeats of the stress-responsive element (StRE) motif, also known as the antioxidant responsive element (ARE) (201,202).

Hmox1 transcription is strictly regulated by two proteins: NRF2 and BACH1 (203). The nuclear factor erythroid 2-related factor 2 (NRF2) recognizes and binds to StRE motifs and represents the major transcriptional activator of Hmox1. Under basal condition, NRF2 is retained in the cytoplasm by the Keap1, which inhibits its transcriptional activity. Keap1 facilitates the ubiquitination of NRF2 by the Cullin 3-based E3 ubiquitin ligase complex, which marks NRF2 for proteosomal degradation. When cells are under stress, such as in the presence of heme or pro-oxidants, NRF2 dissociates from Keap1 and translocates to the nucleus where it binds to small Maf proteins and to the Hmox1 promoter, resulting in gene transcription (204). BACH1 has been identified as the main transcriptional repressor of Hmox1. Under basal condition, BACH1 forms a complex with small Maf proteins and competes with NRF2 for binding at the StRE. When heme is present in the cell it can bind to BACH1, disrupting its interaction with the DNA and promoting its nuclear export (205).

Emerging studies suggest a critical role for miRNAs in the regulation of HO-1 gene expression. In particular, hsa-miR-155 targets Bach1 mRNA for its degradation, promoting hmox1 gene transcription (155). Other miRNAs indirectly target NRF2, for example by downregulating the expression of the E3 ubiquitin ligase involved in the degradation of NRF2.

HO-1 belongs to a larger family of stress-inducible proteins whose transcriptional regulation is also related to adverse environmental conditions. Of the

known mammalian stress protein families, the expression of the heat shock proteins (HSPs) constitutes a global cellular response to protein denaturation associated with hyperthermia (206). HO-1 is sometimes been classified as a heat shock protein (Hsp32) due to its transcriptional responsiveness to hyperthermia; this response is however largely restricted to rodent systems (207,208).

Accumulating evidence indicates that many inducers of HO-1 activate protein phosphorylation-dependent signaling cascades that ultimately converge on the transcription factors that regulate the Hmox1 gene. Several studies have implicated a major role for the mitogen activated protein kinases (MAPKs) in HO-1 activation, although other kinases, including tyrosine kinases, phosphatidylinositol 3-kinase (PI3K) and protein kinases A, G, and C have emerged as potential contributing factors. The MAPK superfamily comprises three primary signaling cascades named after their terminal MAPKs: the extracellular signal regulated kinases (ERK1/2 pathway), the c-Jun NH2 -terminal kinases or stress-activated kinases (JNK/SAPK), and the p38 MAPKs. Each pathway consists of a hierarchy of kinases that sequentially phosphorylate and activate their downstream target kinases. A number of studies have focused on the resolution of MAPK pathways in the activation of hmox-1 in diverse cell types in response to various inducing conditions, supporting a role for the MAPK cascades in inducible hmox-1 gene activation (201,202,209).

1.6.2.2 Role of HO-1 in cancer

HO-1 is highly induced in several cancers, including lymphosarcoma, prostate cancer, brain cancer, adenocarcinoma, hepatoma, squamous carcinoma, glioblastoma, melanoma, pancreatic cancer and Kaposi sarcoma. HO-1 induction in cancer cells has been shown to contribute to tumor progression by promoting cell

proliferation, cytoprotection, resistance to cancer therapy and angiogenesis (202,210,211).

HO-1 is induced by many stress-inducing factors and its expression confers protection from oxidative damage and reduces the rate of apoptosis. Cytoprotective and anti-apoptotic properties of HO-1 have been demonstrated in cancer cells as well as in knockout mice: pharmacological or exogenous expression of HO-1 significantly increases survival of different tumor cell lines, whereas HO-1 inhibition reduces their viability (209).

Mechanisms of HO-1-derived cytoprotection in tumor cells are still not fully understood but a likely explanation involves the cytoprotective activity of the HO-1 metabolites: bilirubin, CO, and ferrous iron.

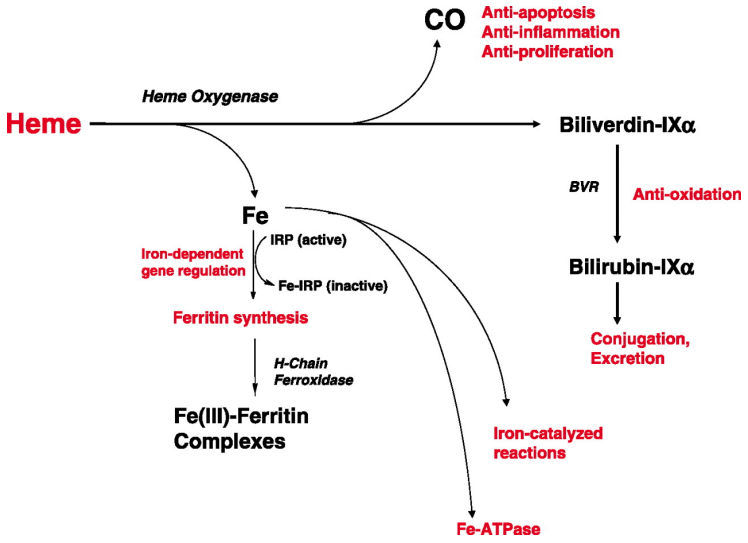

Figure 1.11 Heme catabolism

With permission from Ryter SW and Choi AMK. Translational Research, 2015.

Biliverdin and Bilirubin Biliverdin (BV) and bilirubin (BR) are both considered anti-oxidants: BR effectively quenches singlet molecular oxygen ($^1O_2$) in organic solvents (212), while both BV and BR can react with enzymatically generated O_2^-, resulting in bleaching of pigments (213). By contrast, high concentration of unconjugated BR can

be toxic to cells; thus, its expression is tightly regulated by HO-1.

Carbon monoxide Recent studies have revealed that CO has profound consequences on intracellular signaling processes, which culminate in anti-inflammatory, anti-proliferative, anti-apoptotic, and anti-coagulative effects. CO not only blocks mitochondrial cytochrome c release, the crucial event in induction of apoptosis, but also inhibits expression of pro-apoptotic p53 (214). Exogenous CO can increase the viability of multiple cell types, including endothelial cells (215). CO also modulates the activation of several MAPKs, which represent crucial mediators of both inflammatory and stress responses. These include p38 MAPK, c-Jun NH2 - terminal kinase, and ERK1/2, although the proximal targets remain unclear (209). The anti-inflammatory effect of CO, as demonstrated in LPS-stimulated macrophages, requires activation of the p38-MAPK pathway and may also require the inhibition of TLR4 and NADPH oxidase–dependent signaling. The discovery of novel compounds, termed “carbon monoxide releasing molecules (CORMs)”, have provided further mechanistic insight into the role of CO in biological systems (216). CORMs are transition metal carbonyls with the capacity to release CO. These compounds contain a central metal (i.e., Mn, Bo, Ru, Fe) that is coordinated by carbonyl groups. CORM-2, or [Ru(CO)3Cl2]2, can release CO in organic solvent, depending on ligand displacement by the solvent (i.e., DMSO) (202,209).

Iron Iron that exists in biological systems independently of heme and/or metalloprotein pools resides in complexes with low-molecular-weight organic compounds. This iron appears in a loosely bound form accessible to metal chelating agents (217). The iron released from heme by HO activity potentially becomes part of the transient and “chelatable” iron pool, where it may be available for cellular

processes that depend on iron. One hypothesis states that the iron released from HO activity is transiently available for the promotion of intracellular ROS production (210). Ferritin has also been implicated as a cytoprotective molecule in a number of *in vitro* models. Thus, ferritin synthesized as a consequence of HO activity has been proposed as a contributory mechanism underlying HO-dependent cytoprotection (218).

1.6.2.3 Therapeutic strategies against HO-1 activity

The application of HO-1 activity inhibitors was first proposed as a clinical therapy for neonatal jaundice. More recently, they have been used for the treatment of other diseases, such as prostate cancer. First generation competitive inhibitors of HO-1 are represented by synthetic metalloporphyrins, e.g., heavy metal chelates of protoporphyrins, mesoporphoryins and deuteroporphyrins. Of these, stannate mesoporphyrin (SnMP) was described as the most potent HO inhibitor (202). Despite their potency, the disadvantage of metalloporphyrins is the lack of isoform selectivity. Additionally, off-target effects have been reported in some settings, such as induction of Hmox1 gene transcription, inhibition of iNOS and phototoxicity. Several clinical trials using metalloporphyrins showed their efficacy in reducing bilirubin in neonates, however phototoxicity (erythema) was reported as a concern.

The imidazole-dioxolanes represent a second generation of HO activity inhibitors (219). The first in this class of compound is azalanstat (QC-1). Additional derivatives of this molecule have been shown to inhibit HO activity; QC-15 in particular demonstrated high selectivity for HO-1 (220). Another small-molecule inhibitor of HO-1, OB-24, (221), is a competitive and reversible inhibitor that selectively inhibits HO-1 but not HO-2 and prevents the growth and metastasis of

prostate cancer in a preclinical xenograft model (209).

Recent studies have explored the possibility of targeting HO-1 by using retroviral expression of miRNAs (222). An example is represented by the use of lentiviral vectors expressing miRNAs against HO-1 in the lungs of mice, resulting in enhanced susceptibility to oxidant stress and apoptosis (223).

1.6.3 HO-1 and infection

Up-regulation of HO-1 has been recognized in the context of several pathogens. Infections by influenza virus (224), encephalomyocarditis virus (225), *Listeria monocytogenes* (226), and *Rickettsia rickettsia* (227) all result in significant upregulation of HO-1, suggesting that this enzyme may participate in cellular responses to several intracellular pathogens. Interestingly, recent studies have also demonstrated significant antiviral properties of HO-1. Specifically, upregulation of HO-1 was shown to suppress infection of enterovirus, HCV, HBV, and human immunodeficiency virus (HIV), while protecting infected tissues from virus-induced oxidative injury (228). Another study showed that HO-1 activity significantly attenuates Ebola virus (EBOV) EBOV infection, indicating that, similarly to the other RNA viruses mentioned above, EBOV is also sensitive to the antiviral properties of HO-1 (229). Collectively, these studies suggest that HO-1 can play different roles in the context of specific pathogen infection.

1.6.4 HO-1 and KSHV

Dr. Ashlee Moses' research group was the first to report HO-1 induction in KSHV-infected endothelial cells, both *in vitro* and in KS biopsy tissue (153). The group demonstrated that HO-1 activity in KSHV-infected endothelial cells resulted in

increased cell proliferation, following exposure to free heme. By contrast, uninfected cells grown under the same heme-rich conditions, did not exhibit a proliferative response. Interestingly, these proliferative advantages were reversed in the presence of an HO-1 activity inhibitor (CrMP), suggesting HO-1 as a potential cellular therapeutic target for KS (153). There is evidence that KS lesions have locally elevated concentrations of hemoglobin and free heme and therefore are rich in substrate for HO-1. KS endothelial cells, like other neoplastic endothelial cells, have leaky junctions allowing the extravasation of a large number of erythrocytes from the blood vessels into the surrounding tissue (230-233). Erythrophagocytosis by KS cells is also a common feature (231). Many spindle cells contain engulfed erythrocytes (erythrophagosomes) surrounded by lysosomal granules. These erythrophagosomes show various stages of degradation leading to the expulsion of hemoglobin and dead red blood cells (RBCs). With KS progression, there is an accumulation of hyaline globules in the tissue, and histologic staining has revealed that these are the remnants of degenerated erythrocytes (233). Because of the heme-rich microenvironment KS develops in, it is conceivable that upregulation of HO-1 by KSHV infection could confer a selective growth and/or survival advantage to the spindle cells. The availability of potent inhibitors of HO-1 in clinical use elsewhere (202),(209) makes this enzyme a potentially important treatment target in KS.

1.7 Concluding remarks

As discussed above, KS is one of the cancers in which HO-1 is highly expressed. KSHV infection is itself a potent inducer of HO-1 in target endothelial cells, and evidence supports a role for HO-1 in the development of KS (153). In this thesis, I determine the mechanisms through which KSHV induces HO-1 (Chapter 2) and provide evidence that HO-1 is important not only for viral oncogenesis but also for antagonizing the host antiviral response to facilitate a successful viral infection (Chapter 3). Collectively, these studies characterize for the first time the complex relationship between KSHV and its host regarding HO-1 expression and function, and validate the proposal that HO-1 be considered a viable therapeutic target for KS.

CHAPTER 2

Kaposi Sarcoma Herpesvirus Induces HO-1 During *De Novo* Infection of Endothelial Cells via Viral miRNA-Dependent and -Independent Mechanisms.

Sara Botto[1], Jennifer E. Totonchy[2], Jean K. Gustin[1] and Ashlee V. Moses[1]

[1]Vaccine and Gene Therapy Institute; Oregon Health and Science University; Beaverton, OR 97006 USA; [2] Department of Pathology and Laboratory Medicine, Weill Cornell Medical College, New York, N.Y. 10065, USA

Running title: KSHV induction of HO-1 in endothelial cells

- Manuscript written by Sara Botto and Ashlee V. Moses.
- All experiments were conducted by Sara Botto, except for Figure S2.1A, Figure 2.2B executed by Jen Totonchy, and the construction of AdBACH1, which was made with the help of Lisa Clepper.
- KSHV-BAC16-WT and miRNA mutants viruses and iSLK cell lines were donated by Dr. Rolf Renne.

- This manuscript was received on 21 April 2015. Accepted on 29 April 2015. Published on 4 June 2015 in *mBio Journal*.

2.1 Abstract

KSHV infection of EC is associated with strong induction of *heme oxygenase-1* (*HO-1*), a stress-inducible host gene that encodes the rate-limiting enzyme responsible for heme catabolism. Kaposi sarcoma (KS) is an angioproliferative tumor characterized by the proliferation of KSHV-infected spindle cells, and HO-1 is highly expressed in such cells. HO-1 converts the pro-oxidant, pro-inflammatory heme molecule into metabolites with anti-oxidant, anti-inflammatory and proliferative activity. Published work has shown that KSHV-infected EC *in vitro* proliferate in response to free heme in a HO-1-dependent manner, thus implicating virus-enhanced HO-1 activity in KS tumorigenesis. The current study investigates the molecular mechanisms underlying KSHV induction of HO-1 in lymphatic EC (LEC), which are the likely spindle cell precursors. In a time course analysis of KSHV-infected cells, HO-1 expression displays biphasic kinetics characterized by an early transient induction that is followed by a more sustained upregulation co-incident with the establishment of viral latency. A KSHV mutant deleted for the viral microRNA miR-K12-11 was found to be defective for induction of HO-1 during latency. A potential mechanism for this phenotype was provided by BACH1, a cellular *HO-1* transcriptional repressor targeted by miR-K12-11. In fact, in KSHV-infected LEC, *BACH1* message is reduced, BACH1 subcellular localization is altered, and miR-K12-11 mediates the inverse regulation of *HO-1* and *BACH1* during viral latency. Interestingly, the data indicate that neither miR-K12-11 nor *de novo* KSHV gene expression are required for the burst of HO-1 expression observed at early times post-infection, which suggests that additional virion components promote this phenotype.

2.2 Importance

While the mechanisms underlying KSHV induction of HO-1 remain unknown, the cellular mechanisms that regulate HO-1 expression have been extensively investigated in the context of basal and pathophysiological states. The detoxifying action of HO-1 is critical for the protection of cells exposed to high heme levels. KS spindle cells are erythrophagocytic and contain erythrocyte ghosts. Erythrocyte degeneration leads to the localized release of heme, creating oxidative stress that may be further exacerbated by environmental or other co-factors. Our previous work showed that KSHV-infected cells proliferate in response to heme, and that this occurs in a HO-1-dependent manner. We therefore hypothesize that KSHV induction of HO-1 contributes to KS tumor development via heme metabolism and propose that HO-1 be evaluated as a therapeutic target for KS. Our current work, which aims to understand the mechanisms whereby KSHV induces HO-1, will be important for the design and implementation of such a strategy.

2.3 Introduction

Kaposi sarcoma herpesvirus (KSHV, also HHV-8), an oncogenic γ-2-herpesvirus, is the etiologic agent of the multifocal endothelial tumor known as Kaposi sarcoma (KS). KSHV infection can also result in primary effusion lymphoma (PEL), an aggressive non-Hodgkin B cell lymphoma, or multicentric Castleman disease (MCD), a systemic lymphoproliferative disorder (9,52). KSHV establishes persistent viral infection in endothelial and B cell targets by actively suppressing apoptosis, and by escaping immune detection through various immune evasion strategies (19). These survival mechanisms are thought to contribute to host cell transformation and tumor development. We previously showed that *de novo* KSHV infection of human dermal microvascular endothelial cells (DMVEC) leads to

upregulation of cellular heme oxygenase-1 (HO-1), a phenotype that is validated by the robust HO-1 expression observed in spindle cells in KS biopsies (153,234).

Two functional HO isoforms have been identified, including the stress-inducible HO-1 and the constitutive HO-2. The HO-1 enzyme catabolizes heme into carbon monoxide, ferrous iron and biliverdin. Regarding expression kinetics, HO-1 shows ubiquitous tissue distribution, and is rapidly and strongly induced in response to various cellular stresses (235,236). HO-1 is also highly expressed in several types of cancer. In the tumor setting, HO-1 is thought to contribute to cytoprotection, proliferation and angiogenesis via the conversion of pro-oxidant, cytotoxic heme into metabolites with antioxidant, pro-angiogenic, anti-apoptotic, and anti-inflammatory activity (237-240). Our previous work demonstrated that KSHV-infected DMVEC proliferate in response to low-dose heme and are protected from high-heme toxicity. We further showed that the proliferative and survival advantages of KSHV-infected EC were neutralized when HO-1 enzymatic activity was inhibited (153), suggesting an important role for the enzyme in KS pathophysiology. Despite an extensive body of literature describing the cellular regulation of HO-1 expression under both normal and pathological states (202,241,242), the mechanism(s) of HO-1 induction by KSHV remains to be defined.

MicroRNAs (miRNA) are small non-coding RNA molecules that regulate gene expression post-transcriptionally. miRNAs are encoded by both animal and plant cells as well as by the viruses that infect them (132). Within the KSHV latency-associated region (KLAR) is encoded a set of viral proteins critical for the maintenance of the viral episome and for KSHV oncogenesis (143). Also encoded within the KLAR is a set of 12 miRNAs. Among these, miR-K12-11 is known to target the mRNA encoding the *HO-1* transcriptional repressor BACH1 (147,148) . BACH1 is a transcriptional repressor of genes such as *HO-1* that participate in the NRF2-

dependent oxidative stress pathway (243). Under normal physiological conditions, NRF2 is prevented from entering the nucleus and activating transcription. However, under conditions of oxidative stress, NRF2 enters the nucleus and binds to the antioxidant response elements (ARE) found upstream of over 200 anti-oxidant and cytoprotective genes (244), thereby activating their transcription.

For a subset of these genes, BACH1 functions to counter NRF2 activation; under non-stress conditions, BACH1 binds to ARE, repressing transcription of their associated genes. Interestingly, BACH1 is a heme-binding protein, allowing it to function as a heme sensor. Thus, above a toxic heme concentration, heme binds to BACH1 and causes BACH1 to disengage from the ARE, thereby alleviating HO-1 repression and allowing heme degradation (245,246). BACH1 is then exported from the nucleus and degraded within the cytoplasm (205). Targeting of the *BACH1* mRNA by miR-K12-11 thus enables KSHV to lower BACH1 levels thereby deregulating oxidative stress pathways and facilitating infected cell survival. Notably, miR-K12-11 exhibits high homology with cellular miR-155, which is also known to regulate *BACH1*. Cellular miR-155 is observed to be overexpressed in several types of B-cell lymphoma, and its ectopic expression in mice causes B-cell malignancies (247). Because cellular miR-155 and viral miR-K12-11 contain the same seed sequence (nucleotides 2–7 of the miRNA) required for their interaction with mRNAs, the two miRNAs share many targets, including *BACH1* (147,148,155). Interestingly, miR-155 levels are not altered by KSHV infection, which suggests that miR-K12-11 functions in part by disrupting regulation of host genes that are normally controlled by miR-155 (155). Several reports have described miR-K12-11 activity and function in both ectopic expression and non-endothelial *in vitro* infection systems (147,148). Additionally, miR-K12-11 has been shown to upregulate expression of xCT, an amino acid transport protein subunit encoded by another ARE-containing gene, in

endothelial cells, thereby protecting them from oxidative stress (248). However, the potential influence of miR-K12-11 on *HO-1* during *de novo* infection of EC has yet to be investigated.

In the present study, we explore the mechanisms whereby KSHV upregulates *HO-1* in lymphatic endothelial cells (LEC) at both early times post-infection and following the establishment of viral latency. We demonstrate that miR-K12-11 is one of the viral components responsible for *HO-1* upregulation during latency, and that *HO-1* is transiently upregulated during the early phase of *de novo* infection via a mechanism that is independent of miR-K12-11 activity. We further show that miR-K12-11-targeting of the mRNA encoding the HO-1 transcriptional repressor BACH1 contributes to *HO-1* induction during latency.

2.4 Results

2.4.1 KSHV infection modulates HO-1 expression in LEC in a biphasic manner

We previously reported the upregulation of *HO-1* expression in both primary and immortalized DMVEC latently infected with wild type KSHV (153,234). Using a recently-developed KSHV bacterial artificial chromosome (BAC) system (KSHV-BAC16), we have confirmed the robust induction of HO-1 in LEC infected with BAC-derived recombinant KSHV (249). Considering both the recent recognition that lymphatic EC are the likely precursors of KS spindle cells and reports that KSHV induces lymphatic reprogramming of blood vascular EC (250), we decided to perform mechanistic studies with recombinant KSHV in lymphatic-lineage EC. We elected to use immortalized LEC (iLEC) for the majority of these studies because, like immortalized DMVEC, KSHV-infected iLEC can be maintained *in vitro* for the extended periods that are required for the establishment of viral latency. To initiate

these mechanistic studies, iLEC were infected with wild type, BAC-derived KSHV (BAC16-WT) and cultured for 6 days to allow for establishment of latency. Cells were fixed, immuno-stained for both the viral latency protein LANA-1 (LANA) and HO-1, and then evaluated using deconvolution microscopy (Figure 2.1A). Control cells expressed low basal levels of HO-1, with sporadic cells expressing slightly higher amounts. In contrast, infected cells, which were identified by LANA and GFP positivity, consistently expressed significantly higher levels of HO-1. In both mock and infected cells, HO-1 was predominantly localized to the cytoplasm, reflecting its well-characterized ER localization. Importantly, this pattern was also observed in mock and KSHV-infected primary LEC (Figure 2.2A). To determine the kinetics of HO-1 expression in infected iLEC, we performed a time-course experiment measuring HO-1 mRNA (Figure 2.1B) and protein (Figure 2.1C) levels at sequential times post-infection. Using reverse transcription quantitative PCR (qPCR), we observed induction of *HO-1* mRNA as early as 4 hours post-infection (hpi). This early burst of expression was followed by a decline to basal levels by 24 hpi. Subsequently, coincident with the establishment of latency, HO-1 was re-induced, reaching a sustained phase of expression by 3 days post-infection (dpi) that persisted with time (Figure 2.1B). HO-1 protein levels followed similar bi-phasic kinetics, with an early peak of expression at 6-8 hpi and sustained expression during latency (3-21 dpi). Parallel-extended time course experiments using uninfected cells confirmed that long-term culture of iLEC had no impact on *HO-1* expression (Figure 2.2B). Thus, data from these experiments confirm that, similar to what we have previously described in both primary and transformed DMVEC (153), HO-1 is induced during KSHV latency. In addition, we now show that KSHV also alters HO-1 expression during the initial stages of *de novo* infection.

Our observation that the initial peak of HO-1 expression occurs within 4 hours of virus exposure suggests that early HO-1 induction is independent of viral gene expression. Instead, HO-1 expression is likely to be triggered by component(s) of the virus particle. To test this hypothesis, a time course experiment was performed in which iLEC were infected with either live or UV-inactivated BAC-derived KSHV. Samples were harvested at early times post-infection and then tested for both HO-1 mRNA (Figure 2.1D) and protein levels (Figure 2.1E). The efficacy of UV-inactivation was confirmed by our inability to detect both latent (LANA) and lytic (ORF59) viral transcripts from cells infected with UV-treated viral preparations (Figure 2.3A). This finding was further corroborated by the lack of KSHV gene expression and the absence of HO-1 induction by UV-inactivated KSHV at later times post-infection (Figure 2.3B). Interestingly, at early times post-infection (0-24 hours), both live and UV-inactivated KSHV induced HO-1 to equivalent levels and with similar kinetics, indicating that *de novo* expression of viral genes is not required for the early peak of HO-1 expression. These experiments suggest that one or more components of the viral particle itself are responsible for the early transient expression of HO-1.

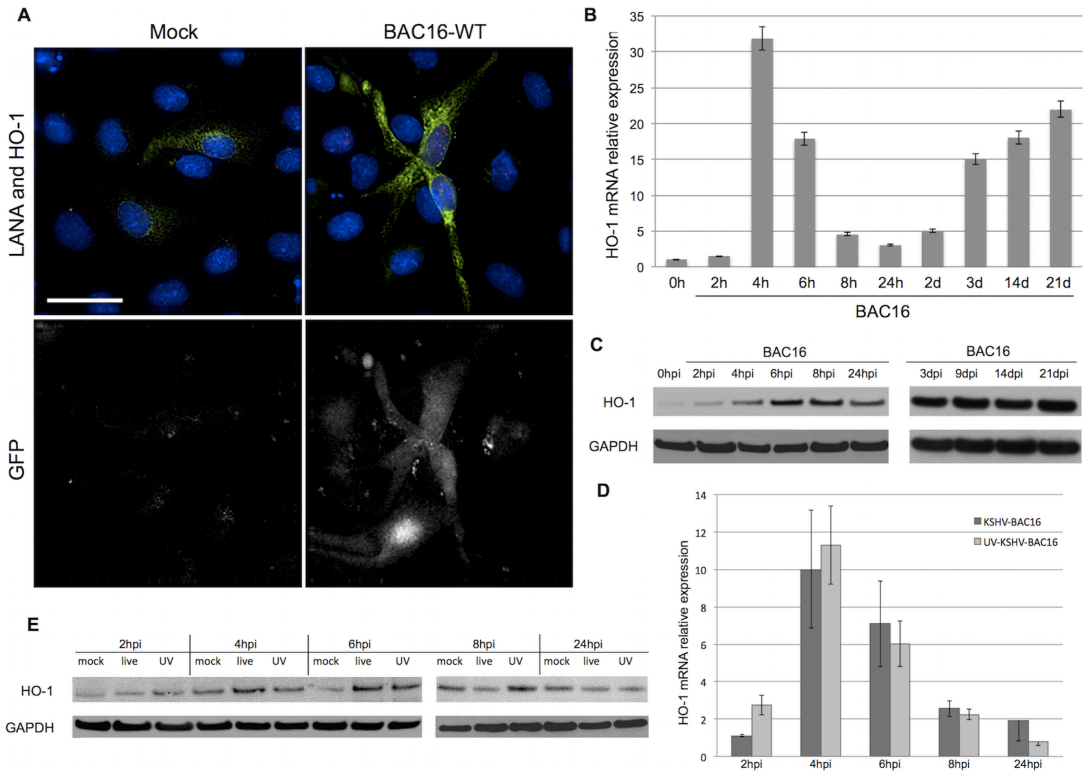

Figure 2.1. KSHV infection induces a biphasic induction of HO-1 in LEC. **A**. IFA of mock and KSHV-infected iLEC 6 dpi. Top panels: LANA (red), HO-1 (green), and DAPI (blue). Bottom panels: GFP (greyscale, same cells as shown in top panels). Left panels correspond to mock-infected cells, and the right panels correspond to KSHV-infected cells. Images were captured at 60X magnification (scale bar = 30μm). **B.** qPCR showing mRNA levels for HO-1 in KSHV infected iLEC at various times post-infection. Message levels are normalized to GAPDH, and fold change is calculated relative to mock samples at each timepoint (n=3). **C.** A western blot showing HO-1 protein levels in KSHV infected iLEC at various times post-infection. GAPDH was used as loading control. **D.** qPCR for *HO-1* mRNA levels in iLEC infected with either live or UV-inactivated KSHV. Cells were collected for analysis at the indicated times post-infection (n=3). **E**. A western blot showing HO-1 protein levels in iLEC infected with either live or UV-inactivated KSHV. Cells were collected at the indicated times post-infection. GAPDH was used as loading control.

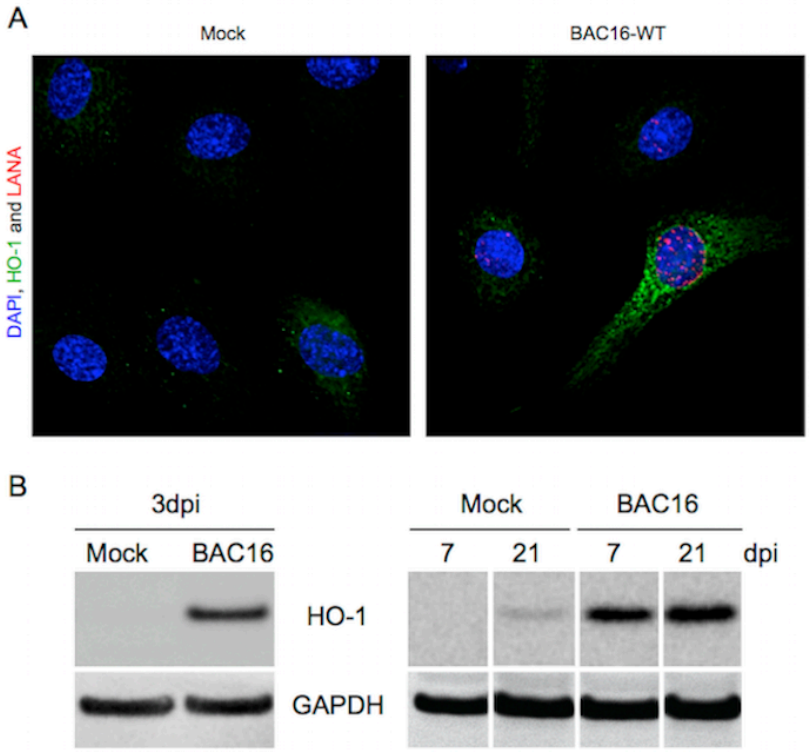

Figure 2.2: A. IFA showing HO-1 expression in KSHV-infected primary LEC (pLEC) at 6dpi. Mock-infected pLEC are shown in the left panel; KSHV-infected pLEC infected are shown in the right panel. HO-1 expression is shown in green, KSHV LANA in red and DAPI nuclear stain in blue. **B.** Western blot showing HO-1 levels in a time course of infection after the establishment of stable latency. Mock and KSHV-infected cells cultured for 3dpi, and for extended times (7dpi and 21dpi) are shown.

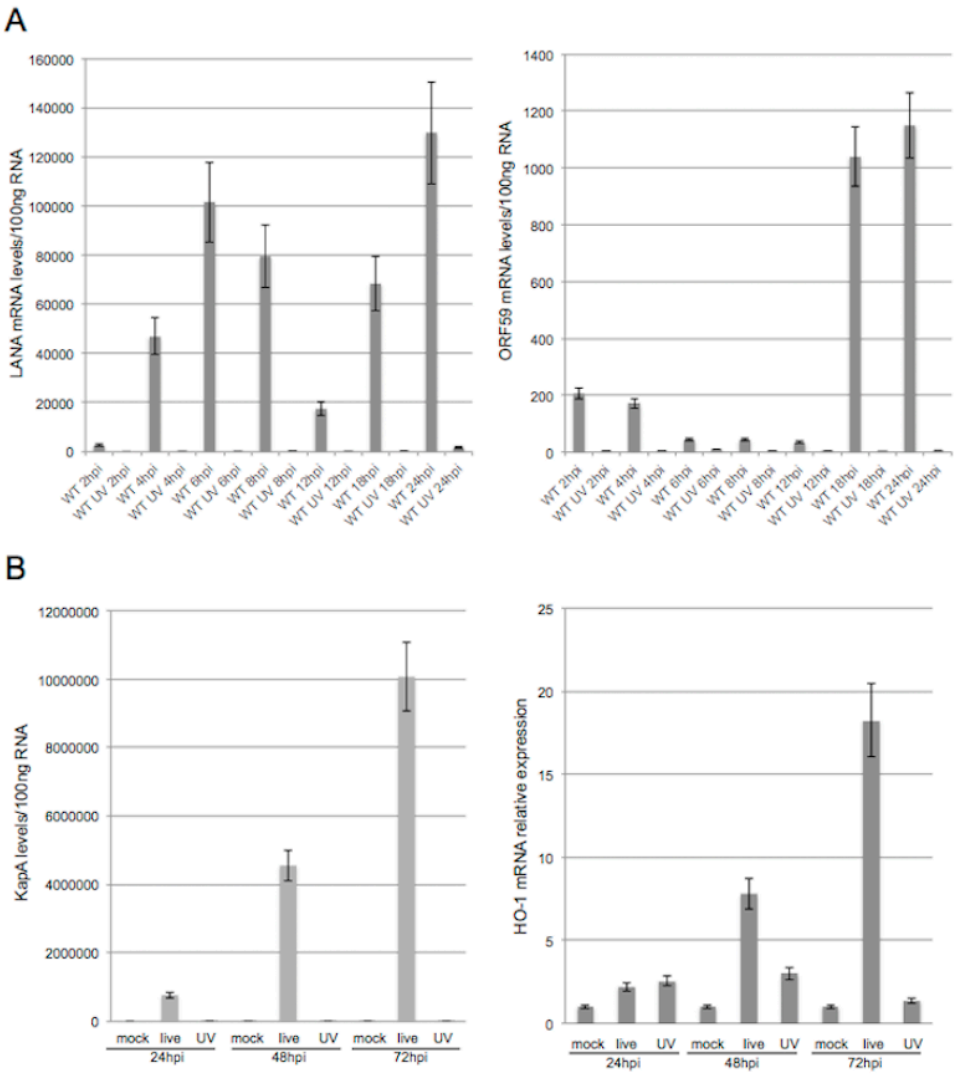

Figure 2.3 : Demonstration of the efficacy of UV inactivation of KSHV. **A.** pPCR for both latent and lytic viral transcripts (LANA and ORF59, respectively) in iLEC infected with live or UV-inactivated virus at the indicated times post-infection. **B.** Detection of the viral *KapA* message by qPCR in iLEC infected with live or UV-inactivated virus at the indicated times post-infection. *HO-1* mRNA levels iLEC infected with either live or UV-infected virus at the indicated times post-infection. *HO-1* levels are normalized to *GAPDH*.

2.4.2 KSHV miR-K12-11 contributes to HO-1 induction during latent infection of LEC

It was recently reported that exogenous expression of KSHV-encoded miR-K12-11 was sufficient to induce HO-1 protein expression in 293 cells, and that BACH1 levels were concomitantly reduced (251). In order to determine if miR-K12-11 influenced HO-1 levels in the context of *de novo* KSHV infection of LEC, we made use of a BAC16-derived KSHV mutant that no longer expressed a functional miR-K12-11 (generously provided by Dr. Rolf Renne, University of Florida, Gainesville, FL). This mutant was generated by deleting one arm of the pre-miRNA, which prevents maturation to the active miRNA (252). For these experiments, iLEC were infected with WT or mutant viruses lacking either miRNA-K12-11 or miRNA-K12-1 (included as a control mutant virus; also provided by Dr. Renne), and then cultured for 6 days to allow for establishment of stable latency. Proper expression of miR-K12-11 in WT-infected cells was confirmed by stem-loop qPCR (Table 2.1). Compared to iLEC infected with either WT or the control mutant (ΔK12-1), we observed significantly lower levels of HO-1 mRNA and protein (Figures 2.4A and 2.4B) in iLEC infected with the ΔK12-11 mutant. Although HO-1 expression in ΔK12-11-infected cells was substantially reduced, some induction above basal levels in mock-infected cells was observed, indicating that KSHV induction of HO-1 during latency is not exclusively regulated by miR-K12-11. Flow cytometric analysis (Figure 2.4C) of KSHV-infected (GFP-positive) iLEC confirmed the reduced HO-1 levels in cells infected with the ΔK12-11 mutant. Similarly, IFA (Figure 2.4D) demonstrated a clear decrease in cytoplasmic HO-1 expression in ΔK12-11-infected cells. In summary, these experiments support a key role for miR-K12-11 in HO-1 induction during latent KSHV infection of LEC. At the same time, our data show that additional viral and/or cellular

factors contribute to maximal HO-1 expression in latently-infected cells. Since miR-K12-11 is a viral ortholog of miR-155, we also considered the possibility that KSHV infection could influence expression of miR-155 in LEC. In keeping with a published study in B cells however (155), expression of miR-155 in LEC was unaffected by KSHV infection (Figure 2.5).

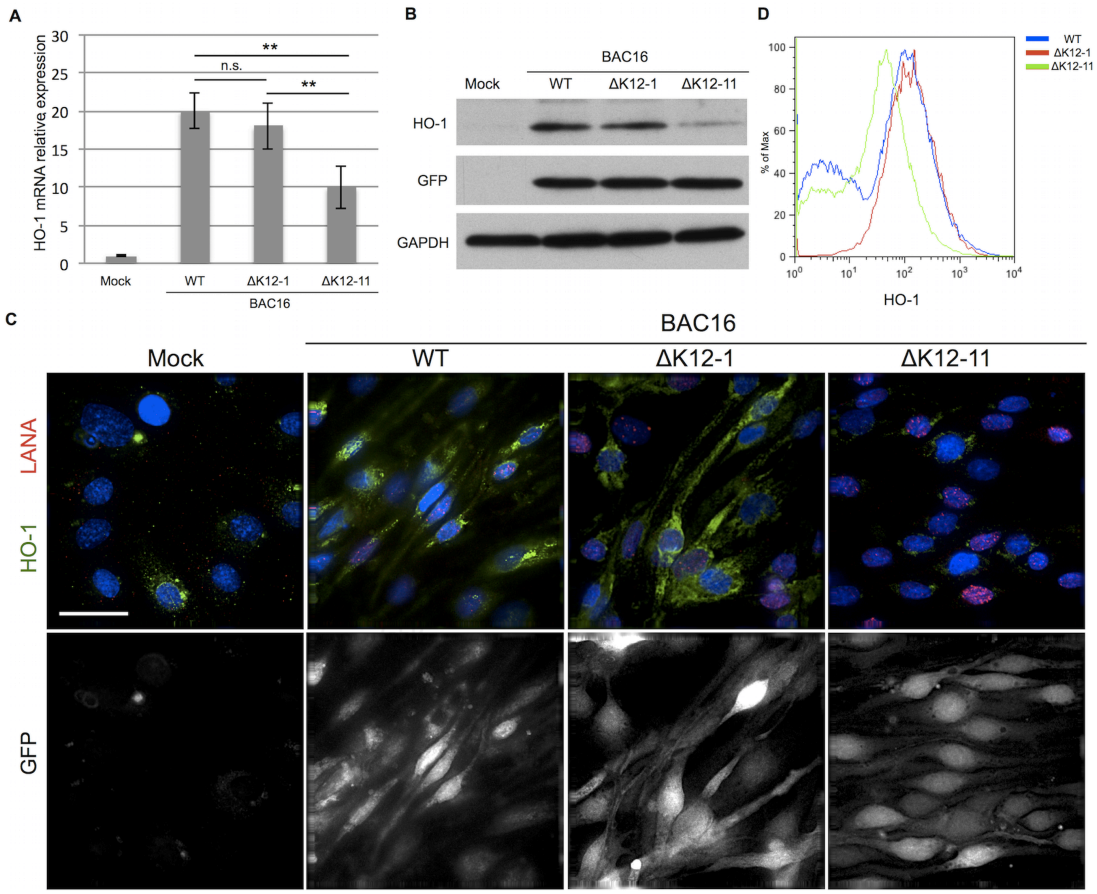

Figure 2.4. The KSHV-ΔK12-11 mutant induces reduced levels of HO-1 in latently infected LEC. Time course experiments showing HO-1 protein and mRNA levels at 6 dpi in iLEC infected with either KSHV WT, ΔK12-11 mutant, or ΔK12-1 mutant (as control) viruses (n=3). **A.** qPCR results. n.s.= not significant, ** = p-value ≤ 0.01. A one-way ANOVA test was used for statistical analysis. **B.** Western blot analysis. GAPDH was used as a loading control. **C.** IFA images. Top panels: HO-1 (green), LANA (red), DAPI (blue). Bottom panels: GFP in greyscale (same cells as shown in top panels). Images were captured at 60X magnification (scale bar= 30μm). **D.** Flow cytometric analysis of infected cells gated on GFP.

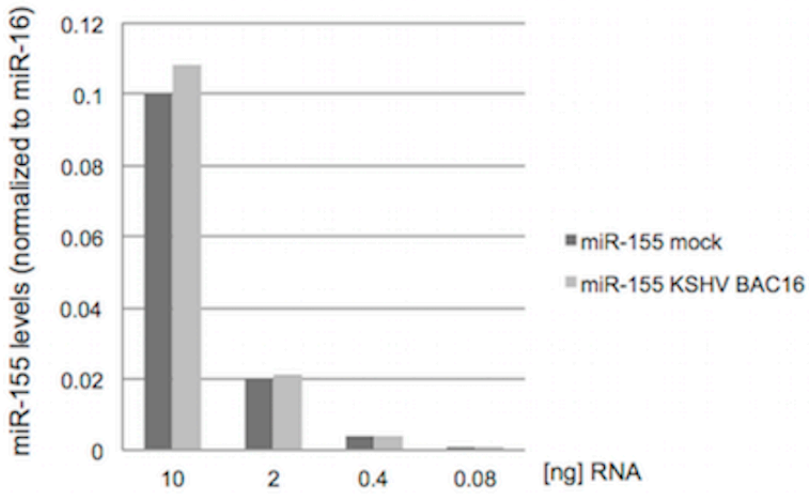

Figure 2.5: miR-155 is not perturbed in KSHV-infected iLEC. Stem-loop qPCR for mir-155 in mock (dark grey) and WT infected iLEC (light grey) at 6dpi.

Samples	miR-K12-11 levels normalized to miR-16
Mock- infected iLEC	N.D.
BAC16-WT infected iLEC	0.584±2.45x10^-3
BAC16-ΔK12-11- infected iLEC	N.D.

Table 2.1: Stem-Loop qPCR for miR-K12-11 levels in infected iLEC 6dpi. iLEC were infected with either WT or ΔK12-11 viruses and then incubated for 6 days, at which time cells were harvested and RNA was isolated. Data are normalized to levels of cellular miR-16. miRNA levels are expressed as the mean ± SEM (n=3). N.D.: not detectable levels.

2.4.3 Exogenous miR-K12-11 restores HO-1 expression in KSHV-ΔK12-11 infected LEC

To provide further support for the hypothesis that miR-K12-11 plays a role in HO-1 induction during latent KSHV infection of LEC, a miR-K12-11 mimic was tested for its ability to complement the HO-1 induction defect observed for the ΔK12-11 mutant virus. This was accomplished by infecting iLEC with either WT or ΔK12-11 viruses for 6 days, transfecting the cells with 100ng of either a negative control miRNA or a miR-K12-11 mimic, and then testing for levels of both HO-1 and miR-K12-11 at 24hpi. Confirming the results shown in Figure 2.2, in cells infected with the ΔK12-11 mutant and then transfected with the control miRNA, levels of HO-1 message (Figure 2.6A) and protein (Figure 2.6B) were 3-4 fold lower than those in similarly transfected cells infected with the WT virus. Conversely, in the presence of the miR-K12-11 mimic, HO-1 levels in ΔK12-11-infected cells were restored to levels approaching those seen in cells infected with WT virus. Transfection of mock-infected cells with the miR-K12-11 mimic was sufficient to induce HO-1 message and protein (Figure 2.6A and 2.6B), which demonstrates that the KSHV miRNA alone is able to induce HO-1 expression. Results from stem loop qPCR (Figure 2.6C) confirmed that the expression levels of miR-K12-11 in transfected cells were comparable to those in cells infected with WT virus.

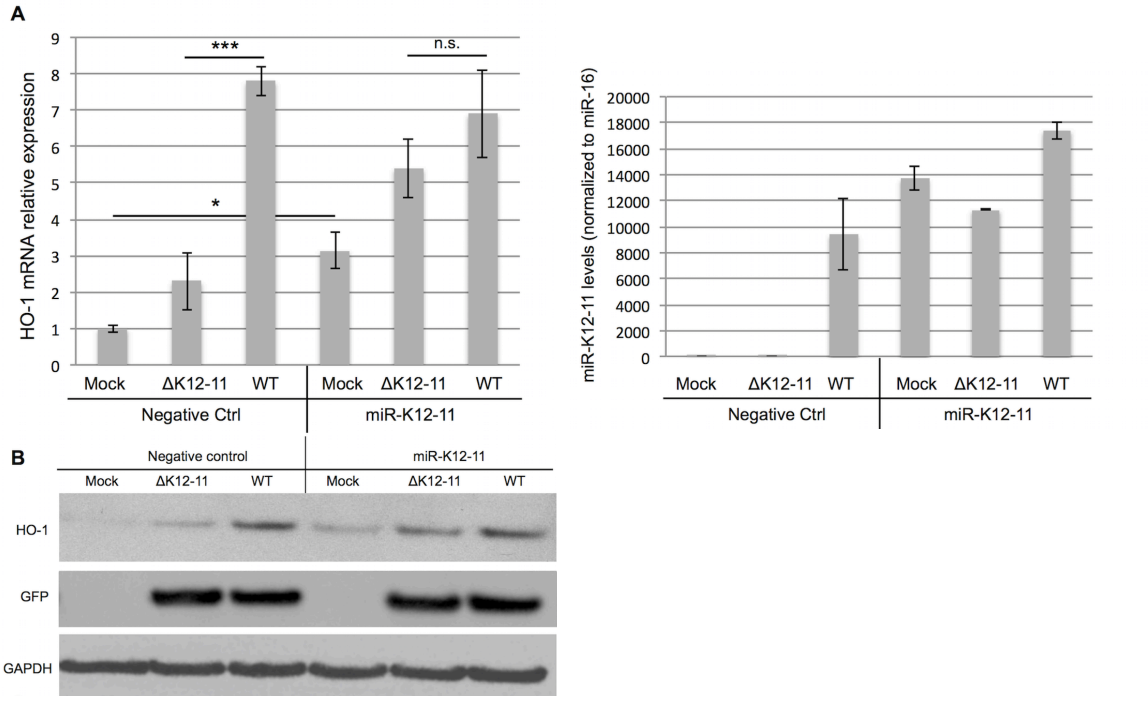

Figure 2.6. Exogenous expression of miR-K12-11 partially restores HO-1 induction in ΔK12-11-infected LEC.

iLEC were sequentially infected with KSHV WT or ΔK12-11 viruses for 6 days, transfected with a miR-K12-11 mimic, and then incubated for another 24 hours. Samples were then harvested and prepared for various HO-1 assays. **A**. qPCR analysis. For each sample, the data is normalized to *GAPDH*, and then fold change is determined relative to the mock sample (n=3). n.s.= not significant; ***=p-value≤0.0001, *= p-value≤0.05. A one-way ANOVA test was used for statistical analysis. **B.** Western blot showing HO-1 protein levels. GAPDH was used as a loading control. **C.** Demonstration of miR-K12-11 levels as determined by stem-loop qPCR. miR-K12-11 levels are normalized to expression of the internal control miR-16 (n=3).

2.4.4 The HO-1 transcriptional repressor BACH1 is downregulated and redistributed in KSHV-infected LEC.

As discussed above, the function of BACH1 is influenced both by its abundance and its sub-cellular localization. It has been previously shown that BACH1 protein levels are low in the stably KSHV-infected PEL cell line BCBL-1, and that miR-K12-11 plays a role in this phenotype (253). However, since BACH1 levels have not been examined in the context of a *de novo* KSHV infection in endothelial cells, we investigated BACH1 expression in LEC at 6 days post-infection with either WT or ∆K12-11 mutant viruses. While WT-infected iLEC expressed significantly less BACH1 mRNA (Figure 2.7A) and protein (Figure 2.7B) than mock-infected cells, BACH1 levels were not significantly reduced in cells infected with the ∆K12-11 mutant. Interestingly, IFA revealed that in KSHV-infected cells BACH1 was consistently redistributed to the cytoplasm, and that this redistribution occurred even in the absence of miR-K12-11 (Figure 2.7C). Thus, our data indicate that *de novo* KSHV infection of LEC results in a decrease of total BACH1 protein, dependent on miR-K12-11, and in its redistribution to the cytoplasm, which appears to be miR-K12-11 independent. The identity of the other viral and/or cellular components that are responsible for BACH1 relocalization is currently under investigation.

To further examine the contribution that BACH1 makes towards the downregulation of HO-1 in the context of KSHV infection, we next asked if ectopic BACH1 expression could overcome KSHV-induced HO-1 induction in infected iLEC. For these studies, we expressed BACH1 from the adenoviral vector pAdTET7 (254). Expression of BACH1 from the adenoviral vector AdBACH1 was verified by IFA of transduced iLEC (Figure 2.8). In subsequent studies, latently infected iLEC were transduced with AdBACH1 or with the transactivator only (Trans, as control), and

then HO-1 levels were examined 1 day later. In cells not infected with KSHV, adenoviral expression of BACH1 reduced basal HO-1 protein levels below the limit of detection (Figure 2.7E), while mRNA levels could not be further reduced below the existing detection threshold (Figure 2.7D). In KSHV-infected cells, the high levels of HO-1 message and protein that we typically observe were significantly reduced by BACH1 overexpression. Thus, our data shows that ectopic expression of BACH1 can effectively overcome KSHV-dependent HO-1 induction.

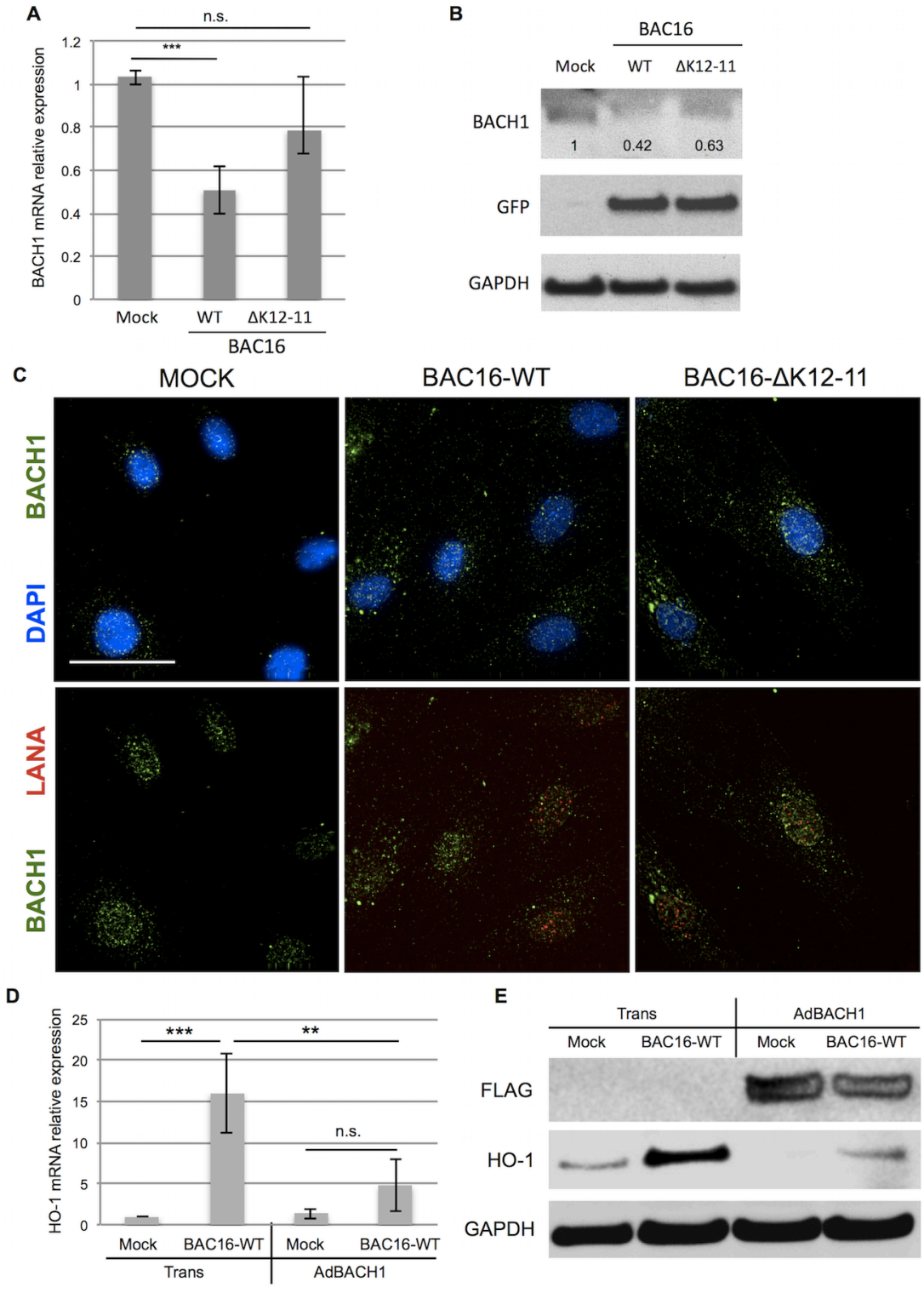
A
n.s.
***
BACH1 mRNA relative expression
1.2
1
0.8
0.6
0.4
0.2
0
Mock
WT
ΔK12-11
BAC16
B
BAC16
Mock
WT
ΔK12-11
BACH1
1
0.42
0.63
GFP
GAPDH
C
MOCK
BAC16-WT
BAC16-ΔK12-11
BACH1
DAPI
LANA
BACH1
D
HO-1 mRNA relative expression
25
20
15
10
5
0
***
**
n.s.
Mock
BAC16-WT
Mock
BAC16-WT
Trans
AdBACH1
E
Trans
AdBACH1
Mock
BAC16-WT
Mock
BAC16-WT
FLAG
HO-1
GAPDH

Figure 2.7. BACH1 levels and sub-cellular location are altered in KSHV infected LEC.

A-C. iLEC were infected with either mock, WT or ΔK12-11 viruses, samples were harvested at 6 dpi, and then BACH1 levels were determined. **A**. qPCR analysis. The raw data for each sample was first normalized to *GAPDH*. The normalized data was then compared to the mock sample in order to determine fold change (n=6). n.s.= not significant; *= p-value ≤ 0.05. Significance was determined using a Kruskal-Wallis test. **B.** BACH1 western blot. GFP expressed by the virus is used as marker of infection; GAPDH is used as a loading control. **C**. IFA images. Top row: DAPI (blue), BACH1 (green); Bottom row: BACH1 (green) and LANA (red). Labels at the top of each panel correspond to the virus used. Images were recorded at 60X magnification; scale bar = 30μm. **D-E.** iLEC were first infected with WT virus for 6 days and then transduced with either Trans (control) or both Trans and AdBACH1. Cells were harvested after a further 24hr incubation, and samples were prepared for either qPCR or WB (n=3). **D**. qPCR analysis of *HO-1* levels. n.s.= not significant; ***= p-value ≤ 0.001; **= p-value≤0.01. Significance was assessed using a One-way ANOVA test. **E.** WB showing exogenous BACH1 (FLAG) and endogenous HO-1 protein levels. GAPDH is used as a loading control.

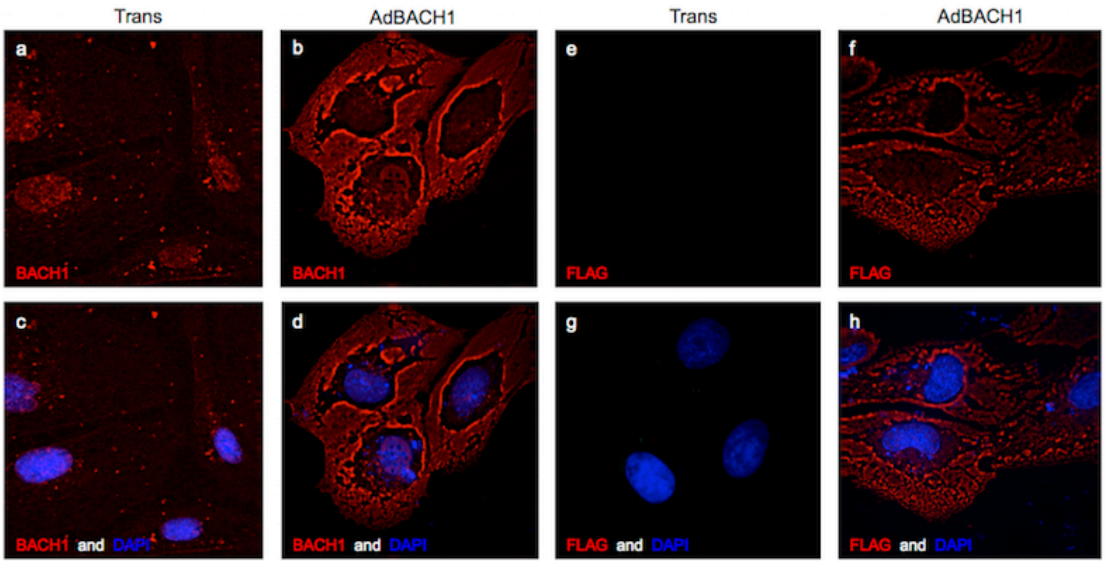

Figure 2.8: IFA analysis of exogenous BACH1 expression in iLEC. iLEC were transduced with Trans only (control) or both Trans and AdBACH1 and then incubated for 24 hrs. Panels A-D: Total (endogenous and exogenous) BACH1 levels (red) were detected using an anti-BACH1 antibody. Bottom panels C and D show the DAPI (nuclei) BACH1 overlay staining. Panels E-H: Exogenous BACH1::FLAG levels (red), were detected using an anti-FLAG antibody. Panels G and H show the DAPI and FLAG overlay.

2.4.5 KSHV induces HO-1 in LEC at early times post infection in a miRNA-independent manner

Figure 2.1 shows that that as early as 4hpi, KSHV transiently induces HO-1, and that this induction does not depend upon *de novo* viral gene expression. A previous study has shown that KSHV miRNAs, including miR-K12-11, can be detected in viral particles, and that these miRNAs remain active even after UV-inactivation (255). In light of this finding, we asked if miR-K12-11 could be delivered to host cells within the virus particle, thereby inducing the early peak of HO-1 expression. We first examined purified virus preparations for their miRNA content, and we found that a standard, purified WT virus preparation (100 μl) contained detectable levels of miR-K12-11, as well as other representative miRNAs and messenger RNAs (Table 2.2). As expected, miR-K12-11 was not detected in the ΔK12-11 virus preparation, but we did observe measurable levels of other miRNAs and mRNAs therein. Using samples collected at multiple intervals over the first 24 hrs post-infection, we used stem-loop qPCR to measure miRNA levels in iLEC infected with live or UV-inactivated WT (Figure 2.9A). Interestingly, despite the capacity of UV-inactivated virus to induce early transient HO-1 (Figure 2.1 D-E), no miR-K12-11 was detected in cells infected with UV-inactivated virus; cells infected with live virus showed appreciable levels of the miRNA only by 12hpi, presumably as a consequence of *de novo* transcription. Thus, considering the low volume of inoculum used for KSHV infection (less than 1 μl of the stock preparation) and the inability to detect any miR-K12-11 prior to 12 hpi, our data suggests that miR-K12-11 is not responsible for the early HO-1 induction. In order to confirm this conclusion, iLEC were infected with WT, ΔK12-11 or ΔK12-1 mutant viruses, and HO-1 levels were determined at early times post-infection (Figures 2.9B and 2.9C). As expected,

we were unable to detect miR-K12-11 in ΔK12-11-infected iLEC (Figure 2.10). HO-1 levels in ΔK12-11-infected iLEC were however comparable to those in cells infected with WT and ΔK12-1 viruses, confirming that this miRNA does not play a role in the early transient induction of HO-1 in KSHV-infected cells. Given the role of BACH1 in negative regulation of HO-1 (Figure 2.7), we also considered that BACH1 could influence early HO-1 expression independent of miR-K12-11 action. Thus, we examined expression of BACH1 in KSHV-infected LEC over the first 8 hours of infection (Figure 2.11). BACH1 expression was unaffected during this time, indicating that early induction of HO-1 is not as a consequence of BACH1 downregulation.

			miRNA/mRNA levels/100µl virus preparation
Virus	**ORF59**	**mir-155**	**miR-k12-11**
BAC16-WT	6.72x10^8±4.70x10^3	4.75x10^5±3.32x10^2	2.32x10^4±1.6x10^1
BAC16-ΔK12-11	5.22x10^8±5.18x10^2	3.89x10^5±1.89x10^2	N.D.

Table 2.2: Detection of *ORF59* mRNA, mir-155, and miR-K12-11 in KSHV viral particles. qPCR was performed on RNA extracted from 100µl of purified WT or ΔK12-11 viruses. miRNA levels are normalized to spiked in control. Data are expressed as the mean ± SEM (n=2). N.D.: not detectable levels.

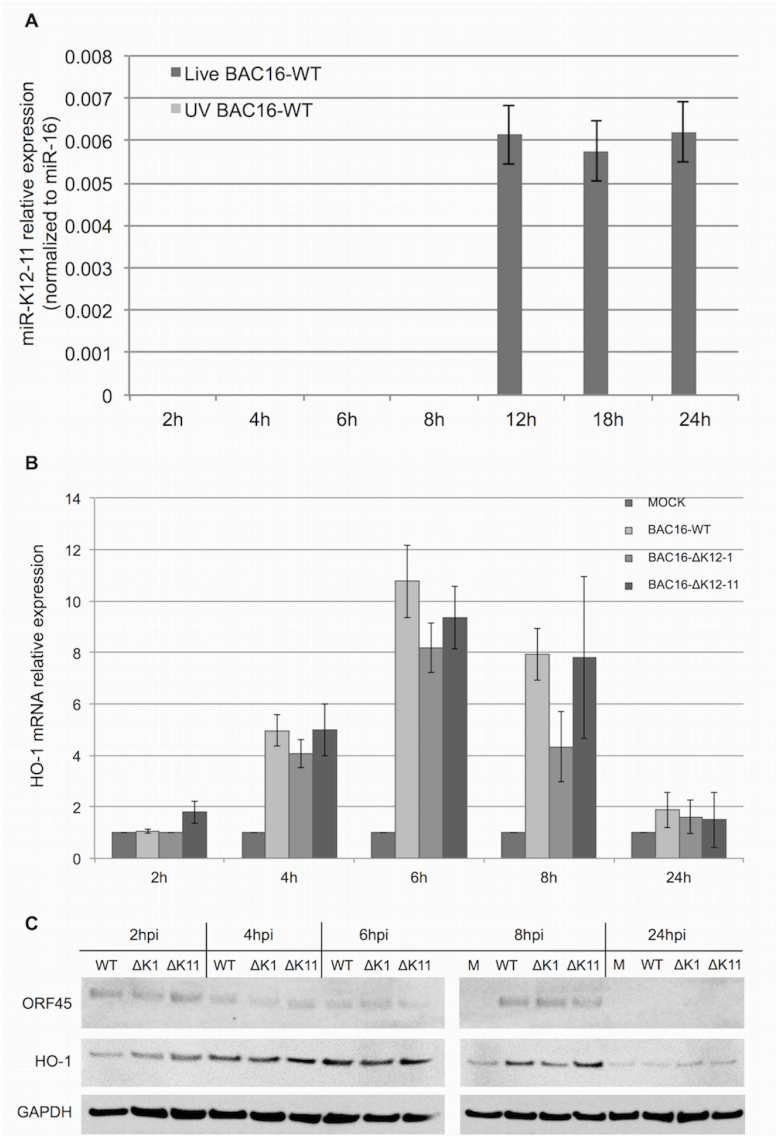

Figure 2.9. KSHV miR-K12-11 is not responsible for the early peak of HO-1 induction.

A-C. Time course experiments in which iLEC were infected with KSHV and then harvested at the indicated times thereafter. **A.** Stem-loop qPCR for miR-K12-11 in cells infected with either live or UV-inactivated virus. miR-K12-11 expression is normalized to levels of the cellular internal control miR-16 (n=3). **B.** qPCR showing HO-1 mRNA levels (n=3) in cells infected with either KSHV WT, ΔK12-11 mutant, or ΔK12-1 mutant (as control) viruses. **C.** Western blot showing HO-1 protein levels in cells infected with either WT, ΔK12-11 (ΔK11), or ΔK12-1 (ΔK1) (control) viruses. The KSHV-encoded ORF45 protein was used as marker of infection; GAPDH serves as a loading control.

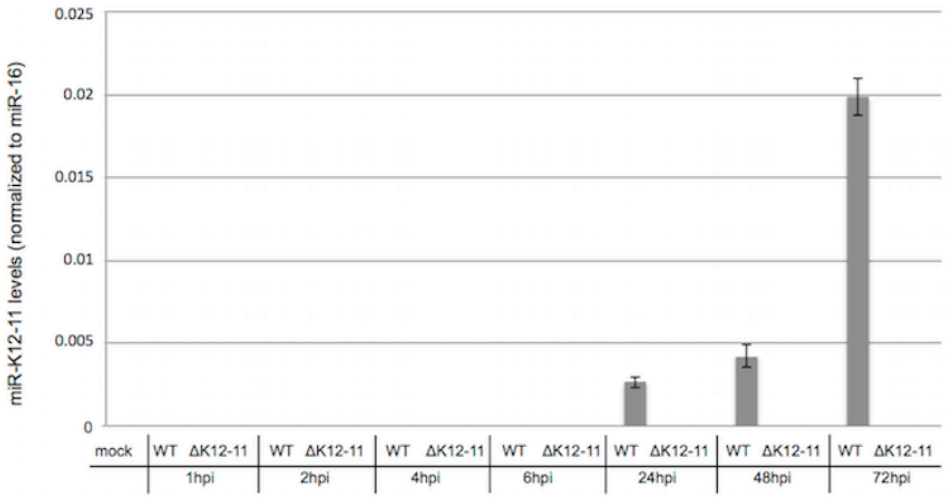

Figure 2.10: Stem-loop qPCR detection of miR-K12-11 in KSHV-infected iLEC. iLEC were infected with either KSHV WT or the ΔK12-11 mutant, and then the cells were harvested at the indicated times post-infection. The data are normalized to the cellular control miR-16.

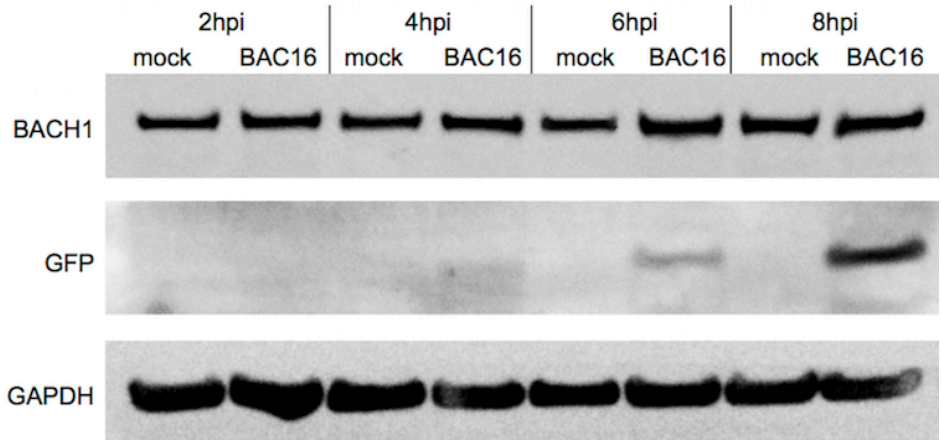

Figure 2.11: BACH1 protein levels do not significantly change within the first 8hrs post KSHV infection. WB showing BACH1 expression KSHV-infected iLEC at the indicated times post-infection. GFP (expressed by the virus) is used as marker of infection.

2.5 Discussion

In the current study we confirmed HO-1 upregulation in lymphatic EC (LEC) infected with a BAC-derived KSHV. Under basal conditions, HO-1 expression is tightly regulated by the transcriptional repressor BACH1 (205). BACH1 mRNA is downregulated by KSHV through the action of the viral miRNA miR-K12-11, which targets the BACH1 3'-UTR (147,148). It was recently shown that exogenous expression of miR-K12-11 in 293 cells is sufficient both for the induction of HO-1 and the concurrent downregulation of BACH1, suggesting an inverse correlation between the regulation of these two proteins (251). Our current study is the first to demonstrate that miR-K12-11 also targets BACH1 during *de novo* infection of LEC, with a concomitant increase in HO-1. Importantly however, HO-1 levels in LEC infected with KSHV lacking miR-K12-11 (ΔK12-11) are not restored to those in mock-infected cells, indicating that the viral miRNA is not the sole element responsible for modulation of this antioxidant pathway. It is not uncommon for viruses to adopt more than one mechanism to regulate key cellular proteins and pathways. Therefore, it is likely that other viral and/or cellular components modulate the expression of BACH1 and/or other HO-1 regulators, such as the transcriptional activator NRF2 (256). NRF2 (a.k.a. NFE2L2) is a member of the basic region-leucine zipper (bZip) protein family and, as described above, plays a critical role in the induction of oxidative stress responsive genes such as HO-1 (204). Consequently, it is plausible that KSHV has developed the ability to modulate HO-1 expression by regulating both BACH1 and NRF2. A recent report suggests that the KSHV latency protein vFLIP, by virtue of its ability to induce NRF2 during latent infection of dermal microvascular EC (HMVEC-d) (257) could provide yet another means whereby KSHV modulates HO-1 expression.

Another intriguing result is our finding that the subcellular localization of

BACH1 is altered by KSHV infection of LEC, with a percentage of the predominantly nuclear protein being redistributed to the cytoplasm; as previously stated, BACH1 functions as a HO-1 transcriptional repressor when bound to the *HO-1* promoter in the nucleus. Accordingly, KSHV could also impair BACH1-mediated repression of ARE-containing genes such as HO-1 by preventing its translocation to the nucleus or inducing its nuclear export. Further investigation will be needed to evaluate how KSHV mediates the relocalization of BACH1 and to identify the viral and/or host factors involved.

While investigating the expression kinetics of HO-1 in *de novo* infected LEC, we discovered that HO-1 is also rapidly and transiently upregulated at early times post infection (6-8 hpi). This early induction was not dependent on *de novo* expression of viral genes, since UV-inactivated virus induced similar levels of HO-1. This suggests that one or more virion components might be responsible for the transient upregulation. A recent paper demonstrated the presence of biologically functional viral miRNAs in KSHV virions (255). Thus, we investigated whether miR-K12-11 was also responsible for the early induction of HO-1. Despite detecting miR-K12-11 in stock virus preparations, our data indicate that this viral miRNA is not responsible for the early induction of HO-1. Consequently, we predict that other virion component(s) are responsible for the early induction of HO-1. Since cellular pathways regulated by early *de novo* KSHV infection are thought to participate in orchestrating an effective viral infection (83), it is reasonable to speculate that early induction of HO-1 by KSHV could protect the cell from virus-induced oxidative stress and contribute to a cellular environment permissive for successful infection. The recent finding that NRF2 induction in KSHV-infected HMVEC-d is regulated by early *de novo* infection events, including virus binding and early signaling (257), suggests that KSHV induction of NRF2 contributes to the early peak of HO-1 seen in KSHV-

infected LEC. The long-term goal of our studies is to develop a novel therapy for KS. Due to the selective pressure on the virus that can lead to mutations within its genome, drug resistance is a recurrent problem when targeting viral genes (258,259). Therefore, a more attractive strategy involves the identification of cellular genes that are uniquely expressed or overexpressed during the development of the pathology. HO-1 may represent such a target for the treatment of KS: HO-1 is selectively upregulated in KS spindle cells (153), KS lesions are characterized by high free heme and hemoglobin as a result of erythrocyte extravasation and degradation (54,260,261), and HO-1 induction affords survival and proliferation advantages to infected cells within the unique tumor microenvironment that would otherwise be hostile to normal cells. For these reasons, and because HO-1 targeting has been successful for treatment of other types of cancer, we propose that a similar approach should be considered for the treatment of KS.

2.6 Materials And Methods

Cells and viruses

Primary adult human LEC were obtained from Lonza (Allendale NJ). Immortalized LEC (iLEC) were generated from these cells via transduction with a retrovirus expressing papilloma virus E6/E7, as previously described (103). LEC were cultured in EGM-2 medium prepared by supplementing basal medium (EBM-2; Lonza) with 10% FBS, penicillin/streptomycin/L-glutamine (PSG, Hyclone, Logan, UT) and additional EC growth supplements (EGM-2MV Bullet Kit; Lonza). HEK293T cells were grown in DMEM supplemented with 10% FBS and PSG. Epithelial iSLK cell lines (generously provided by Dr. Rolf Renne at the University of Florida, Gainesville, FL with kind permission from Dr. Jae Jung at the University of Southern California, Los Angeles, CA and Dr. Don Ganem at the University of California, San Francisco,

CA) were used to produce stocks of recombinant KSHV (249,252,262). iSLK were grown in DMEM supplemented with 10% FBS, PSG, puromycin (1 μg/ml), neomycin (200 μg/ml) and hygromycin (1.5 mg/ml). The KSHV bacterial artificial chromosome clone BAC16 was kindly provided by Dr. Jae Jung (249). KSHV-BAC16 was derived from recombinant rKSHV.219, which expresses GFP under the control of the human EF1α promoter (263). The independent regulation of GFP and viral gene expression in this virus leads to occasional cells that express discordant levels of KSHV and LANA (264,265). To produce stocks of recombinant KSHV, iSLK cells harboring BAC16 were treated with doxycycline (1 μM) and sodium butyrate (3 mM) for 72 hours. Supernatants were then collected, and cell debris was removed via low-speed centrifugation. Clarified supernatants were then transferred to ultracentrifuge tubes, underlaid with 25% sucrose in TNE (150 mM NaCl, 10 mM Tris pH8.0, 2 mM EDTA pH 8.0) and centrifuged at 78,000 x *g* for 2 hours at 4°C. The resulting virion pellets were resuspended in TNE. Stocks of BAC16-derived KSHV were titrated by infecting iLEC with serially diluted virus preparations. After a 48hr incubation, the cells were harvested and evaluated for GFP expression via flow cytometry. For latent infection experiments, MOI (multiplicity of infection) were normalized to the volume of viral supernatant required for 20% GFP+ iLEC. For acute infection experiments, MOI's corresponding to 80% GFP+ iLEC were used, and centrifugation was omitted in order to prevent mechanical stress-induced HO-1 upregulation.

Antibodies and other reagents

HO-1 protein levels were assessed using a mouse anti-HO-1 mAb (BD Transduction Laboratories, Franklin Lakes, NJ) at a concentration of 1:1000 for WB and 1:200 for IFA and flow cytometry. An Anti-GFP (Goat) horseradish peroxidase (HRP)-

conjugated antibody (Rockland-600-103-215, Limerick PA) was used at 1:2000 in order to detect GFP. Mouse anti-BACH1 (F-9) antibody (sc-271211; Santa Cruz Biotechnologies, Santa Cruz, CA) was used at either 1:200 (WB), or 1:100 (IFA). GAPDH levels were used as WB loading controls and were detected with a mouse anti-GAPDH antibody (ab8245; AbCam, Cambridge, England) at a concentration of 1:20,000. Mouse anti-ORF45 antibody (ab36618; AbCam) was used at 1:500 (WB). A rabbit anti-LANA antibody (UK183), kindly provided by Dr Bala Chandran (Rosalind Franklin University, Chicago, IL) was used at 1:100 for IFA. For FLAG epitope detection, a monoclonal anti-FLAG M2 HRP-conjugated antibody (Sigma, St. Louis, MO) was used at 1:5000. For WB, donkey anti-rabbit (sc-2313; Santa Cruz Biotechnologies) or goat-anti mouse (GAM-HRP Millipore, Billerica, MA) HRP-conjugated secondary antibodies were each used at a concentration of 1:10,000. For IFA, anti-mouse IgG1 Alexa Fluor 594 and anti-rabbit Alexa Fluor 647 secondary antibodies (both from Invitrogen, Eugene, OR) were used at 1:1000. miRNA mimics were transfected into iLEC using Effectene (Qiagen, Valencia, CA). Both the miR-K12-11 mimic (KSHV-miR-K12-11-5p *mir*Vana miRNA mimic) and the negative control miRNA (FAM-dye-labeled control Pre-miR) were purchased from Ambion (Life Technologies, Carlsbad, CA).

BACH1 Adenovirus Vector

A FLAG-tag was fused to the BACH1 N-terminus using standard PCR techniques. The resulting DNA fragment was cloned into the adenoviral vector pAdTet7. In this vector, transgene expression is driven by a minimal CMV promoter that is preceded by multiple tet-repressor binding sites. Expression from this chimeric promoter only takes place in presence of the tet transactivator, as well as the absence of tetracycline or doxycycline (a so-called, “tet-off” system). In this system, the tet

transactivator is expressed from a second co-infecting adenovirus, hereafter referred to as Trans. In all AdBACH1 experiments, cells infected with Trans alone were used to control for nonspecific effects resulting from adenoviral infection (266). Adenovirus was prepared from these vectors as described previously (254).

Reverse Transcription Quantitative PCR (qPCR)

Extraction of total RNA was performed using miRNeasy Mini Kits (Qiagen, Valencia, CA), which allow for isolation of both miRNAs and mRNAs. DNase I (Qiagen) digestion was included to remove any contaminating DNA from the samples. Total cDNA was generated from these samples using the SuperScript III First-Strand Synthesis System (Invitrogen; Life Technologies, Carlsbad, CA). The following stem-loop PCR primers were used for the reverse transcription of miRNAs (Stem-loop RT), as previously described (267): mir-k12-11: SL 5′-GTCGTATCCAGTGCAGGGTCCGAGGTATTCGCACTGGATACGACTCGGAC- 3’; mir-k12-1: SL 5′-GTCGTATCCAGTGCAGGGTCCGAGGTATTCGCACTGGATACGACGCTTAC-3’; mir16: SL 5′-GTCGTATCCAGTGCAGGGTCCGAGGTATTCGCACTGGATACGACCGCCAA- 3’; mir-155: SL 5′-GTCGTATCCAGTGCAGGGTCCGAGGTATTCGCACTGGATACGACACCCCT- 3’. The following primers were used for qPCR: mRNAs: GAPDH F 5’-GAAGGTGAAGGTCGGAGT-3’, GAPDH R 5’-GAAGATGGTGATGGGATTTC-3’; HO-1 F 5’-GCCCTTCAGCATCCTCAGTTC-3’, HO-1 R 5’-GGTTTGAGACAGCTGCCACA-3’; BACH1 F 5’-TGAGAAGCTGCAAAGTGAAAAGG-3’, BACH1 R 5’-CTGCTTTGTCTCACCCAGAGT-3’; ORF59 F 5’- CGAGTCTTCGCAAAAGGTTC-3’,

ORF59 R 5'- AAGGGACCAACTGGTGTGAG-3'.miRNAs: miR-K12-11 F 5'-CGAGCCTTAATGCTTAGCCUG- 3'; miR-K12-1 F 5'-GCGAGCATTACAGGAAACTGG-3'; miR16 F 5'-CGGCAGTAGCAGCACGTAAAT-3'; miR-155 F 5'- CGCGAGCTTAATGCTAATCGTG-3'. The reverse primer for all miRNA detection was Universal SL Rev 5′-CCAGTGCAGGGTCCGAGGTA-3′. To perform qPCR, 5 µl of cDNA (typically 1-10 ng) was mixed with gene-specific primers and 12.5 µl Power SYBR Green PCR Master Mix (ABI, Foster City, CA) to a final volume of 25 µl. Optimization of primer/sample concentrations was performed for all targets. For qPCR experiments, standard curves were set up using appropriate control samples and a dilution series ranging from 100 ng to 3.2 pg cDNA. Sample amplification was performed using an ABI Real Time PCR 7500 System. For relative quantitation experiments, the signal for each cDNA was normalized to GAPDH levels, thereby allowing for the comparison of mRNA expression levels in different samples.

Western Blot analysis

Cells were lysed in RIPA buffer (50mm Tris, pH 7.5, 150mm NaCl, 1% Nonidet P-40, 0.5% deoxycholate, 0.1% SDS, 1X Complete inhibitors [Roche Applied Science, Pleasanton, CA]), incubated on ice for 30min, and then centrifuged at 13,400 x *g* for 10min at 4°C. Cleared supernatants were transferred to fresh tubes, and their protein concentrations were determined via bicinchoninic acid assay (BCA, Thermo Fisher Scientific, Waltham, MA). The resulting proteins were separated via reducing SDS-PAGE, transferred to PVDF membranes, incubated in blocking buffer (5% nonfat dry milk in Tris-buffered saline with 0.1% Tween 20 [TBST]) for 1h with agitation, and then probed with the appropriate primary antibody diluted in blocking buffer. Blots

were then washed 3 times with TBST, incubated with the appropriate secondary antibodies in blocking buffer, and then washed a further 3 times with TBST. Blots were developed using an ECL Plus kit (Amersham Biosciences/GE Healthcare, Pittsburgh, PA), and the resulting data was captured using either Kodak XAR film or a G:Box (Syngene). The ImageJ software package (Rasband, W.S., ImageJ, U. S. National Institutes of Health, Bethesda, Maryland, USA, http://imagej.nih.gov/ij/, 1997-2014) was used for band quantitation. Images shown are representative of three independent experiments.

Indirect Immunofluorescence and Image Analysis

For IFA, cells were seeded on collagen-coated coverslips (BD Biosystems, Franklin Lakes, NJ) in 6-well tissue culture plates. At the end of the experiment, cells were fixed in 2% paraformaldehyde (PFA) for 8 min, washed 3 times in PBS, and permeabilized in 0.25% Triton-X100 for 8 min. Cells were blocked in IFA blocking buffer (20% normal goat serum [NGS] in PBS) for 20 mins at 37°C, and incubated with the appropriate primary antibody incubation buffer (1% NGS in PBS) for 1 hr at 37°C. After primary antibody incubation, coverslips were washed 3 times in PBS and incubated with both the appropriate secondary antibody and the nuclear stain 4',6-diamidino-2-phenylindole (DAPI) for 45 min at 37°C. Coverslips were then washed 3 times in PBS and mounted on glass slides with FluoromountG (Southern Biotech, Birmingham, AL). The slides were then analyzed using a Deltavision real-time deconvolution fluorescence microscope (DVRT, Applied Precision, Issaquah, WA) and images were captured using a Photometrics CoolSNAP HQ camera. Image analysis was performed using Softworx (Applied Precision). Stacks of images (0.2 μm z-step) were captured at 60X magnification. Stacks were subjected to deconvolution, and 2–3 section projections were made by superimposing

representative z-planes to generate the final image. Images shown are representative of three independent experiments. Where necessary to facilitate visualization of GFP and more than one fluorescently-tagged target protein of interest, GFP was pseudocolored to greyscale.

Flow cytometry

Cells to be analyzed via flow cytometry were dissociated from tissue-culture plates using non-enyzmatic Cellstripper (25-056-CI; CellGro/Corning, Manassas, VA) and then pelleted at 1800 x *g* at 4°C for 5 min. The cells were then fixed using BD Cytofix/Cytoperm, incubated on ice for 15 min, pelleted, and then resuspended in 1X BD Permwash containing primary antibody. After a further 15 min incubation on ice, the cells were washed three times and then resuspended in 1X BD Permwash containing the appropriate dilution of secondary antibody. After a subsequent 15 min on ice, the cells were washed in 1X BD Permwash and finally analyzed on a BD FACSCalibur flow cytometer (BD Biosciences).

Statistical analysis

Quantitative PCR data is expressed as the mean ± Standard Error of the Mean (SEM). Statistical analysis was performed on R Software (R Core Team (2013). R: A language and environment for statistical computing. R Foundation for Statistical Computing, Vienna, Austria). One-way ANOVA and Kruskal-Wallis tests were used to compare means from different groups.

CHAPTER 3

HO-1 Promotes KSHV Infection Of Endothelial Cells Through Inhibition Of TLR4 Signaling.

Sara Botto[1], and Ashlee V. Moses[1]

[1]Vaccine and Gene Therapy Institute; Oregon Health and Science University; Beaverton, OR 97006 USA

Running title: HO-1 inhibits TLR4 in KSHV-infected endothelial cells

- Manuscript written by Sara Botto and Ashlee V. Moses.
- All experiments were conducted by Sara Botto.

- This manuscript is ready for submission on *mBio Journal*.

3.1 Abstract

KSHV is the etiologic agent of Kaposi sarcoma (KS) an endothelial cell (EC)-derived tumor and rare lymphoproliferative disorders. KSHV infection of EC results in induction of heme oxygenase-1 (HO-1), the rate-limiting enzyme of heme catabolism that converts pro-oxidant heme into metabolites with cytoprotective properties. Previous work has shown that HO-1 expression in KSHV-infected EC is characterized by an early transient induction followed by a sustained upregulation co-incident with the establishment of viral latency. These two phases of HO-1 induction are independently regulated, suggesting distinct roles in the virus life cycle. In the current chapter, we investigated the role of HO-1 at the early stage of *de novo* infection. The initial stage of KSHV infection involves virion binding to the cell membrane, leading to activation of host innate immune effectors, including TLR4. TLR4 signaling in infected cells is then targeted by viral immune evasion factors. TLR4-deficient EC are more susceptible to KSHV infection than wild-type controls, while the heme metabolite carbon monoxide (CO) is a TLR4 signaling inhibitor. In the light of these two findings, we investigated a potential role for CO in blocking TLR4 activation to facilitate KSHV infection of EC. Indeed, we report that CO is able to partially block TLR4 signaling in *de novo* infected EC through inhibition of the TRIF-dependent pathway. Further, elevation of intracellular CO resulted in reduced expression of TLR4 downstream anti-viral genes, thus dampening the innate immune response against KSHV. By contrast, inhibition of HO-1 activity resulted in higher innate immune response and reduced KSHV infection.

3.2 Importance

The HO-1 enzyme has been extensively investigated in both physiological and pathological conditions. HO-1 is induced in several types of cancer, where it is considered a therapeutic target. Our goal is to understand how HO-1 promotes KS tumorigenesis and to explore its potential role as a KS treatment target. Our previous work showed that KSHV strongly induces HO-1 and that KSHV-infected cells proliferate in response to heme in a HO-1-dependent manner, suggesting that HO-1 promotes infection and tumorigenesis. In the current study we investigate the contribution of HO-1 to the early stage of virus infection. Investigation of HO-1 in the context of KSHV infection is key to understanding the biology of the virus and to develop targeted therapies for KS.

3.3 Introduction

The oncogenic human γ-herpesvirus Kaposi sarcoma herpesvirus (KSHV) is the causative agent of Kaposi's sarcoma (KS) (9) and the lymphoproliferative disorders primary effusion lymphoma (PEL) and multicentric Castleman disease (MCD) (9,45). KSHV establishes persistent infection in B-cells and endothelial cells by evading the host immune system and by promoting survival of infected cells. The importance of the balance between KSHV and host immunity is underscored by the increased development of KSHV-associated malignancies in the setting of immunodeficiency (98). Viruses adopt several mechanisms to evade the host immune response. In particular, KSHV encodes different proteins and micro-RNAs able to target host factors of both the innate and the adaptive immune system (268). The innate immune system is the first inducible layer of host defense against pathogens and appropriate sensing of non-self components is critical for initiating an

effective immune response (166). Virus detection is carried out by a class of immune sensors known as pattern recognition receptors (PRR). The Toll-like receptors (TLRs) are a class of evolutionarily-conserved PRRs that detect a broad range of pathogens (269).

KSHV is known to induce activation of several TLRs including TLR9, which recognizes unmethylated CpG motifs of double-stranded DNA (dsDNA) (270), TLR3, which senses viral replication intermediates such as dsRNA (271) and TLR4, which is most well-known for recognizing gram-negative bacterial lipopolysaccharide (LPS) (175). Although the KSHV component(s) that activate TLR4 signaling remain to be identified, UV-inactivated KSHV induces TLR4 signaling, suggesting that one or more glycoproteins are responsible (175). Accordingly, treatment of fibroblasts with a purified soluble version of KSHV glycoprotein K8.1 is sufficient to induce expression of IFNβ and a panel of interferon-stimulated genes (ISGs) (181,182). The significance of TLR4 in the regulation of KSHV infection is highlighted by the evidence that KSHV employs strategies to evade TLR4-triggered immunity. For example, the viral proteins vIRF-1 (ORF K9) and vGPCR (ORF74) are able to suppress TLR4 signaling (175). Furthermore, KSHV encodes proteins and miRNAs that block the TLR4 adaptor proteins MyD88 and TRIF: the transactivator protein RTA (ORF50) degrades TRIF (272), while the viral microRNAs miR-K9 and miR-K5 downregulate IRAK1 and MyD88, respectively (273). From a functional standpoint, downregulation of TLR4 in EC, the precursors of KS tumor cells, leads to higher susceptibility to KSHV infection (175), suggesting an important role of this PRR in the prevention of endothelial infection and the progression of KS.

In a previous work, we demonstrated that *de novo* KSHV infection of lymphatic EC results in induction of the stress-inducible host enzyme heme oxygenase-1 (HO-1) at both early times post infection and during established viral

latency (Chapter 2). Early HO-1 expression was independent of viral gene expression, suggesting that one of more virion components is responsible for the initial response (Chapter 2). These data were corroborated by an independent study showing induction of HO-1 early post infection via a mechanism involving upregulation the HO-1 transcriptional activator NRF2 in response to infection-associated oxidative stress (274).

HO-1 catalyzes the degradation of heme into carbon monoxide, ferrous iron, and biliverdin (210). HO-1 is ubiquitously expressed and rapidly induced in response to diverse cellular stressors, and is also strongly expressed in several types of cancer (209). HO-1 induction is thought to contribute to cytoprotection, proliferation and angiogenesis via the conversion of pro-oxidant, cytotoxic heme into metabolites with antioxidant, pro-angiogenic, anti-apoptotic, and anti-inflammatory activity (202,210). Of particular relevance to the current study, the heme metabolite carbon monoxide (CO) is involved in activation of intracellular signaling pathways, which culminate in anti-inflammatory, anti-proliferative, anti-apoptotic, and anti-coagulative properties (209,214,215,275). Notably, CO is able to block TLR4 signaling by preventing the interaction between this receptor and its adaptor proteins MyD88 and TRIF (276-279). This downmodulatory influence reveals an important anti-inflammatory role for CO in pathogen-exposed cells and suggests a potential role for CO in immune evasion by pathogens such as KSHV that have the capacity to release CO. The discovery of compounds eponymously named “carbon monoxide releasing molecules” (CORM), have provided further mechanistic insight into the role of CO in biological systems (216).

In the present chapter we investigated the potential role of HO-1’s CO-releasing activity in the inhibition of TLR4 signaling during *de novo* KSHV infection of endothelial cells.

3.4 Results

3.4.1 *De novo* KSHV infection of endothelial cells activates TLR4

It is known that *de novo* KSHV infection of LEC induces an early transient expression of HO-1 message and protein (Chapter 2). However, the significance of this early phase of HO-1 induction to establishment of KSHV infection remains unknown. KSHV binding to the surface of EC leads to activation of several PRRs, including TLR4 (175). KSHV in turn employs mechanisms to counteract TLR4 signaling (174), suggesting that TLR4 plays an important role in KSHV infection. Besides activating the innate immune response, TLR4 has also been shown to induce expression of HO-1 (279). HO-1 in turn promotes a CO-driven feedback mechanism that attenuates TLR4 signaling (279). Considering the ability of CO to attenuate TLR4, we hypothesized that the transient peak of HO-1 observed during initial KSHV infection of EC might inhibit TLR4 signaling to facilitate KSHV infection. In order to verify this hypothesis, iLEC were infected with live or UV-inactivated BAC16 recombinant KSHV, then collected at different times post infection and analyzed for expression of HO-1 and of TLR4-induced transcripts. Confirming previous observations (Chapter 2) Figure 3.1A shows a transient peak of HO-1 message between 4 and 6 hours post infection (hpi), in both live and UV infected cells. To determine if TLR4 signaling was concurrently activated, transcription levels of the downstream cytokine IL-1β was determined; similar levels of IL-1β message were observed both in cells infected with live or UV-inactivated KSHV as early as 2 hpi (Figure 3.1B). At 4 hpi, IL-1β was sustained in UV-inactivated virus-infected cells, but decreased in live virus-infected cells, possibly due to *de novo* expression of viral immune evasion proteins. Similar trends were observed for TNFα and IFNβ transcripts (dns). Interestingly, virions devoid of the viral genome (B-capsids) were

also able to induce transcription of HO-1 message and cytokines involved with TLR4 signaling activation (dns), supporting the supposition that a virus particle component may be responsible for TLR4 activation. Since HO-1 can be induced through activation of the TLR4 signaling pathway (279,280), we next investigated whether the early induction of HO-1 observed in KSHV-infected LEC was TLR4-triggered. Accordingly, iLEC were pretreated with DMSO or with the TLR4-specific inhibitor CLI-095 for 2 hours and then exposed to LPS for 2 or 4 hours. As expected, LPS stimulation induction IL-1β transcripts in cells pretreated with DMSO, while cells pretreated with CLI-095 showed only basal levels of IL-1β (Figure 3.1C). By contrast, LPS treatment, regardless of the presence of the TLR4 inhibitor, did not significantly influence HO-1 message levels (Figure 3.1D). These experiments were then repeated using KSHV as inducer of TLR4 signaling: iLEC were pretreated with CLI-095 for 2 hours, KSHV-infected and then harvested at 2, 4 and 6 hpi for measurement of HO-1 transcripts, KSHV genomes and an immediate early viral transcript (K5). As observed with LPS treatment, CLI-095 did not significantly change the expression of HO-1 message in KSHV-infected iLEC (Figure 3.1E), confirming that TLR4 does not play a role in the induction of HO-1 in the system under study. However, iLEC pretreated with CLI-095 contained higher level of KSHV genomes (Figure 3.1G) and K5 transcripts (Figure 3.1H) as compared to control cells at early times hpi, which was reflected by a significant increase in the percentage of GFP-positive cells by 24 hpi (Figure 3.1F). Additionally, cells treated with the TLR4 inhibitor showed higher genome copies in the supernatant of infected cells at 24 hpi (Figure 3.2). Thus, these data imply that TLR4 plays an important inhibitory role against *de novo* KSHV infection and support a previous study showing that downregulation of TLR4 in EC using siRNA enhances their susceptibility to KSHV infection (175).

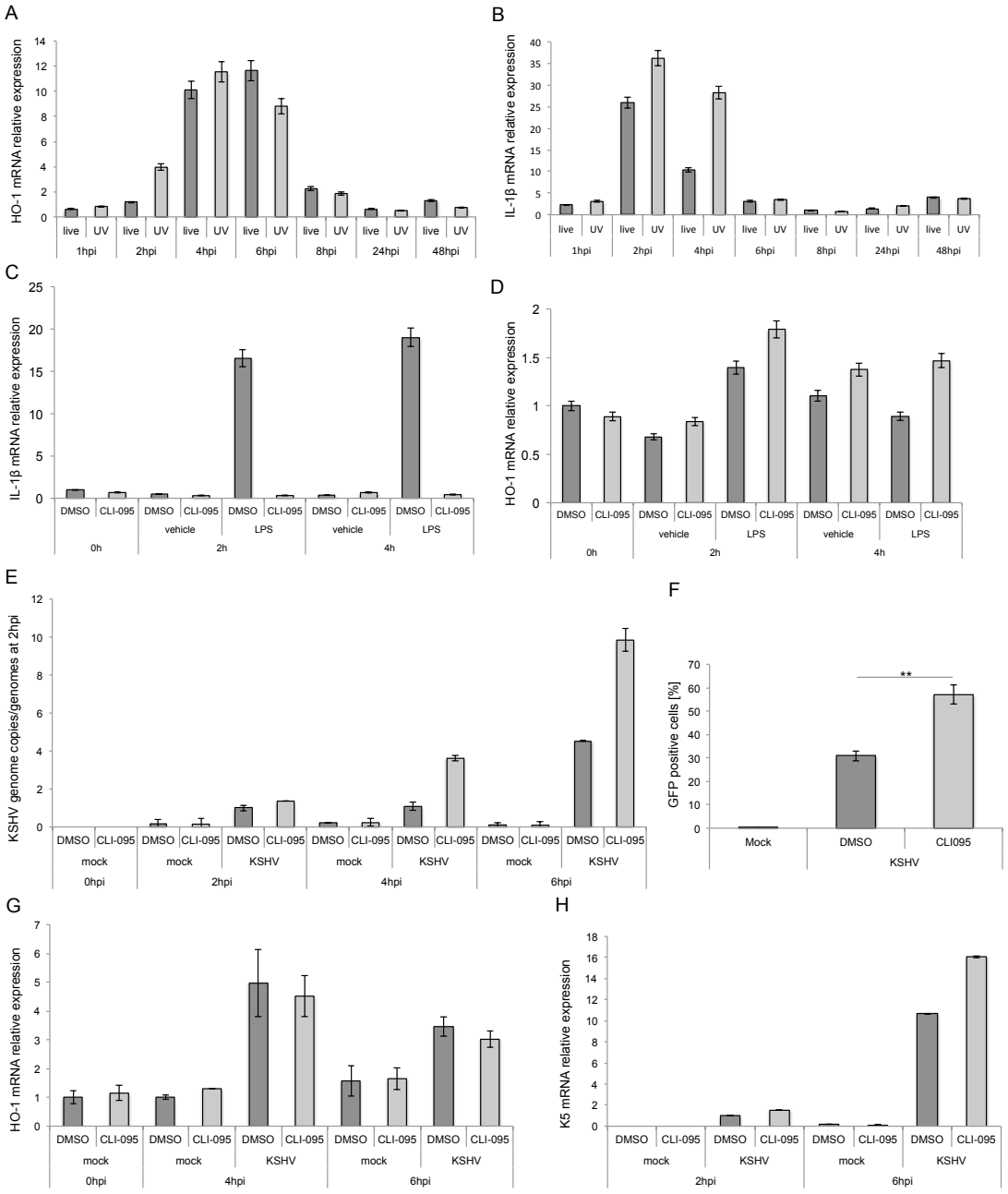

Figure 3.1. KSHV activates TLR4 signaling in EC while TLR4 inhibition enhances susceptibility to KSHV infection. A and B. qPCR for HO-1 (A) or IL-1β (B) transcripts in iLEC infected with infectious KSHV (live) or UV-inactivated KSHV (UV), at different times post infection (hpi). Data are expressed as the mean ± SEM (n=3). **C and D.** qPCR for IL-1β (C) and HO-1 (D) transcripts in cells pretreated with DMSO or CLI-095 and then stimulated with PBS (vehicle) or LPS. Data are expressed as the mean ± SEM (n=3). **E.** qPCR for KSHV genomes in cells pretreated with DMSO or CLI-095 prior

to infection (KSHV) or mock-infection (mock) with KSHV. Data are expressed as the mean ± SEM (n=3) **F.** Flow cytometric analysis of cells treated as in E; infected cells are gated on GFP (n=2). ** = p-value ≤ 0.01. A one-way ANOVA test was used for statistical analysis. **G and H.** qPCR for HO-1 (G) and KSHV K5 (H) transcripts in cells pretreated with DMSO or CLI-095 prior to infection (KSHV) or mock-infection (mock) with KSHV. Data are expressed as the mean ± SEM (n=2).

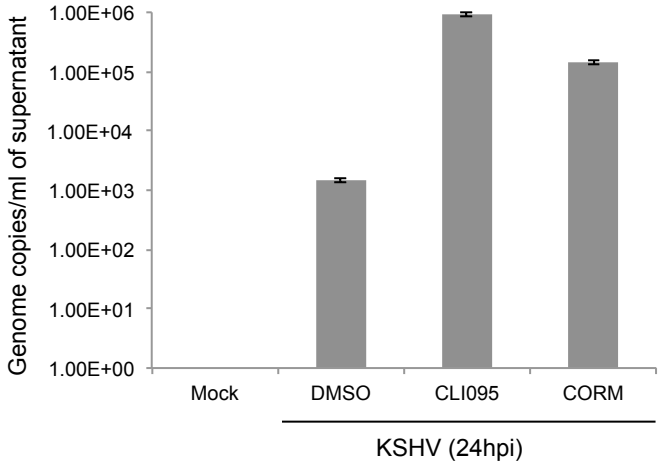

Figure 3.2. qPCR for KSHV genome copies in supernatant of iLEC pretreated with DMSO, CLI-095 or CORM-2 and then infected with KSHV for 24 hpi.

3.4.2 Carbon monoxide treatment renders iLEC more permissive to KSHV infection

As previously stated, HO-1 has been associated with inhibition of TLR4 signaling (279). In particular, carbon monoxide (CO) has the ability to block TLR4 signaling pathway by preventing its interaction with the adaptor proteins, MyD88 and TRIF (279). Thus, we hypothesized that the HO-1 inhibition of TLR4 signaling might occur as a consequence of CO production. We first confirmed that CO was able to inhibit LPS-induced TLR4 signaling in their system. iLEC were pretreated with DMSO or CORM-2, a carbon monoxide releasing molecule, for 2 hours, then stimulated with DMSO (vehicle) or LPS for 4 and 6 h. As shown in Figure 3.3A, cells stimulated with LPS in the presence of CORM-2 showed reduced levels of IL-1β message as compared to DMSO-treated cells. Interestingly, the decrease in cytokines in cells pretreated with CORM-2 was not as profound as the decrease observed in iLEC treated with CLI-095 (Figure 3.1C), indicating that CO did not inhibit TLR4 signaling as potently as a chemical inhibitor of TLR4. As previously mentioned, CO is itself an inducer of HO-1 (281) and indeed, iLEC pretreated with CORM-2 showed increased levels of HO-1 transcripts by 6 hours (Figure 3.3B), regardless of LPS treatment. Next, we investigated whether CO could also promote KSHV infection: iLEC were pretreated with CORM-2 for 2 h, infected with KSHV, and harvested at 2, 4 and 6 hpi to monitor infection efficacy. Cells pretreated with CORM-2 showed a higher number of intracellular KSHV genome copies compared to control (DMSO) cells (Figure 3.3C) as well as a significant increase in transcription of the IE gene K5 (Figure 3.3D), suggesting that, similarly to CLI-095, CO is able to render iLEC more susceptible to KSHV infection. In order to verify successful inhibition of the TLR4 pathway by CORM-2 treatment in the context of KSHV, we also examined cytokine transcription in virus-infected iLEC. As expected, CORM-2 pretreatment significantly

reduced IL-1β transcription in infected cells (Figure 3.3E); similar trends were observed for IL-6 and IL-8 (Figure 3.4).

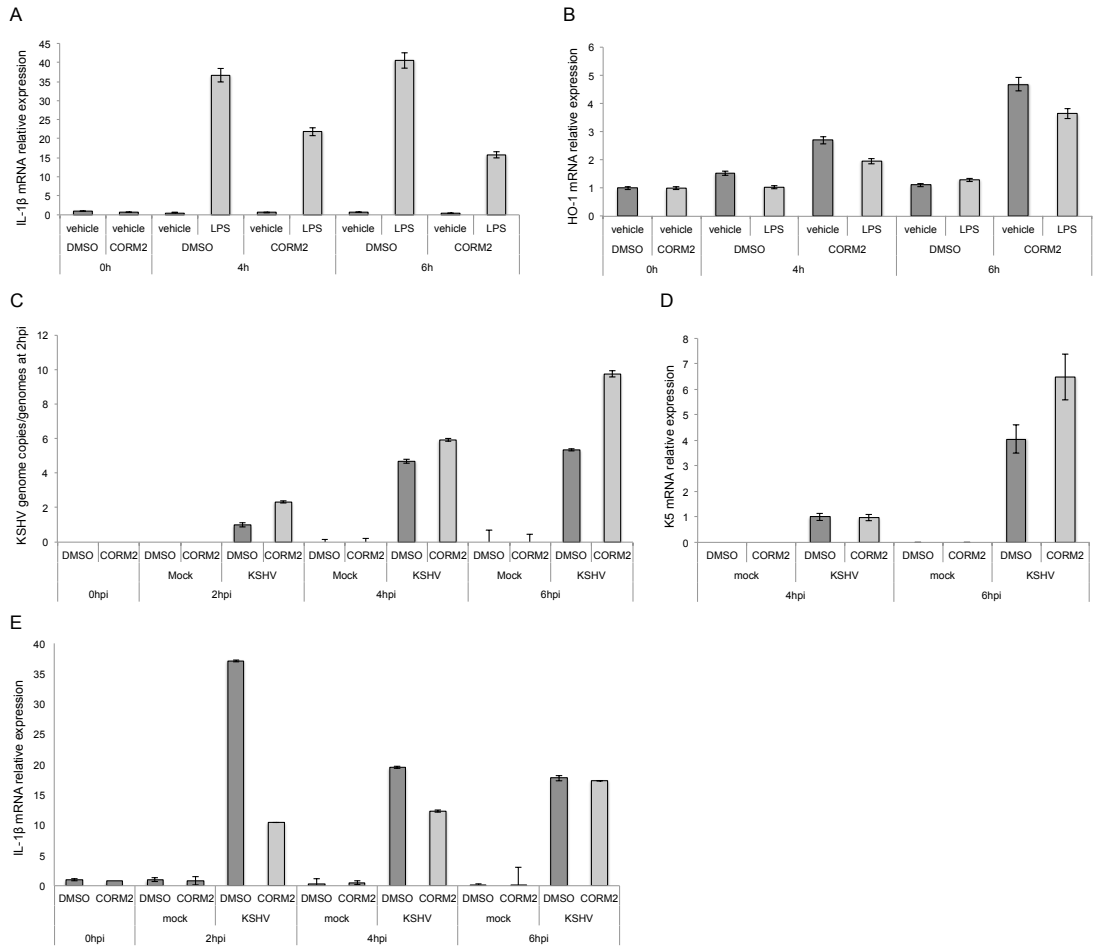

Figure 3.3. CO inhibits TLR4 signaling and renders EC more susceptible to KSHV infection. A and B. qPCR for IL-1β (A) and HO-1 (B) transcripts in iLEC pretreated with DMSO (vehicle) or CORM2 and then stimulated with DMSO or LPS. Data are expressed as the mean ± SEM (n=3). **C.** qPCR for KSHV genomes in iLEC pretreated with DMSO or CORM2 and then infected with KSHV. Data are expressed as the mean ± SEM (n=3) **D and E.** qPCR for KSHV K5 (D) or IL1-β (E) transcripts in iLEC pretreated with DMSO or CORM2 and then infected with KSHV. Data are expressed as the mean ± SEM (n=3).

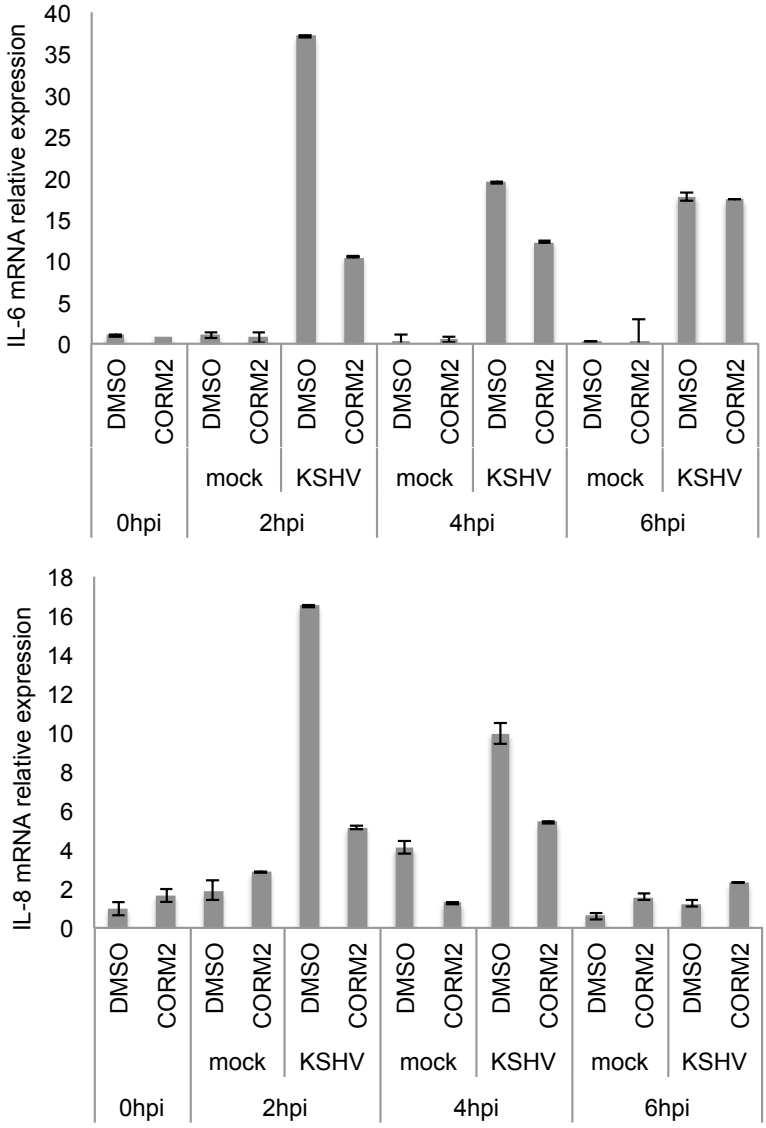

Figure 3.4. qPCR for mRNA levels of IL-6 (top) and IL-8 (bottom) in iLEC pretreated with DMSO or CORM-2 and then infected with KSHV for 2, 4 or 6h. Data are expressed as the mean ± SEM (n=3).

3.4.3 HO-1 inhibition affects KSHV infection of iLEC

As shown in Figure 3.3 above, enhancing intracellular CO levels facilitates KSHV infection through inhibition of TLR4 signaling (Figure 3.3). To verify that HO-1 activity was required for this phenotype, an inhibitor of HO-1 activity, OB-24, was used. OB-24 is a water-soluble small-molecule inhibitor synthesized from the imidazole class that has potent anti-tumor and anti-metastatic activity in preclinical models of prostate cancer (221). Contrarily to other commonly used HO-1 inhibitors, OB-24 selectively inhibits HO-1 and does not perturb HO-1 expression (221,282). OB-24 was first tested in iLEC to determine a non-cytotoxic range and inhibition of HO-1 activity confirmed by measuring bilirubin concentration in cell lysates (Figure 3.5). Next the drug was tested in the presence of KSHV infection. iLEC were pretreated overnight with OB-24 or PBS as vehicle, then infected with KSHV and collected at different times post infection (2, 4, 6, 8 hpi) for analysis. Cells pretreated with OB-24 showed higher levels of IFNβ transcripts (Figure 3.6A) and contained lower levels of K5 message (Figure 3.6B) as compared to PBS-treated cells or CORM-2 treated cells, suggesting that inhibition of HO-1 activity leads to an increase in anti-viral cytokines and results in less KSHV infection. To confirm this data, cells pretreated with OB-24 showed significant decrease in expression of both early (ORF59) (Figure 3.6C) and latent (LANA-1) viral transcripts at 24 hpi (Figure 3.6D). Next, we investigated TLR4 signaling activation in CORM-2 or OB-24 pretreated cells by examining intracellular levels of phosphorylated TBK1 (TRIF-dependent pathway) and total IRAK1 (MyD88-dependent pathway). iLEC pretreated with CORM-2 and infected with KSHV showed lower levels of phosphorylated TBK1 compared to DMSO-treated cells, while similar levels of total TBK1 were observed in both conditions (Figure 3.6E). No significant differences were observed in IRAK1 levels suggesting that, in this system, CO seems to mainly affect the TRIF-

dependent pathway. This finding may also explain the partial block of TLR4 signaling observed with CORM-2 treatment in Figure 3.3A. Cells pretreated with OB-24 showed higher levels of phospho-TBK1 as compared to DMSO-treated cells (vehicle) and in particular CORM-2-treated cells (Figure 3.6E). By contrast, no significant changes were detected for the levels of total TBK1 or IRAK1 (Figure 3.6E). Together, these results suggest that HO-1 activity is responsible for the inhibition TLR4 signaling, resulting in promotion of viral infection.

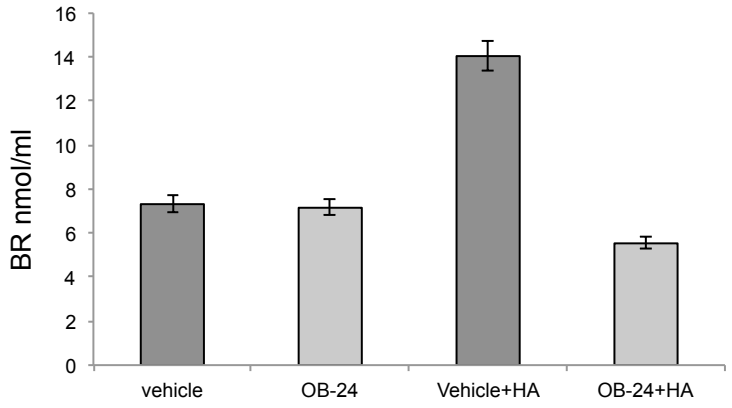

Figure 3.5. ELISA for intracellular bilirubin (BR) to verify efficacy of the HO-1 inhibitor OB-24. iLEC were pretreated with PBS (vehicle) or OB-24 (20μM) overnight, then stimulated with HO-1 inducer heme arginate (HA) for 3h. Data are expressed as the mean (n=2).

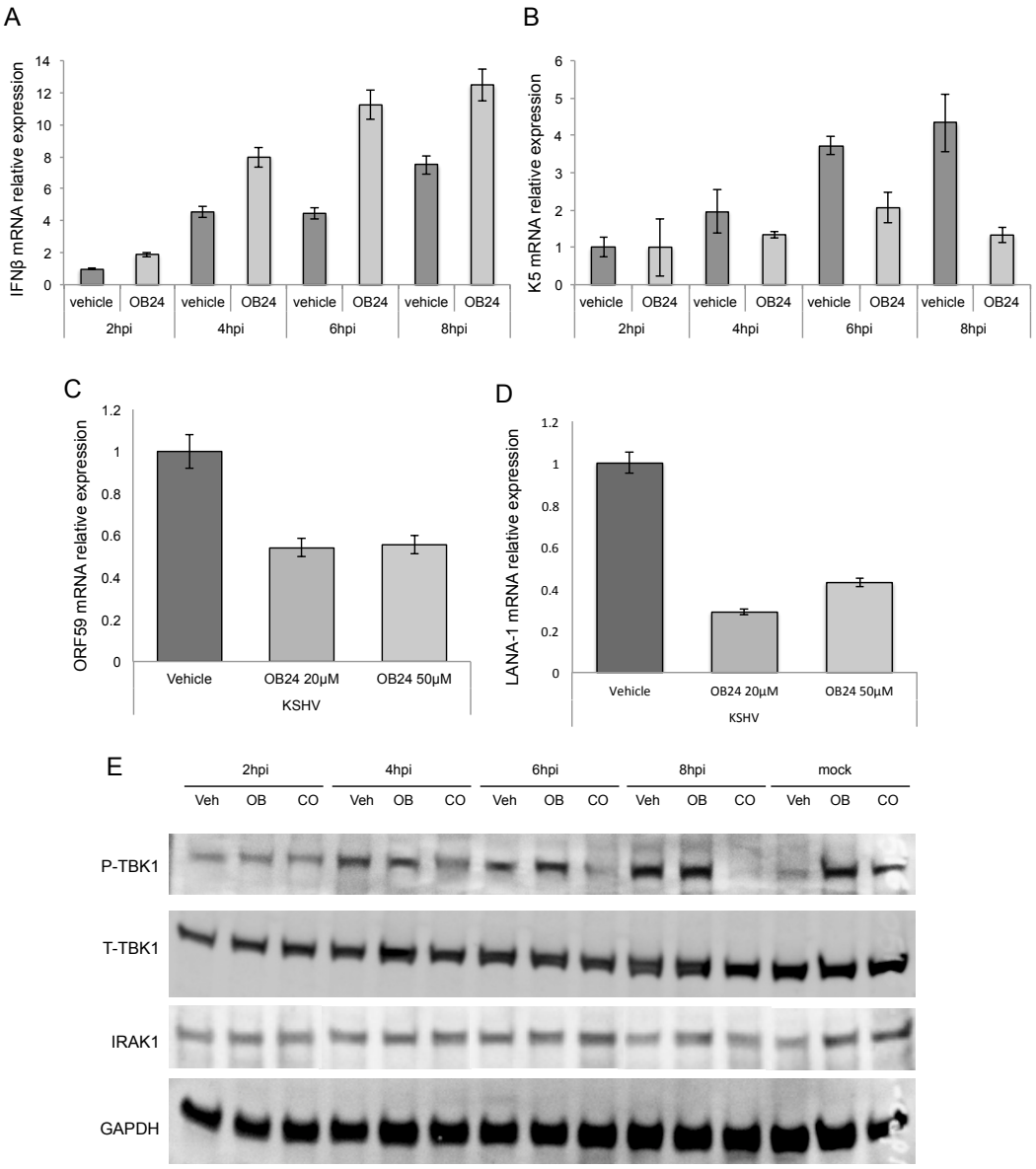

Figure 3.6. HO-1 inhibition decreases KSHV infection of EC. A and B. qPCR for IFNβ (A) and K5 (B) transcripts in iLEC pretreated with PBS (vehicle) OB-24 (20μM) overnight and then infected with KSHV. Data are expressed as the mean ± SEM (n=2). **C and D.** qPCR for KSHV ORF59 (C) and LANA-1 (D) transcripts in iLEC pretreated with PBS (vehicle) or OB-24 (20 or 50 μM) and then infected with KSHV for 24 h. Expression levels are shown relative to those in vehicle-treated iLEC. Data are expressed as the mean ± SEM (n=3). **E.** Western blot of iLEC pretreated with DMSO (vehicle), 20μM OB-24 (OB) or CORM2 (CO), infected with KSHV and then harvested at intervals post-infection. Mock refers to mock-infected samples harvested at 8 hpi. P-TBK1= phospho-TBK1. T-TBK1= total-TBK1. GAPDH was used as a loading control. (n=2).

3.4.4 TLR4 signaling affects a step of KSHV infection beyond capsid delivery to the nucleus

In Figure 3.1 and 3.3 we demonstrated that TLR4 inhibition through either CLI-095 or CORM-2 pretreatment renders iLEC more permissive to KSHV infection. To determine which step of KSHV infection was affected by TLR4 signaling, KSHV binding, entry and capsid delivery to the nucleus were evaluated by immunofluorescence microscopy (IFA). iLEC were first treated with DMSO, CORM-2 or CLI-095 for 2 h, then infected with KSHV at 4°C, to allow virus binding but preventing entry. After 30 min at 4°C, cells were washed and either fixed to determine the number of bound virions or further incubated at 37°C for 60 or 120 min to allow for virus entry and nuclear trafficking. All cells were then stained for viral capsids (ORF65). IFA for ORF65 revealed no significant difference in the number of capsids at 30 min (binding), 60 min (entry), or 120 min (delivery to nucleus) post infection regardless of the treatment (Figure 3.7A and Table 3.1). These data thus suggest that TLR4 signaling does not have an impact on these initial infection stages. Next, we used the viral polymerase inhibitor ganciclovir (GCV) to evaluate intracellular levels of viral DNA in the absence of viral replication, thus allowing detection of only input viral genomes. iLEC were pretreated with GCV alone or with CORM-2 and GCV concomitantly for 1h, and then infected with KSHV for 2, 3 and 4 h. Collected cells were then analyzed for viral DNA content by qPCR. As expected (Figure 3.7B), treatment with GCV successfully blocked DNA replication. Importantly, in the presence of GCV similar amounts of viral DNA reached the nucleus (2hpi) in CORM- and DMSO-treated cells, confirming that CORM-2 treatment does not promote virus delivery to the nucleus. Corresponding to results shown in Figures 2 and 3, CORM-2 treatment in the absence of GCV resulted in higher viral DNA content at later time points (3 and 4 hpi). Thus, these data suggest that TLR4

activation affects a phase of KSHV infection post viral genome delivery to the nucleus, potentially by inducing expression of ISGs that are dedicated to the inhibition of viral transcription/replication.

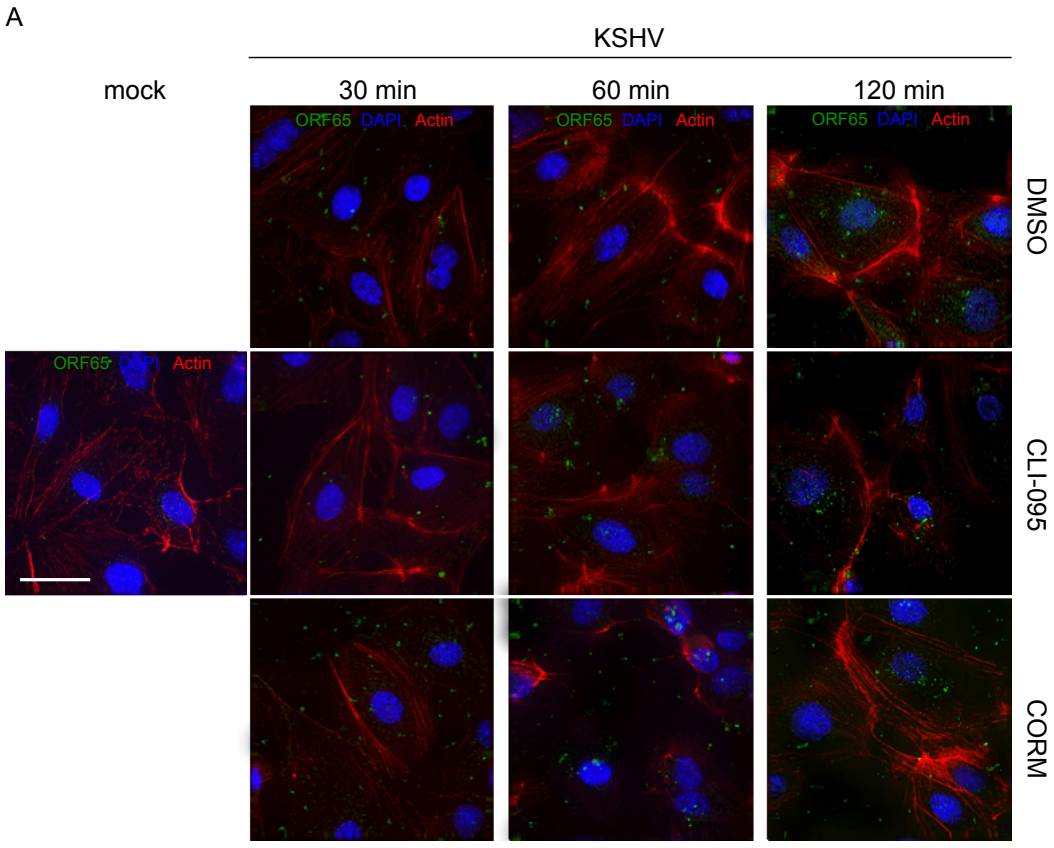

Table 1: Quantification of ORF65 staining in Figure 4A

	Infection time [min]		
Treatment	**Binding [30]**	**Entry [60]**	**Delivery to nucleus (120)**
DMSO	28±3	25±4	30±4
CLI-095	28±2	29±2	25±3
CORM2	25±2	30±3	29±5

Figure 3.7. TLR4 signaling affects a step of KSHV infection beyond capsid delivery to the nucleus. A. IFA of iLEC pre-treated with DMSO, CLI-095 or CORM-2, infected with KSHV for 30, 60 or 120 minutes and then imaged for expression of KSHV ORF65 (green), host actin (red) and DAPI

nuclear stain (blue). Cells were maintained at 4°C for the first 30 min and then warmed to 37°C for 60 or 120 min. Single left panel shows mock-infected cells. Top three panels show DMSO treated iLEC. Middle three panels show CLI-095 treated iLEC. Bottom three panels show CORM2-treated iLEC. Images were captured at 60X magnification (scale bar = 30μm). **B.** qPCR for viral DNA in iLEC pretreated with vehicle or GCV, in the presence or absence of CORM2, then infected with KSHV. Data are expressed as the mean ± SEM (n=3).

3.5 Discussion

KSHV infection results in robust expression of the inducible form of heme oxygenase, HO-1 both *in vivo* and *in vitro* (153). HO-1 is known to be upregulated by KSHV not only in stably-infected EC but also during the early phase of *de novo* infection, through two distinct mechanisms (Chapter 2). HO-1 induction during latency is associated with downregulation of the HO-1 transcriptional repressor BACH1, which is targeted by the KSHV miRNA miR-K12-1 (Chapter 2). Conversely, early HO-1 transient induction has been attributed to ROS production and consequent upregulation of NRF2, a HO-1 transcriptional activator (274). In the present chapter we investigated whether expression of HO-1 in the early stages of KSHV infection has any effect on the virus-host interaction and the success of the infection process. This was of interest since KSHV binding and entry into permissive cells is known to activate several cellular pathways, some of which facilitate infection while others activate anti-viral immunity or antagonize this host response. For example, KSHV infection triggers activation of several cellular signaling pathways, which promote entry and delivery of the virus to the nucleus (83). Concomitantly, KSHV infection activates host innate immune responses including theTLR4 pathway (175). Here we describe a novel mechanism of TLR4 inhibition in KSHV-infected cells, which occurs through induction of cellular HO-1. The HO-1 metabolite carbon monoxide has been shown to block TLR4 signaling activation by preventing

interaction of TLR4 with its adaptor proteins MyD88 and TRIF (279). Here, we show that KSHV infection leads to activation of the TLR4 pathway in endothelial cells and that CO is able to partially block its signaling and promote infection. Indeed, cells pretreated with a TLR4 inhibitor or with exogenous CO show higher level of viral genes and genomes as compared to control cells. Moreover, cells subjected to CO exposure show reduced levels of inflammatory cytokines associated with TLR4 activation. By contrast, cells pretreated with an inhibitor of HO-1 enzyme activity show less permissiveness to KSHV infection as well as higher levels of inflammatory cytokines, thus suggesting an important role for HO-1 at early stages of KSHV infection.

To further understand the role that TLR4 plays in KSHV infection, we investigated which step of KSHV infection is affected by TLR4 signaling. TLR4 signaling activates a series of pathways that results in transcription of inflammatory cytokines and chemokine, as well as in transcription of type I IFN genes. IFNβ secretion from infected cells leads to activation of a set of genes, denominated IFN-stimulated genes (ISGs), which show a variety of antiviral properties (283,284). ISGs antagonize the virus by initiating an antiviral program able to act on infected cells and neighboring cells. Some of the ISGs induced upon infection are involved in the amplification and regulation of the IFN response, including MDA5, RIG-1, and TRIM proteins (283). Some other ISGs are involved in antiviral mechanisms that interfere with the virus life cycle, example of these are Mx protein, OAS, RNaseL, APOBEC3 and PKR (283). We showed that pretreatment of cells with CO or with a TLR4 inhibitor leads promotes KSHV infection. Interestingly, we observed no significant difference in the amount of virus that binds, enters or reaches the nucleus. By contrast, we detected differences at later time points coincident with viral

transcription and viral genome replication. Possibly, CO treatment, by blocking TLR4-TRIF-dependent pathways, is able to decrease the magnitude of ISGs induced, thus allowing the virus to continue its life cycle and either establish latency or spread to neighboring cells. Accordingly, treatment of endothelial cells with an inhibitor of HO-1 activity led to an increase in the production of inflammatory cytokines and reduced levels of KSHV infection, suggesting that HO-1 plays a role in the inhibition of innate immune responses against KSHV.

HO-1 is highly induced in several cancer types, where it has been shown to contribute to tumor progression by promoting cell proliferation, angiogenesis, cytoprotection and resistance to chemotherapy (202,210,211). Previous work by Dr. Ashlee Moses' group showing that KSHV-enhanced HO-1 activity could promote the growth of KSHV-infected EC provided evidence that HO-1 is a driver of KS tumorigenesis (153). In the current study, we show for the first time that HO-1 induction by KSHV is not only beneficial for KS tumorigenesis, but is also important for attenuating critical anti-viral mechanisms. This dual role for HO-1 enhances its importance as a therapeutic target for KS.

3.6 Materials and methods

Cells and viruses

Primary adult human lymphatic endothelial cells (LEC) were obtained from Lonza (Allendale, NJ). Life-extended iLEC were generated from these cells via transduction of a retrovirus expressing the E6 and E7 genes of HPV16 as previously described (103). LEC were cultured in EGM-2 medium prepared by supplementing basal medium (EBM-2; Lonza) with 10% fetal bovine serum (FBS), penicillin-streptomycin–L-glutamine (PSG; HyClone, Logan, UT), and additional EC growth supplements (EGM-2MV Bullet Kit; Lonza). Epithelial iSLK cells (generously provided by Dr. Rolf

Renne at the University of Florida, Gainesville, FL, with kind permission from Dr. Jae Jung at the University of Southern California, Los Angeles, CA, and Dr. Don Ganem at the University of California, San Francisco, CA) were used to produce stocks of recombinant KSHV. iSLK cells were grown in DMEM supplemented with 10% FBS, PSG, puromycin (1 μg/ml), neomycin (200 μg/ml), and hygromycin (1.5 mg/ml). The KSHV BAC clone BAC16 was kindly provided by Dr. Jae Jung (249). To produce stocks of recombinant KSHV, iSLK cells harboring BAC16 were treated with doxycycline (1 μM) and sodium butyrate (3 mM) for 72 h. Supernatants were collected, clarified via low-speed centrifugation and transferred to ultracentrifuge tubes underlaid with 25% sucrose in TNE (150 mM NaCl, 10 mM Tris [pH 8.0], 2 mM EDTA [pH 8.0]) for centrifugation at 78,000 x *g* for 2 h at 4°C. The resulting virion pellets were resuspended in TNE. Stocks of BAC16-derived KSHV were titrated by infecting iLEC with serially diluted virus preparations. After a 48-h incubation, the cells were harvested and evaluated for GFP expression via flow cytometry. Infections were conducted using an MOI corresponding to 80% GFP+ iLEC.

Antibodies and other reagents

HO-1 protein was detected using a mouse anti-HO-1 monoclonal antibody (BD Transduction Laboratories, Franklin Lakes, NJ) at concentrations of 1:1,000 for Western blotting (WB). An anti-GFP (goat) horseradish peroxidase (HRP)-conjugated antibody (600-103-215; Rockland, Limerick, PA) was used at 1:2,000 to detect GFP. Actin was used as WB loading controls and detected with a mouse anti-β-actin-HRP antibody at a concentration of 1:100,000 (company). Rabbit anti-total TBK1 and phospho-TBK1 were used at 1:1,000 for WB (Cell signaling). Rabbit anti-IRAK1 was used at 1:1,000 for WB (Pierce). Rabbit anti-ORF65 was kindly provided by Dr. Bala Chadran and used to detect viral capsid by IFA at 1:200 dilution. For WB,

donkey anti-rabbit (sc-2313; Santa Cruz Biotechnologies) or HRP-conjugated goat anti-mouse (Millipore, Billerica, MA) secondary antibodies were each used at a concentration of 1:10,000. For IFA, Alexa Fluor 488-conjugated anti-rabbit secondary antibody (Invitrogen, Eugene, OR) was used at 1:1,000. Rhodamine Phalloidin (Invitrogen, Eugene, OR) was used at 1:40 dilution to detect actin filaments by IFA. LPS was used to induce TLR4 signaling at a concentration of 100ng/ml. The TLR4 inhibitor CLI-095 (Invivogen) was used at a concentration of 3 μM. The HO-1 inhibitor OB-24 (221) was kindly provided by Dr. Ajay Gupta (McGill University, Montreal, Canada) and used at a concentration of 20 μM. Ganciclovir (GCV), a viral DNA polymerase inhibitor, was used at a concentration of 200 μM (Sigma). CORM-2 a carbon monoxide-releasing molecule was used at a concentration of 10 μM (Sigma).

Reverse transcription-qPCR assay.

Extraction of total RNA was performed with RNeasy minikits (Qiagen, Valencia, CA). DNase I (Qiagen) digestion was included to remove any contaminating DNA from the samples. Total cDNA was generated from these samples with the SuperScript III First- Strand Synthesis System (Invitrogen; Life Technologies, Carlsbad, CA). Extraction of DNA was performed with Blood and Tissue DNA kits (Qiagen, Valencia, CA). The following primers were used for qPCR assays of mRNAs: GAPDH F, 5'-GAAGGTGAAGGTCGGAGT-3'; GAPDH R, 5'-GAAGATGGTGATGGGATTTC-3'; HO-1 F, 5'-GCCCTTCAGCATCCTCAGTTC-3'; HO-1 R, 5'-GGTTTGAGACAGCTGCCACA-3'; ORF59 F 5'-CGAGTCTTCGCAAAAGGTTC-3'; ORF59 R, 5'-AAGG GACCAACTGGTGTGAG-3'; IL-1β F 5'- GCCAATCTTCATTGCTCAAGTGT-3', IL-1β R 5'-AGCCATCATTTCACTGGCGA-3'; LANA-1 F 5'- CGCGAATACCGCTATGTAC-

3', LANA1 R 5'- CTGGAAGGCCTGAGATAA-3'; K5 F 5'-ACAAGGACCGTCAATTCGATG-3', K5 R 5'-TGCCATACCGACGGCC-3'; IL-6 F 5'-CCAGGAGCCCAGCTATGAAC-3', IL-6 R 5'-CCCAGGGAGAAGGCAACTG-3'; IFNβ F 5'-ACGCCGCATTGACCATCTA-3', IFNβ R 5'-TAGTCTCATTCCAGCCAGTGC-3'. For detection of genomic targets, the following primers were used: ORF26 F 5'-ACGCGAAAGGATTCCACCAT-3', ORF26 R 5'-TCCGTGTTGTCTACGTCCA-3'; GAPDH F GAPDH R

To perform qPCR assays, 5 µl of cDNA or DNA (typically 10 ng) was mixed with gene specific primers and 12.5 µl of Power SYBR green PCR master mix (ABI, Foster City, CA) to a final volume of 25 µl. Optimization of primer and sample concentrations was performed for all targets. For all qPCR experiments, standard curves were set up with the appropriate control samples using a dilution series ranging from 100 ng to 3.2 pg of cDNA/DNA. Sample amplification was performed with an ABI real-time PCR 7500 system. For relative quantitation experiments, the signal for each cDNA/DNA was normalized to GAPDH levels, thereby allowing the comparison of message and genomic expression levels in different samples.

Western Blot analysis

Cells were lysed in radio immunoprecipitation assay buffer (50 mm Tris [pH 7.5], 150 mm NaCl, 1% Nonidet P-40, 0.5% deoxycholate, 0.1% SDS, 1x Complete inhibitors [Roche Applied Science, Pleasanton, CA] and Phosphatase inhibitors), incubated on ice for 30 min, and then centrifuged at 13,400 x g for 10 min at 4°C. Cleared supernatants were transferred to fresh tubes, and their protein concentrations were determined via bicinchoninic acid assay (Thermo Fisher Scientific, Waltham, MA). The resulting proteins were separated via reducing SDS-PAGE, transferred to polyvinylidene difluoride membranes, incubated in blocking buffer (5% Bovine Serum

Albumin in Tris-buffered saline with 0.1% Tween 20 [TBST]) for 1 h with agitation, and then probed with the appropriate primary antibody diluted in blocking buffer. Blots were then washed three times with TBST, incubated with the appropriate secondary antibodies in blocking buffer, and then washed a further three times with TBST. Blots were developed with an ECL Advance (check company), and the resulting data were captured with G:BOX (Syngene). The images shown are representative of two independent experiments.

IFA and image analysis

For IFA, cells were seeded onto collagen-coated coverslips (BD Biosystems, Franklin Lakes, NJ) in six-well tissue culture plates. At the end of each experiment, cells were fixed in 2% paraformaldehyde for 8 min, washed three times in phosphate-buffered saline (PBS), and permeabilized in 0.25% Triton X-100 for 8 min. Cells were blocked in IFA blocking buffer (20% normal goat serum [NGS] in PBS) for 20 min at 37°C and incubated with the appropriate primary antibody incubation buffer (1% NGS in PBS) for 1 h at 37°C. After primary antibody incubation, coverslips were washed three times in PBS and incubated with the appropriate secondary antibody, rhodamine phalloidin for actin filaments staining, and the nuclear stain 4,6-diamidino-2-phenylindole (DAPI) for 45 min at 37°C. Coverslips were then washed three times in PBS and mounted on glass slides with Fluoromount-G (Southern Biotech, Birmingham, AL). Slides were analyzed with a DeltaVision real-time deconvolution fluorescence microscope (Applied Precision, Issaquah, WA), and images were captured with a Photometrics CoolSNAP HQ camera. Image analysis was performed with SoftWoRx (Applied Precision). Stacks of images (0.2-μm z step) were captured at 60X magnification. Stacks were subjected to deconvolution, and two- or three-section projections were made by superimposing representative z planes to generate the final image. Images shown are representative of two independent experiments.

Flow cytometry

Cells to be analyzed via flow cytometry were dissociated from tissue-culture plates using the non-enyzmatic Cellstripper reagent (25-056-CI; CellGro/Corning, Manassas, VA) and then pelleted at 1800 x *g* at 4°C for 5 mins. Cells were then fixed using 2% PFA, incubated on ice for 15 min, pelleted, resuspended in 1X Washing Buffer (1X PBS, 2% normal goat serum, 0.1% sodium azide) and analyzed on a LSR2 Flow Cytometer.

Statistical analysis

Quantitative PCR data is expressed as the mean ± Standard Error of the Mean (SEM). Statistical analysis was performed on R Software (R Core Team (2013). R: A language and environment for statistical computing. R Foundation for Statistical Computing, Vienna, Austria). One-way ANOVA was used to compare means from different groups.

CHAPTER 4

DISCUSSION AND FUTURE DIRECTIONS

KSHV infection of endothelial cells is associated with development of KS and results in upregulation of several cellular oncogenes (234). One of the cellular oncogenes that is strongly induced by KSHV infection is the heme-degrading enzyme HO-1 and HO-1 activity promotes the selective growth of KSHV-infected endothelial cells exposed to free heme (153,234). High levels of HO-1 have been reported in several types of cancer and the protein has become an attractive target for cancer therapy (201,202). Inhibition of HO-1 activity has been shown to decrease survival of tumor cells and reduce resistance to chemotherapeutic agents (209). KSHV infected cells express high levels of HO-1 *in vivo* as well as *in vitro*, while the erythrophagocytic nature of KS spindle cells leads to a heme-rich tumor microenvironment. These two interesting features prompted us to investigate the role of HO-1 expression and activity in KSHV infection. The main two foci of this dissertation were a) to investigate the mechanism of KSHV-induced HO-1 expression and b) to understand the role that HO-1 plays in KSHV infection. I chose to perform my studies in lLEC since EC of the lymphatic lineage are considered the likely precursors of KS spindle cells (105,106,285).

4.1 The mechanisms of KSHV-induced HO-1 expression

The induction of HO-1 in KSHV-infected cells has been associated with overexpression of the viral GPCR protein, which is expressed during the lytic phase of the virus life cycle (286-288). Dr. Enrique Mesri's group showed that exogenous expression of the vGPCR is sufficient for induction of HO-1 messenger RNA, and that inhibiting HO-1 activity interferes with the transforming activity of vGPCR

(286,287). In the aforementioned studies, the authors explored the role of one lytic protein in the upregulation of HO-1. The vGPCR was not evaluated in the context of KSHV infection, and the impact of latent infection was not examined. In Chapter 2, I describe my work on the mechanisms of HO-1 induction in KSHV-infected endothelial cells. Briefly, KSHV infection results in a bi-phasic induction of HO-1 represented by an initial, transient peak during early times post infection and a later sustained upregulation during latency (Chapter 2, figure 1). Subsequent investigation of latently-infected endothelial cells revealed that the miRNA miR-K12-11 encoded by KSHV is partially responsible for the induction of HO-1 through downregulation of the HO-1 transcription regulator BACH1 (Chapter 2) (147,148). miR-K12-11 has been extensively studied for its role in modulating a variety of cellular pathways in KSHV-infected cells or when expressed ectopically in isolation (140,155-157,252,289-291). For example, by targeting IKKε, mir-K12-11 inhibits IRF3/7-dependent expression of ISGs and prevents the virus from reactivating by blocking expression of RTA (156). Interestingly, by downregulating BACH1, miR-K12-11 significantly increases levels of xCT, a membrane transport protein that exchanges intracellular glutamate for extracellular cysteine. This allows for the restoration of intracellular glutathione (GSH) and protects cancer cells from oxidative stress and cell death (292,293). xCT was also recently identified as a fusion-entry receptor for KSHV and may mediate KSHV entry either alone or as part of a complex with other receptors (78,294). Since miR-K12-11 regulates a cellular pathway that is involved in viral entry and tumorigenesis, it represents a possible therapeutic target for KSHV infection and/or tumorigenesis. miR-K12-11 is an ortholog of the cellular miR-155, the expression of which is elevated in EBV-infected B-cells, which do not express an EBV ortholog (295). Interestingly, a recent paper showed that targeting of the cellular miR-155 in EBV-infected cells results in inhibition of cellular growth supporting the

hypothesis that miRNAs can be used as targets for cancer therapy (295,296). To better understand the role that miR-K12-11 plays in KS tumorigenesis, it is important to understand if and how deletion of miR-K12-11 from the virus affects the phenotype of infected cells (e.g., proliferation, angiogenesis and migration). Accordingly, at the annual international KSHV meeting in 2015, Dr. Rolf Renne presented his recent research on the effects of KSHV miRNAs on telomerase-immortalized vein endothelial (TIVE) cells (oral presentation, unpublished data). He showed that TIVE cells infected with a virus lacking miR-K12-11 display a reduced rate of migration and cell division, while angiogenic activity is similar to that of WT-infected cells. It would be interesting to study these phenotypes in iLEC cells infected with wild type versus ∆miR-K12-11 KSHV. In addition, studying phenotypes such as apoptosis and wound healing in the presence of the mutant virus would further shed light on the role of miR-K12-11 in KS tumorigenesis. TIVE cells and iLEC originated from different primary EC, human umbilical vein and lymphatic endothelium, respectively. Because KSHV infection of blood cells and lymphatic cells alters different cellular pathways (250,285,297,298), it is plausible that different phenotypes would be detected using these two cell systems, allowing for a more complete picture of the tumorigenic activity of KSHV.

Because miR-K12-11 is only partially responsible for HO-1 induction during latency, it is important to investigate if and how other viral or cellular components contribute to HO-1 expression in KSHV infected cells. Along these lines, a recent study demonstrated that KSHV upregulates the host NRF2 protein during latent infection of EC (257). As mentioned in Chapter 1, NRF2 is a transcriptional activator for HO-1 and other genes involve in oxidative stress. More recently, novel target genes for NRF2 have been discovered, including the anti-apoptotic Bcl-2/Bcl-xL, some members of the proangiogenic HIF-1/VEGF pathway (299), the prometastatic

matrix metalloproteinase 9 (MMP9) (300), members of the proliferative pentose phosphate pathway (301), the drug resistance Mrp1 and Mrp2 (302,303), and the proinflammatory COX-2 (257). All these genes share the ability to promote survival of cancer cells, suggesting that KSHV might also benefit from their upregulation. Thus, it will be important to investigate the role of all these genes during KSHV-infection. Additionally, a recent publication by Dr. Zhiqian Qin's group suggests an additional viral mechanism of HO-1 induction during latency. The authors showed that exogenous expression of KSHV LANA-1 results in HO-1 upregulation in endothelial cells (304). In order to determine the role of LANA-1 in HO-1 induction during latency, it will be necessary to perform additional experiments in the context of the virus. Because only a limited number of viral genes are expressed during KSHV latency (305), it would be interesting to evaluate whether other latent genes might be involved in HO-1 regulation.

In Chapter 2, I demonstrated that KSHV induces HO-1 at very early times post infection (between 4-8 hpi) through a mechanism that is independent of miR-K12-11 and *de novo* viral gene expression. Interestingly, Dr. Bala Chandran's research group has recently shown that induction of ROS following KSHV infection results in the upregulation of several stress-inducible genes, including HO-1, in endothelial cells (257). Additionally, they discovered that anti-oxidant treatment prior to infection reduces KSHV infection. Interestingly, it has also been shown that treatment of latently-infected cells with oxidants (i.e. hydrogen peroxide) promotes KSHV reactivation (306), while treatment with anti-oxidants (i.e. N-acetyl-L-cysteine) blocks reactivation (306,307). These findings emphasize the critical role of oxidative stress in promoting KSHV infection and suggest that ROS inhibitors may be an attractive target for KS therapy.

4.2 The role that HO-1 plays in KSHV infection

As mentioned in section 4.1 above, early induction of HO-1 in KSHV-infected cells is, at least in part, the result of oxidative stress and upregulation of NRF2 in response to early viral sensing (257). Given that several viruses, including KSHV, modulate target cells to promote an effective infection, I wanted to investigate the role of HO-1 in initial KSHV infection of endothelial cells. The results I present in Chapter 3 suggest that HO-1 induction is responsible for inhibition of TLR4-signaling, therefore representing a novel mechanism of KSHV-mediated innate immune evasion in endothelial cells (See Figure 4.1).

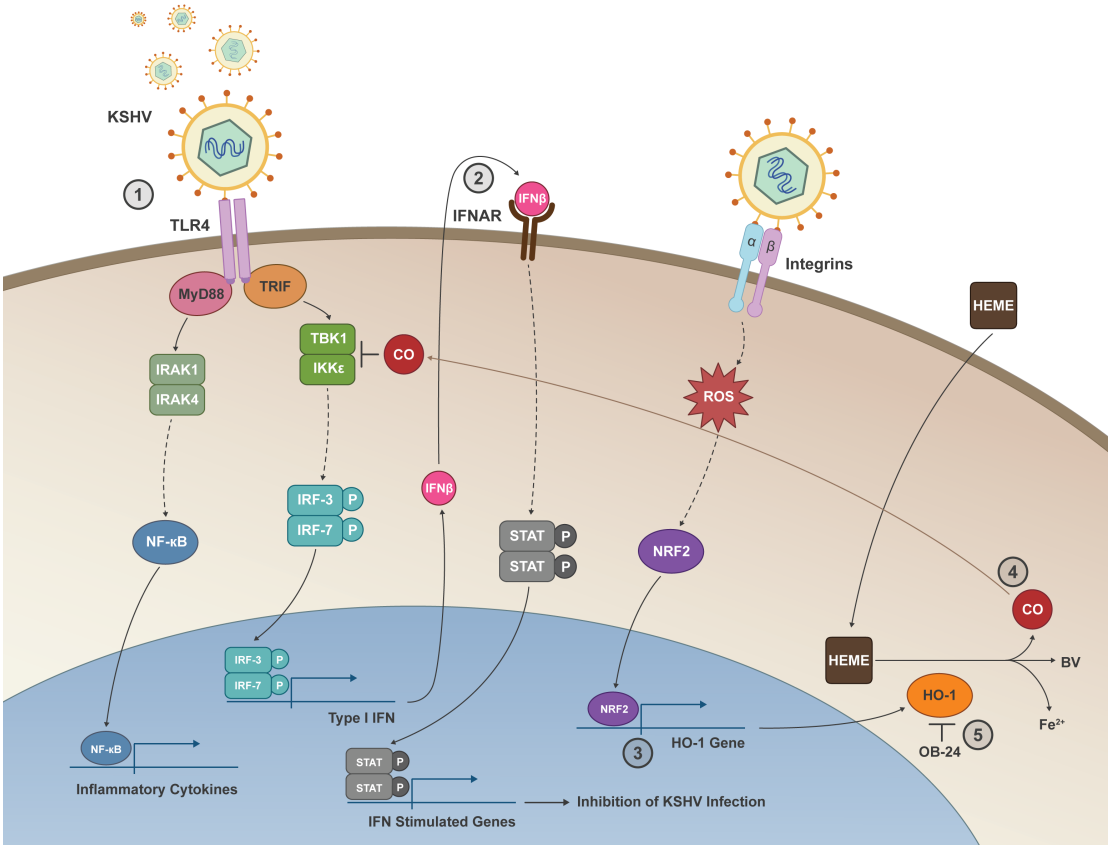

Figure 4.1 TLR4 inhibition by KSHV-induced HO-1. 1. KSHV binds to TLR4 and activates its signaling pathway, which leads to transcription of inflammatory cytokines and Type I IFN. **2.** IFNβ is secreted from the cell and binds to IFNAR, resulting in activation of IFN signaling and transcription of IFN stimulated genes (ISGs), which inhibit KSHV infection. **3.** KSHV binding to integrins leads to activation of several cellular pathways leading to production of ROS and induction of the HO-1 transcriptional activator NRF2. NRF2 activates transcription of HO-1. **4.** HO-1 induction results in enzymatic degradation of heme into biliverdin (BV), ferrous iron and carbon monoxide (CO). CO inhibits TLR4 signaling by blocking the TRIF-dependent pathway, leading to reduced expression of IFNβ and ISGs **5.** OB-24, an inhibitor of HO-1 enzyme activity, blocks production of CO and consequent inhibition of the TLR4 pathway.

Both HO-1 and the heme metabolite CO have been shown to inhibit TLR4-induced cytokines and oxidative stress in cells (276,277,281,308-312). In particular, induction of HO-1 results in a significant decrease of IL-6, TNFα, CCL2, COX-2 transcription in LPS-treated cells (277,312), thereby suggesting a mechanism for inhibiting innate immune responses in KSHV-infected cells and neighboring cells. In addition to TLR4, CO treatment has led to inhibition of other TLRs including TLR2, TLR5, and TLR9 (277). Interestingly, CO had no effect on poly(I:C)-induced ROS production and TLR3 signaling (277). Because of the promiscuity of CO in regards to the different TLRs, it will be critical to investigate whether the phenotype observed in my experiments is attributable to the inhibition of TLR4 signaling alone. The data in Figure 3.3 show that CO is able to block TBK-1 phosphorylation caused by KSHV infection, thus blocking the TLR4-TRIF-dependent pathway; however CO treatment shows no inhibition of the TLR4-MyD88 dependent pathway. To determine the specificity of CO for TLR4 in our system, experiments should be performed in EC treated with different TLR agonists, in the presence or absence of CO. If CO is specific to TLR4 signaling, it should not have any effect on the signaling of the other TLRs. In order to better understand the inhibitory role of CO on TLR signaling in the context of KSHV infection, I propose to evaluate transcription levels of different ISGs in the presence and absence of CO. ISGs are the direct mediators of the antiviral effect (284) and, as previously mentioned in Chapter 3, they affect different steps of the viral cycle. As shown in Figure 3.7, our data suggest that TLR4 signaling affects steps of the viral cycle involving transcription and/or translation of gene expression, thus suggesting the involvement of ISGs in this phenotype.

Only a small subset of TLRs have been shown to be directly activated by KSHV infection. These include TLR9 and TLR4; no data are available for the other TLRs. Interestingly, TLR3 has been shown to be a target of several KSHV proteins,

but the precise role of this PRR in KSHV infection is still unknown. Because TLR4 and TLR3 share the adaptor protein TRIF and the downstream pathway, it will be important to investigate whether CO is able to also block the TLR3-TRIF-dependent pathway in the context of KSHV infection. As previously mentioned, CO showed no inhibition of TLR3 signaling in macrophages (277), suggesting that the TLR3-TRIF-dependent pathway should not be affected in the context of CO treatment. However, because we focus on endothelial cells and KSHV infection, the same has to be validated in our system. It is possible that CO, as showed in the Nakahira et al. paper {Nakahira:2006hw}, has a broad inhibitory effect on TLRs, thus constituting a more generic mechanism of innate immune evasion (277). Along these lines, it would be interesting to evaluate the inhibitory effect of CO on non-TLR PRRs such as the nuclear sensors RIG-1, MDA-5, DDX41, DAI, IFI16 and cGAS in the context of KSHV-infection. In order to investigate activation of these PRRs in the presence of CO, the simplest experiment would be to evaluate the phosphorylation status of IRF-3. IRF-3 and IRF-7 are key transcriptional regulators of type I IFN-dependent responses, which plays a critical role in innate immunity against DNA and RNA viruses (313,314). IRF-3 and IRF-7 regulate transcription of type I IFN genes and ISGs by binding to an interferon-stimulated response element (ISRE) in their respective promoters. In the absence of viral infection, inactive IRF-3 and IRF-7 are maintained as monomers in the cytoplasm. During viral infection, IRF-3 and IRF-7 are phosphorylated leading to their dimerization and nuclear translocation. When in the nucleus, the IRF-3/IRF-7 dimer is able to activate transcription of type I IFN and ISG genes, promoting innate immune responses against the virus (313,314).

Another interesting aspect of CO is its involvement in blocking T-cell proliferation (315) and dendritic cell (DC) maturation (311), suggesting that HO-1 activity also interferes with adaptive immune responses. It would be noteworthy to

study whether KSHV-induction of HO-1 has any impact on recruitment of T-cells or other immune components to the site of viral infection. Additionally, the effect of HO-1 should be examined in KSHV-infected B-cells in order to determine if, similarly to other antigen presenting cells (i.e. DCs), B-cell maturation is impaired.

In Chapter 3, I showed that inhibition of HO-1 activity by the small molecule inhibitor OB-24 results in a reduced rate of KSHV infection in iLEC (Chapter 3, Figure 3.3). These experiments also demonstrated that treatment of infected cells with OB-24 results in enhanced expression of IFNβ and inflammatory cytokines, supporting the observation that HO-1 blocks innate immune responses. Similar results were observed in KSHV-infected iLEC transduced with a HO-1-specific shRNA. Moreover, iLEC expressing the shRNA against HO-1 were less permissive to KSHV infection as compared to control cells (Figure 4.2).

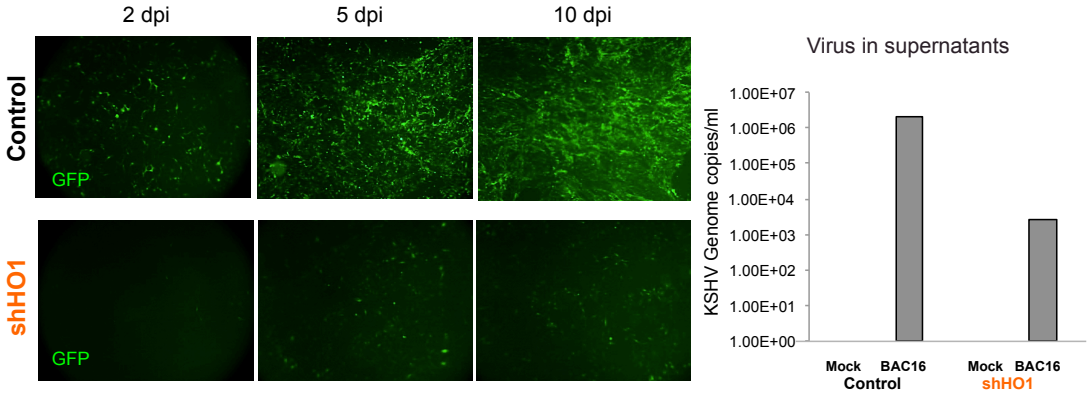

Figure 4.2 KSHV infection is impaired in iLEC expressing shRNA against HO-1 (shHO-1). On the left, top panels: iLEC transduced with control shRNA (control) and infected with KSHV-BAC16 for 2,5,10 days. Bottom panels: iLEC transduced with shRNA against HO-1 (shHO1) and infected with KSHV-BAC16 for 2,5,10 day. GFP is shown as marker of infection. On the right: qPCR for KSHV genome in supernatants from mock and KSHV-BAC16 infected control iLEC and shHO-1 iLEC at 10 dpi.

Additional experiments are required to evaluate how OB-24 treatment affects latent infection of iLEC, such as by investigating apoptosis, angiogenesis and proliferation of infected cells in the presence or absence of OB-24. As previously published by Dr. Moses' group, KSHV-infected DMVEC treated with another HO-1 activity inhibitor, CrMP, showed lower proliferation rate compared to cells treated with an inactive analog (CuMP) (153). A similar outcome is expected with OB-24-mediated inhibition, which has the advantage of being a water-soluble compound with low toxicity (221). Along these lines, a recent paper showed an inhibitory effect of the HO-1 activity inhibitor SnPP using *in vitro* and *in vivo* KS model systems (304). In an *in vitro* model of KS, SnPP treatment promoted cell death in KSHV-infected endothelial cells. More importantly SnPP treatment in a humanized mouse model of KS resulted in reduction of tumor size and decreased KSHV LANA-1 expression in the tumor (304). These data confirm that inhibition of HO-1 activity is able to affect both KS tumorigenesis as well as KSHV infection.

While HO-1 clearly plays an important role in KSHV infection and pathogenesis, whether HO-1 influences other herpesvirus infections remains to be clarified. To date, we have evaluated RRV, which infects macaques and is highly homologous to KSHV: RRV infection of iLEC showed no upregulation of HO-1 mRNA (Figure 4.3).

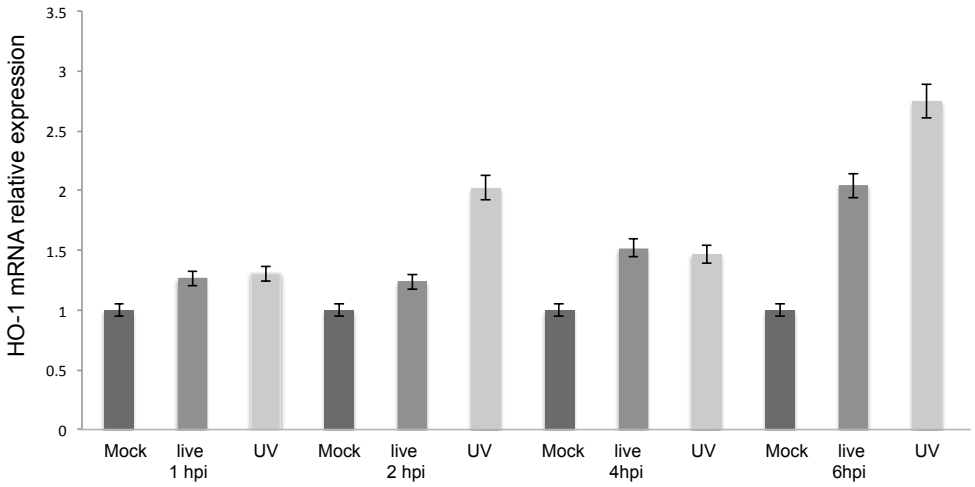

Figure 4.3 HO-1 mRNA levels in iLEC infected with live or UV-inactivated RRV-BAC. HO-1 message levels in iLEC infected with mock, live-RRV-BAC (live) or UV-inactivated RRV-BAC (UV) for either 1h, 2h, 4h or 6h. Data expressed as mean±SEM, n=3.

Similar results were obtained by a previous graduate student in the Moses' laboratory (Dr. McAllister, unpublished data). Because of the homology between KSHV and RRV, it is interesting and somewhat surprising that RRV does not induce HO-1. One explanation might reside in the uniqueness of the KS microenvironment: KS lesions are characterized by disorganized networks of abnormal microvasculature, which do not preserve the integrity of the endothelium and allow for extensive extravasation of erythrocytes which engulf and destroy by KS spindle (tumor) cells. This phenotype is not a feature of RRV-induced retroperitoneal fibromatosis (113). Thus, lesions caused by the two viruses likely have a very different microenvironment and RRV might not benefit from increased expression of HO-1. In addition, it is possible that RRV infection of human endothelial cells does not result in a physiological infection: experiments should be repeated in rhesus cells for further elucidation.

It was recently published that HCMV induces several cellular proteins to protect infected cells from ROS and oxidative stress (316). Specifically, the authors showed that HCMV does not activate NRF2 and does not increase HO-1 expression in telomerized fibroblasts. In contrast, other groups have shown an increase in HO-1 message RNA and protein expression upon HCMV infection in primary fibroblasts (317,318). In order to evaluate the role of HO-1 in HCMV-infected endothelial cells, I infected iLEC with an endotheliotropic strain of HCMV (TB40/E) (319). My experiments showed that HCMV does not upregulate HO-1 message RNA or protein in iLEC.

Next, I infected iLEC expressing HO-1-specific shRNA with TB40/E. HCMV infection was not affected by the downregulation of HO-1, as shown by the percentage of GFP+ cells quantitated by flow cytometry, suggesting that the enzyme is not involved in HCMV infection, at least in this cell type (Figure 4.4).

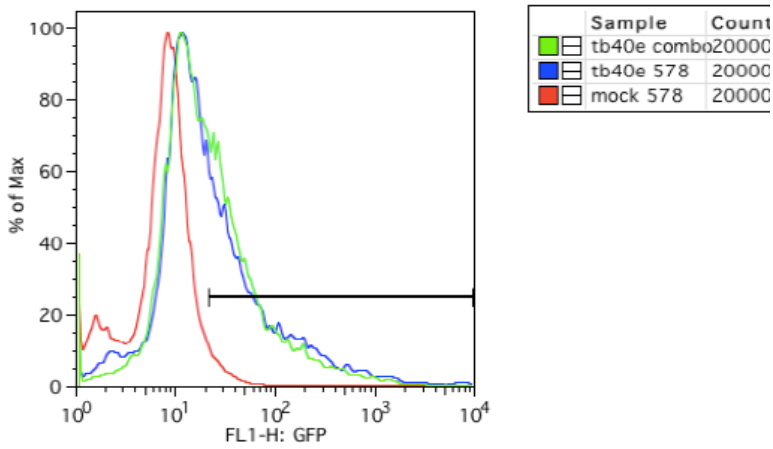

Figure 4.4 HCMV TB40/E infection in iLEC. Infection of iLEC expressing a control shRNA (578) or shRNAs against HO-1 (combo) with HCMV TB40/E for 7 d. Flow cytometry was used to determine the percentage of GFP positive cells in mock-infected cells (red), TB40/E infected control (blue) or TB40/E infected combo (green).

Because HO-1 is highly upregulated during KSHV latency in endothelial cells, it would be informative to investigate HO-1 upregulation in latent reservoirs for HCMV such as monocytes (320), and compare these results to the findings observed in fibroblasts and endothelial cells. To fully understand the role of HO-1 in herpesviral pathogenesis, additional experiments should be performed with other species. However, it is possible that the promotion of viral infection by HO-1 is specific to KSHV, due to the unique heme-rich environment of KS tumors.

Since HO-1 and oxidative stress play such a critical role in KSHV infection and tumorigenesis, I propose that the use of HO-1 inhibitors in combination with anti-oxidants might be a possible therapy for KS and/or to reduce KSHV infection in patients. The two components of the therapy will, on one side, prevent viral reactivation and inhibit active replication and, on the other side, inhibit the tumor by downregulating cellular genes involved in tumorigenesis.

APPENDIX I

VIRAL PURIFICATION AND TITRATION

In order to investigate the mechanisms of early HO-1 induction in KSHV infected EC, I decided to performed experiments with replication-deficient viruses. “Inactive” viruses still have the ability to bind and enter in the target cells without resulting in a productive infection. UV-inactivation is one method used to obtain a replication-deficient virus. However, UV-inactivated viruses have some disadvantages because they still contain the (cross-linked) viral genome, which can potentially trigger innate immune responses (also important for TLRs studies) and additionally, viral proteins are also cross-linked during the process, thus complicating the interpretation of my results. Interestingly, KSHV production *in vitro* results in a combination of immature and mature capsids defined A-, B- and C-type capsids. A and B capsids are immature forms and do not contain any viral genome (321,322). They can be distinguished from one another for the presence of the scaffolding protein (SCAF) contained in B capsids only. Thus, I decided to use B capsids as a source of replication-deficient virus, and C capsids as my infectious virus population. In order to obtain the three individual types of capsids, the virus obtained from producer cells (iSLK) underwent through three purification steps, using a modified version of the protocol described by Dr. Ke Lan’s group (255). The first step involved a centrifugation at 78,000 x *g* for 2 hours at 4°C, using a sucrose cushion (see Material and Methods in Chapter 2). The resulting virus pellets were then resuspended in TNE. The second step involved virus purification on discontinuous gradient. OptiPrep (60% iodixanol in water, Sigma Aldrich) was used to create a discontinuous gradient from 20% to 50% iodixanol, with a 5% step. After loading each dilution on an

ultracentrifuge tube, the resuspended viruses were loaded at the top of the tube and centrifuged for 4h at 78,000 x g at 4°C. After centrifugation, three different bands were visible for each virus representing the A, B and C capsids (shown in Figure A.1). The third step involved isolating each virus population by individually aspirating each band using a syringe. After that, the viruses were purified using a tabletop ultracentrifuge at 78,000 x *g* for 2 h at 4°C. The resulting pellets were then resuspended in TNE and stored at -80°C.

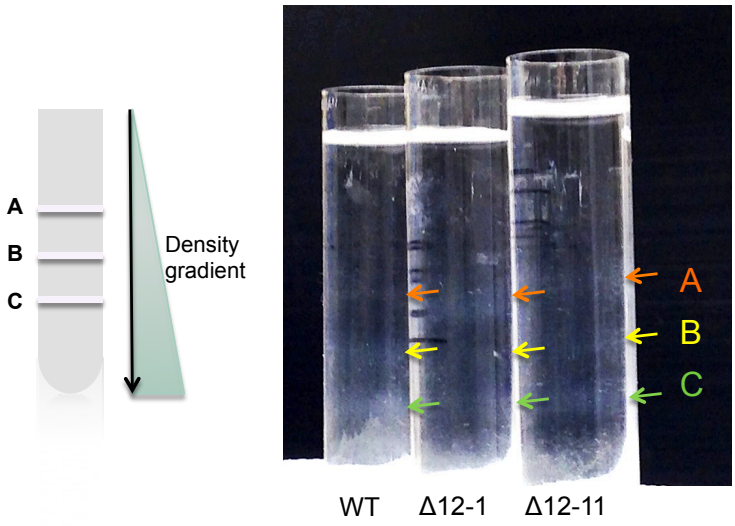

Capsid type	MCP, SCIP and TRI-1,2	SCAF	dsDNA
A	yes	no	no
B	yes	yes	no
C	yes	no	yes

Figure A.1: Virus purification using density gradient. Top two figures show the density gradient with the separation of the three bands representing the A- B- and C-type capsids for KSHV-BAC16-WT (WT), KSHV-BAC16-Δ12-1 (Δ12-1) and KSHV-BAC16-Δ12-11 (Δ12-11).

In order to confirm the purity of each band, detection of viral genome was performed by qPCR on each capsid preparation. As shown in Figure A.2, KSHV genome was detected in C capsids only.

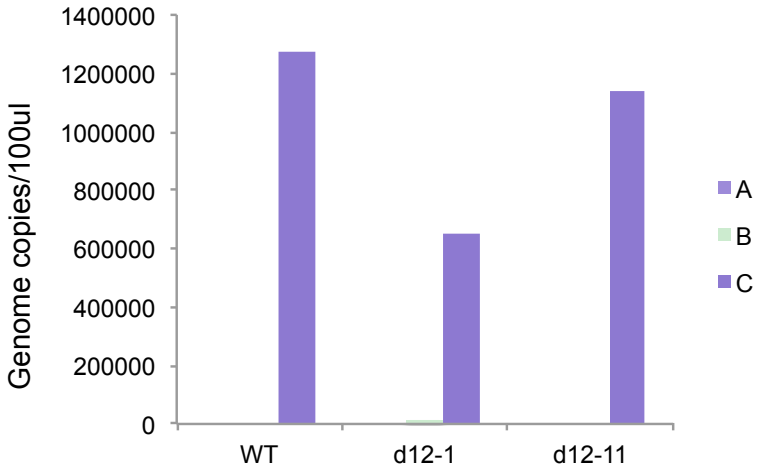

Figure A.2: qPCR for KSHV genomes in the virus preparations. qPCR for ORF26 DNA in a 100ul of virus preparation for KSHV-BAC16-WT (WT), KSHV-BAC16-Δ12-1 (d12-1) and KSHV-BAC16-Δ12-11 (d12-11). Three different preparations were tested for each virus, representing the three bands for A-type capsids (A), B-type capsids (B) and C-type capsids (C).

In order to infect iLEC with equal numbers of virus particles, we decided to normalize the infection to KSHV tegument protein ORF45. As shown in Figure A.3, equal volumes (10 µl) of each preparation were loaded on protein gels and subsequently incubated with an anti-ORF45 antibody (2D4A5-Abcam). Interestingly, KSHV WT virus and the two miRNA mutant viruses (d12-1 and d12-11) appeared different for each of their three capsid populations. For example, in the WT preparation the mature capsids are the predominant ones as opposed to the miRNA-K12-1 mutant preparation where the three capsids are present in equal proportions. To calculate the amounts of virus needed for the experiment, the infection was normalized to "equal ORF45 levels" by quantifying each ORF45 band by densitometry.

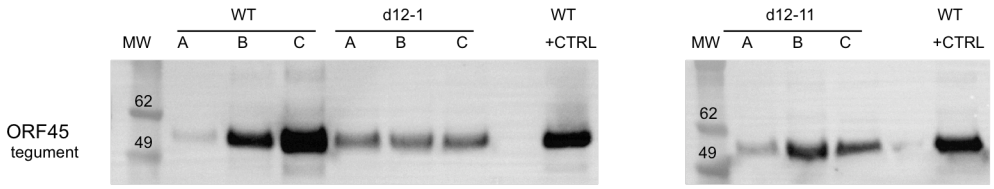

Figure A.3: WB for ORF45 in the different virus preparations. Equal volumes of each virus preparation was loaded on a protein gel. Three different preparations were tested for each virus, representing the three bands for A-type capsids (A), B-type capsids (B) and C-type capsids (C). Each virus is represented by KSHV-BAC16-WT (WT), KSHV-BAC16-Δ12-1 (d12-1) and KSHV-BAC16-Δ12-11 (d12-11). WT+CTRL: standard preparation as control. The blot was then stained for KSHV tegument protein ORF45. MW: Molecular weight.

Interestingly, iLEC infected with either mature (C-type) or genome-devoid (B-type) viruses showed upregulation of HO-1 (Figure A.4), either in the presence (WT) or absence of the miRNAs (d12-1 and d12-11). These results supported the hypothesis that HO-1 induction is indeed due to a component of the virus particle regardless of *de novo* viral gene expression and miR-K12-11.

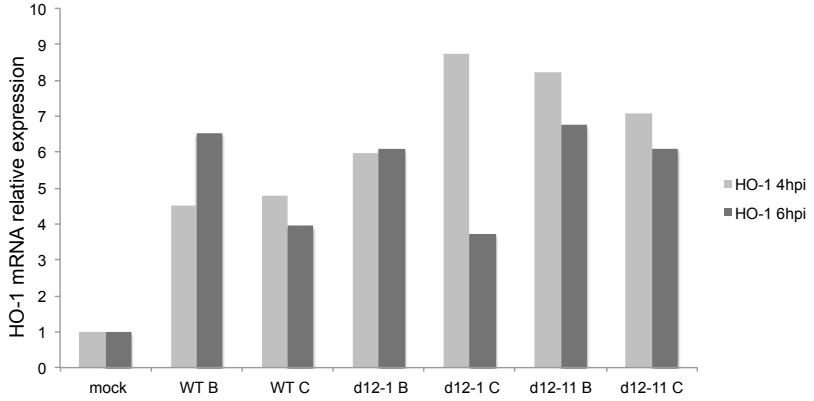

Figure A.4: qPCR for HO-1 mRNA in iLEC infected with B- capsids or C-capsids. iLEC were infected with KSHV-BAC16-WT B-type capsid (WT B) or C-type capsid (WT C), with KSHV-BAC16-d12-1 B-type capsid (d12-1 B) or C-type capsid (d12-1 C), or with KSHV-BAC16-d12-11 B-type capsid (d12-11 B) or C-type capsid (d12-11 C) for 4 h (light grey) or 6 h (dark grey).

References

1. Roizman B, Carmichael LE, Deinhardt F, de-The G, Nahmias AJ, Plowright W, et al. Herpesviridae. Definition, provisional nomenclature, and taxonomy. The Herpesvirus Study Group, the International Committee on Taxonomy of Viruses. Intervirology. 1981;16(4):201–17.

2. Arvin A, Campadelli-Fiume G, Mocarski E, Moore PS, Roizman B, Whitley R, et al. Overview of classification. Cambridge: Cambridge University Press; 2007.

3. Whitley RJ, Roizman B. Herpes simplex virus infections. Lancet. Elsevier; 2001 May 12;357(9267):1513–8.

4. Kinchington PR, Leger AJS, Guedon J-MG, Hendricks RL. Herpes simplex virus and varicella zoster virus, the house guests who never leave. Herpesviridae. BioMed Central; 2012;3(1):5.

5. Oxman MN. Zoster vaccine: current status and future prospects. Clin Infect Dis. Oxford University Press; 2010 Jul 15;51(2):197–213.

6. Oxman MN, Levin MJ, Johnson GR, Schmader KE, Straus SE, Gelb LD, et al. A vaccine to prevent herpes zoster and postherpetic neuralgia in older adults. N Engl J Med. 2005 Jun 2;352(22):2271–84.

7. Arvin A, Campadelli-Fiume G, Mocarski E, Moore PS, Roizman B, Yamanishi K, et al. Pathogenesis and disease. Cambridge: Cambridge University Press; 2007.

8. Arvin A, Campadelli-Fiume G, Mocarski E, Moore PS, Roizman B, Whitley R, et al. Comparative genome and virion structure. Cambridge: Cambridge University Press; 2007.

9. Moore PS, Chang Y. Kaposi's sarcoma-associated herpesvirus-encoded oncogenes and oncogenesis. J Natl Cancer Inst Monographs. 1998;(23):65–71.

10. Bouvard V, Baan R, Straif K, Grosse Y, Secretan B, Ghissassi El F, et al. A review of human carcinogens--Part B: biological agents. Lancet Oncol. 2009 Apr;10(4):321–2.

11. de Martel C, Ferlay J, Franceschi S, Vignat J, Bray F, Forman D, et al. Global burden of cancers attributable to infections in 2008: a review and synthetic analysis. Lancet Oncol. 2012 Jun;13(6):607–15.

12. Hausen zur H. The search for infectious causes of human cancers: where and why (Nobel lecture). Angew Chem Int Ed Engl. WILEY-VCH Verlag; 2009;48(32):5798–808.

13. Hanahan D, Weinberg RA. The hallmarks of cancer. Cell. 2000 Jan

7;100(1):57–70.

14. Hanahan D, Weinberg RA. Hallmarks of cancer: the next generation. Cell. 2011 Mar 4;144(5):646–74.

15. Vogelstein B, Kinzler KW. The multistep nature of cancer. Trends Genet. 1993 Apr;9(4):138–41.

16. Bouvard V, Baan R, Straif K, Grosse Y, Secretan B, Ghissassi El F, et al. A review of human carcinogens--Part B: biological agents. Lancet Oncol. 2009 Apr;10(4):321–2.

17. McFadden K, Luftig MA. Interplay Between DNA Tumor Viruses and the Host DNA Damage Response. In: Intrinsic Immunity. Berlin, Heidelberg: Springer Berlin Heidelberg; 2013. pp. 229–57.

18. Arzumanyan A, Reis HMGPV, Feitelson MA. Pathogenic mechanisms in HBV- and HCV-associated hepatocellular carcinoma. Nat Rev Cancer. 2013 Feb;13(2):123–35.

19. Giffin L, Damania B. KSHV: Pathways to Tumorigenesis and Persistent Infection. 1st ed. ADVANCES IN VIRUS RESEARCH. Elsevier Inc; 2014. 49 p.

20. Mesri EA, Feitelson MA, Munger K. Human viral oncogenesis: a cancer hallmarks analysis. Cell Host and Microbe. 2014 Mar 12;15(3):266–82.

21. Yoshida M. Multiple viral strategies of HTLV-1 for dysregulation of cell growth control. Annu Rev Immunol. Annual Reviews 4139 El Camino Way, P.O. Box 10139, Palo Alto, CA 94303-0139, USA; 2001;19(1):475–96.

22. Matsuoka M, Jeang K-T. Human T-cell leukaemia virus type 1 (HTLV-1) infectivity and cellular transformation. Nat Rev Cancer. Nature Publishing Group; 2007 Apr;7(4):270–80.

23. Zemel R, Issachar A, Tur-Kaspa R. The role of oncogenic viruses in the pathogenesis of hepatocellular carcinoma. Clin Liver Dis. 2011 May;15(2):261–79–vii–x.

24. Martin-Vilchez S, Lara-Pezzi E, Trapero-Marugán M, Moreno-Otero R, Sanz-Cameno P. The molecular and pathophysiological implications of hepatitis B X antigen in chronic hepatitis B virus infection. Rev Med Virol. John Wiley & Sons, Ltd; 2011 Sep;21(5):315–29.

25. Vrancken K, Paeshuyse J, Liekens S. Angiogenic activity of hepatitis B and C viruses. Antivir Chem Chemother. SAGE Publications; 2012;22(4):159–70.

26. Lok AS-F. Navigating the maze of hepatitis B treatments. Gastroenterology. 2007 Apr;132(4):1586–94.

27. Lok AS. Natural history and control of perinatally acquired hepatitis B virus

infection. Dig Dis. 1992;10(1):46–52.

28. Smith MA, Love BL, Mohammad RA. The changing landscape of adverse drug events associated with chronic hepatitis C virus therapy. Expert Opin Drug Saf. Informa Healthcare; 2015 Nov;14(11):1649–52.

29. McLaughlin-Drubin ME, Meyers J, Munger K. Cancer associated human papillomaviruses. Current Opinion in Virology. 2012 Aug;2(4):459–66.

30. Moody CA, Laimins LA. Human papillomavirus oncoproteins: pathways to transformation. Nat Rev Cancer. Nature Publishing Group; 2010 Aug;10(8):550–60.

31. Goodwin EC, Yang E, Lee CJ, Lee HW, DiMaio D, Hwang ES. Rapid induction of senescence in human cervical carcinoma cells. Proceedings of the National Academy of Sciences. National Academy of Sciences; 2000 Sep 26;97(20):10978–83.

32. Roman A, Munger K. The papillomavirus E7 proteins. Virology. 2013 Oct;445(1-2):138–68.

33. Vande Pol SB, Klingelhutz AJ. Papillomavirus E6 oncoproteins. Virology. 2013 Oct;445(1-2):115–37.

34. Zwerschke W, Mazurek S, Massimi P, Banks L, Eigenbrodt E, Jansen-Dürr P. Modulation of type M2 pyruvate kinase activity by the human papillomavirus type 16 E7 oncoprotein. Proceedings of the National Academy of Sciences. National Academy of Sciences; 1999 Feb 16;96(4):1291–6.

35. Russell M, Raheja V, Jaiyesimi R. Human papillomavirus vaccination in adolescence. Perspect Public Health. SAGE Publications; 2013 Nov;133(6):320–4.

36. Kash N, Lee MA, Kollipara R, Downing C, Guidry J, Tyring SK. Safety and Efficacy Data on Vaccines and Immunization to Human Papillomavirus. J Clin Med. Multidisciplinary Digital Publishing Institute; 2015;4(4):614–33.

37. Darus CJ, Mueller JJ. Development and impact of human papillomavirus vaccines. Clin Obstet Gynecol. 2013 Mar;56(1):10–6.

38. Feng H, Shuda M, Chang Y, Moore PS. Clonal integration of a polyomavirus in human Merkel cell carcinoma. Science. American Association for the Advancement of Science; 2008 Feb 22;319(5866):1096–100.

39. Chen T, Hedman L, Mattila PS, Jartti T, Ruuskanen O, Söderlund-Venermo M, et al. Serological evidence of Merkel cell polyomavirus primary infections in childhood. J Clin Virol. 2011 Feb;50(2):125–9.

40. Shuda M, Feng H, Kwun HJ, Rosen ST, Gjoerup O, Moore PS, et al. T antigen mutations are a human tumor-specific signature for Merkel cell

polyomavirus. Proc Natl Acad Sci USA. National Acad Sciences; 2008 Oct 21;105(42):16272–7.

41. Shuda M, Kwun HJ, Feng H, Chang Y, Moore PS. Human Merkel cell polyomavirus small T antigen is an oncoprotein targeting the 4E-BP1 translation regulator. J Clin Invest. American Society for Clinical Investigation; 2011 Sep;121(9):3623–34.

42. Wendzicki JA, Moore PS, Chang Y. Large T and small T antigens of Merkel cell polyomavirus. Current Opinion in Virology. 2015 Apr;11:38–43.

43. Locke FL, Rollison DE, Sondak VK. Merkel cell carcinoma and immunosuppression: what we still need to know. J Natl Cancer Inst. Oxford University Press; 2015 Feb;107(2):dju422–2.

44. Wiedinger K, Bitsaktsis C, Chang S. Reactivation of human polyomaviruses in immunocompromised states. J Neurovirol. Springer US; 2014 Feb;20(1):1–8.

45. Cesarman E, Mesri EA. Kaposi sarcoma-associated herpesvirus and other viruses in human lymphomagenesis. Curr Top Microbiol Immunol. 2007;312:263–87.

46. Kutok JL, Wang F. Spectrum of Epstein-Barr virus-associated diseases. Annu Rev Pathol. Annual Reviews; 2006;1(1):375–404.

47. Young LS, Rickinson AB. Epstein-Barr virus: 40 years on. Nat Rev Cancer. Nature Publishing Group; 2004 Oct;4(10):757–68.

48. Thorley-Lawson DA. Epstein-Barr virus: exploiting the immune system. Nat Rev Immunol. 2001 Oct;1(1):75–82.

49. Geng L, Wang X. Epstein-Barr Virus-associated lymphoproliferative disorders: experimental and clinical developments. Int J Clin Exp Med. e-Century Publishing Corporation; 2015;8(9):14656–71.

50. Chang Y, Cesarman E, Pessin MS, Lee F, Culpepper J, Knowles DM, et al. Identification of herpesvirus-like DNA sequences in AIDS-associated Kaposi's sarcoma. Science. 1994 Dec 16;266(5192):1865–9.

51. Ganem D. KSHV and the pathogenesis of Kaposi sarcoma: listening to human biology and medicine. J Clin Invest. American Society for Clinical Investigation; 2010 Apr;120(4):939–49.

52. Mesri EA, Cesarman E, Boshoff C. Kaposi's sarcoma and its associated herpesvirus. Nature Publishing Group; 2010 Oct 1;:1–13.

53. Bhutani M, Polizzotto MN, Uldrick TS, Yarchoan R. Kaposi sarcoma-associated herpesvirus-associated malignancies: epidemiology, pathogenesis, and advances in treatment. Semin Oncol. 2015 Apr;42(2):223–46.

54. Orenstein JM. Ultrastructure of Kaposi sarcoma. Ultrastruct Pathol. 2008 Sep;32(5):211–20.

55. Douglas JL, Gustin JK, Dezube B, Pantanowitz JL, Moses AV. Kaposi's sarcoma: a model of both malignancy and chronic inflammation. Panminerva Med. 2007 Sep;49(3):119–38.

56. Pantanowitz L, Moses AV, Dezube BJ. The inflammatory component of Kaposi sarcoma. Exp Mol Pathol. 2009 Oct;87(2):163–5.

57. Douglas JL, Gustin JK, Moses AV, Dezube BJ, Pantanowitz L. Kaposi Sarcoma Pathogenesis: A Triad of Viral Infection, Oncogenesis and Chronic Inflammation. Transl Biomed. NIH Public Access; 2010;1(2).

58. Pantanowitz L, Dezube BJ. Kaposi's sarcoma. Ear Nose Throat J. 2004 Mar;83(3):157.

59. Radu O, Pantanowitz L. Kaposi sarcoma. Arch Pathol Lab Med. the College of American Pathologists; 2013 Feb;137(2):289–94.

60. Schulz TF. The pleiotropic effects of Kaposi's sarcoma herpesvirus. J Pathol. John Wiley & Sons, Ltd; 2006 Jan;208(2):187–98.

61. Stebbing J, Pantanowitz L, Dayyani F, Sullivan RJ, Bower M, Dezube BJ. HIV-associated multicentric Castleman's disease. Am J Hematol. Wiley Subscription Services, Inc., A Wiley Company; 2008 Jun;83(6):498–503.

62. Du M-Q, Bacon CM, Isaacson PG. Kaposi sarcoma-associated herpesvirus/human herpesvirus 8 and lymphoproliferative disorders. Journal of Clinical Pathology. 2006 Dec 20;60(12):1350–7.

63. Mylona EE, Baraboutis IG, Lekakis LJ, Georgiou O, Papastamopoulos V, Skoutelis A. Multicentric Castleman's disease in HIV infection: a systematic review of the literature. AIDS Rev. 2008 Jan;10(1):25–35.

64. Carbone A, Gloghini A, Capello D, Gaidano G. Genetic pathways and histogenetic models of AIDS-related lymphomas. Eur J Cancer. 2001 Jul;37(10):1270–5.

65. Fan W, Bubman D, Chadburn A, Harrington WJ, Cesarman E, Knowles DM. Distinct subsets of primary effusion lymphoma can be identified based on their cellular gene expression profile and viral association. Journal of Virology. American Society for Microbiology; 2005 Jan;79(2):1244–51.

66. Dupont C, Vasseur E, Beauchet A, Aegerter P, Berthé H, de Truchis P, et al. Long-term efficacy on Kaposi's sarcoma of highly active antiretroviral therapy in a cohort of HIV-positive patients. CISIH 92. Centre d'information et de soins de l'immunodéficience humaine. AIDS. 2000 May 26;14(8):987–93.

67. Krown SE, Lee JY, Lin L, Fischl MA, Ambinder R, Roenn Von JH. Interferon-

alpha2b with protease inhibitor-based antiretroviral therapy in patients with AIDS-associated Kaposi sarcoma: an AIDS malignancy consortium phase I trial. J Acquir Immune Defic Syndr. 2006 Feb 1;41(2):149–53.

68. Koon HB, Krown SE, Lee JY, Honda K, Rapisuwon S, Wang Z, et al. Phase II Trial of Imatinib in AIDS-Associated Kaposi's Sarcoma: AIDS Malignancy Consortium Protocol 042. Journal of Clinical Oncology. 2014 Feb 7;32(5):402–8.

69. Chaisuparat R, Hu J, Jham BC, Knight ZA, Shokat KM, Montaner S. Dual inhibition of PI3Kalpha and mTOR as an alternative treatment for Kaposi's sarcoma. Cancer Research. American Association for Cancer Research; 2008 Oct 15;68(20):8361–8.

70. Neipel F, Albrecht JC, Fleckenstein B. Human herpesvirus 8--the first human Rhadinovirus. J Natl Cancer Inst Monographs. 1998;(23):73–7.

71. Borchers K, Goltz M, Ludwig H. Genome organization of the herpesviruses: minireview. Acta Vet Hung. 1994;42(2-3):217–25.

72. Arvin A, Campadelli-Fiume G, Mocarski E, Moore PS, Roizman B, Whitley R, et al. Comparative analysis of herpesvirus-common proteins. Cambridge: Cambridge University Press; 2007.

73. Veettil MV. Kaposi's sarcoma associated herpesvirus entry into target cells. Frontiers in Microbiology.2012 Jan 18; 6–19.

74. Veettil MV, Bandyopadhyay C, Dutta D, Chandran B. Interaction of KSHV with host cell surface receptors and cell entry. Viruses. 2014 Oct;6(10):4024–46.

75. Rappocciolo G, Jenkins FJ, Hensler HR, Piazza P, Jais M, Borowski L, et al. DC-SIGN is a receptor for human herpesvirus 8 on dendritic cells and macrophages. The Journal of Immunology. 2006 Feb 1;176(3):1741–9.

76. Garrigues HJ, Rubinchikova YE, Dipersio CM, Rose TM. Integrin alphaVbeta3 Binds to the RGD motif of glycoprotein B of Kaposi's sarcoma-associated herpesvirus and functions as an RGD-dependent entry receptor. Journal of Virology. 2008 Feb;82(3):1570–80.

77. Garrigues HJ, DeMaster LK, Rubinchikova YE, Rose TM. KSHV attachment and entry are dependent on αVβ3 integrin localized to specific cell surface microdomains and do not correlate with the presence of heparan sulfate. Virology. Elsevier; 2014 Sep 1;464-465(C):118–33.

78. Kaleeba JAR. Kaposi's Sarcoma-Associated Herpesvirus Fusion-Entry Receptor: Cystine Transporter xCT. Science. 2006 Mar 31;311(5769):1921–4.

79. Boehmer PE, Lehman IR. Herpes simplex virus DNA replication. Annu Rev Biochem. 1997;66(1):347–84.

80. Lee C-P, Chen M-R. Escape of herpesviruses from the nucleus. Rev Med Virol. John Wiley & Sons, Ltd; 2010 Jul;20(4):214–30.

81. Mettenleiter TC, Müller F, Granzow H, Klupp BG. The way out: what we know and do not know about herpesvirus nuclear egress. Cellular Microbiology. 2013 Feb;15(2):170–8.

82. Purushothaman P, Thakker S, Verma SC. Transcriptome analysis of Kaposi's sarcoma-associated herpesvirus during de novo primary infection of human B and endothelial cells. Longnecker RM, editor. Journal of Virology. 2015 Mar;89(6):3093–111.

83. Chandran B. Early events in Kaposi's sarcoma-associated herpesvirus infection of target cells. Journal of Virology. 2010 Mar;84(5):2188–99.

84. Lieberman PM. Keeping it quiet: chromatin control of gammaherpesvirus latency. Nature Publishing Group. 2013 Dec;11(12):863–75.

85. Gramolelli S, Schulz TF. The role of Kaposi sarcoma-associated herpesvirus in the pathogenesis of Kaposi sarcoma. J Pathol. 2014 Dec 11;235(2):368–80.

86. Ballestas ME, Kaye KM. Kaposi's sarcoma-associated herpesvirus latency-associated nuclear antigen 1 mediates episome persistence through cis-acting terminal repeat (TR) sequence and specifically binds TR DNA. Journal of Virology. 2001 Apr;75(7):3250–8.

87. Renne R, Barry C, Dittmer D, Compitello N, Brown PO, Ganem D. Modulation of cellular and viral gene expression by the latency-associated nuclear antigen of Kaposi's sarcoma-associated herpesvirus. Journal of Virology. 2001 Jan;75(1):458–68.

88. Friborg J, Kong W, Hottiger MO, Nabel GJ. p53 inhibition by the LANA protein of KSHV protects against cell death. Nature. Nature Publishing Group; 1999 Dec;402(6764):889–94.

89. Radkov SA, Kellam P, Boshoff C. The latent nuclear antigen of Kaposi sarcoma-associated herpesvirus targets the retinoblastoma-E2F pathway and with the oncogene Hras transforms primary rat cells. Nat Med. 2000 Oct;6(10):1121–7.

90. Bubman D, Guasparri I, Cesarman E. Deregulation of c-Myc in primary effusion lymphoma by Kaposi's sarcoma herpesvirus latency-associated nuclear antigen. Oncogene. Nature Publishing Group; 2007 Jul 26;26(34):4979–86.

91. Li M, Lee H, Yoon DW, Albrecht JC, Fleckenstein B, Neipel F, et al. Kaposi's sarcoma-associated herpesvirus encodes a functional cyclin. Journal of Virology. 1997 Mar;71(3):1984–91.

92. Grundhoff A, Ganem D. Mechanisms governing expression of the v-FLIP

gene of Kaposi's sarcoma-associated herpesvirus. Journal of Virology. 2001 Feb;75(4):1857–63.

93. Swanton C, Mann DJ, Fleckenstein B, Neipel F, Peters G, Jones N. Herpes viral cyclin/Cdk6 complexes evade inhibition by CDK inhibitor proteins. Nature. Nature Publishing Group; 1997 Nov 13;390(6656):184–7.

94. Verschuren EW, Jones N, Evan GI. The cell cycle and how it is steered by Kaposi's sarcoma-associated herpesvirus cyclin. Journal of General Virology. 2004 Jun;85(Pt 6):1347–61.

95. Leidal AM, Cyr DP, Hill RJ, Lee PWK, McCormick C. Subversion of autophagy by Kaposi's sarcoma-associated herpesvirus impairs oncogene-induced senescence. Cell Host and Microbe. 2012 Feb 16;11(2):167–80.

96. Koopal S, Furuhjelm JH, Järviluoma A, Jäämaa S, Pyakurel P, Pussinen C, et al. Viral oncogene-induced DNA damage response is activated in Kaposi sarcoma tumorigenesis. PLoS Pathog. 2007 Sep 7;3(9):1348–60.

97. Baresova P, Pitha PM, Lubyova B. Distinct roles of Kaposi's sarcoma-associated herpesvirus-encoded viral interferon regulatory factors in inflammatory response and cancer. Journal of Virology. 2013 Sep;87(17):9398–410.

98. Liang C, Lee J-S, Jung JU. Immune evasion in Kaposi's sarcoma-associated herpes virus associated oncogenesis. Seminars in Cancer Biology. 2008 Dec;18(6):423–36.

99. Di Maio TA., Lagunoff M. KSHV induction of angiogenic and lymphangiogenic phenotypes. Frontiers in Microbiology. 2012 Mar 28; 102–112.

100. Jham BC, Ma T, Hu J, Chaisuparat R, Friedman ER, Pandolfi PP, et al. Amplification of the Angiogenic Signal through the Activation of the TSC/mTOR/HIF Axis by the KSHV vGPCR in Kaposi's Sarcoma. Zhang L, editor. PLoS ONE. 2011 Apr 29;6(4):e19103–11.

101. Ojala PM, Schulz TF. Manipulation of endothelial cells by KSHV: Implications for angiogenesis and aberrant vascular differentiation. Seminars in Cancer Biology. Elsevier Ltd; 2014 Jan 31;:1–9.

102. Dai L, Bai L, Lu Y, Xu Z, Reiss K, Del Valle L, et al. Emmprin and KSHV: new partners in viral cancer pathogenesis. Cancer Lett. Elsevier; 2013 Sep 1;337(2):161–6.

103. Moses AV, Fish KN, Ruhl R, Smith PP, Strussenberg JG, Zhu L, et al. Long-term infection and transformation of dermal microvascular endothelial cells by human herpesvirus 8. Journal of Virology. 1999 Aug;73(8):6892–902.

104. McAllister SC, Moses AV. Endothelial cell- and lymphocyte-based in vitro systems for understanding KSHV biology. Curr Top Microbiol Immunol.

2007;312:211–44.

105. Cancian L, Hansen A, Boshoff C. Cellular origin of Kaposi“s sarcoma and Kaposi”s sarcoma-associated herpesvirus-induced cell reprogramming. Trends Cell Biol. Elsevier; 2013 Sep;23(9):421–32.

106. Pyakurel P, Pak F, Mwakigonja AR, Kaaya E, Heiden T, Biberfeld P. Lymphatic and vascular origin of Kaposi's sarcoma spindle cells during tumor development. Int J Cancer. 2006 Sep 15;119(6):1262–7.

107. Lagunoff M, Bechtel J, Venetsanakos E, Roy A-M, Abbey N, Herndier B, et al. De novo infection and serial transmission of Kaposi's sarcoma-associated herpesvirus in cultured endothelial cells. Journal of Virology. 2002 Mar;76(5):2440–8.

108. Brehm MA, Shultz LD, Greiner DL. Humanized mouse models to study human diseases. Curr Opin Endocrinol Diabetes Obes. 2010 Apr;17(2):120–5.

109. Wang LX, Kang G, Kumar P, Lu W, Li Y, Zhou Y, et al. Humanized-BLT mouse model of Kaposi's sarcoma-associated herpesvirus infection. Proceedings of the National Academy of Sciences. 2014 Feb 25;111(8):3146–51.

110. Searles RP, Bergquam EP, Axthelm MK, Wong SW. Sequence and genomic analysis of a Rhesus macaque rhadinovirus with similarity to Kaposi's sarcoma-associated herpesvirus/human herpesvirus 8. Journal of Virology. 1999 Apr;73(4):3040–53.

111. Desrosiers RC, Sasseville VG, Czajak SC, Zhang X, Mansfield KG, Kaur A, et al. A herpesvirus of rhesus monkeys related to the human Kaposi's sarcoma-associated herpesvirus. Journal of Virology. 1997 Dec;71(12):9764–9.

112. Wong SW, Bergquam EP, Swanson RM, Lee FW, Shiigi SM, Avery NA, et al. Induction of B cell hyperplasia in simian immunodeficiency virus-infected rhesus macaques with the simian homologue of Kaposi's sarcoma-associated herpesvirus. Journal of Experimental Medicine. 1999 Sep 20;190(6):827–40.

113. Giddens WE, Tsai CC, Morton WR, Ochs HD, Knitter GH, Blakley GA. Retroperitoneal fibromatosis and acquired immunodeficiency syndrome in macaques. Pathologic observations and transmission studies. Am J Pathol. American Society for Investigative Pathology; 1985 May;119(2):253–63.

114. Orzechowska BU, Powers MF, Sprague J, Li H, Yen B, Searles RP, et al. Rhesus macaque rhadinovirus-associated non-Hodgkin lymphoma: animal model for KSHV-associated malignancies. Blood. American Society of Hematology; 2008 Nov 15;112(10):4227–34.

115. Orzechowska BU, Manoharan M, Sprague J, Estep RD, Axthelm MK, Wong

SW. Viral interleukin-6 encoded by rhesus macaque rhadinovirus is associated with lymphoproliferative disorder (LPD). J Med Primatol. Blackwell Publishing Ltd; 2009 Oct;38 Suppl 1(s1):2–7.

116. Estep RD, Axthelm MK, Wong SW. A G Protein-Coupled Receptor Encoded by Rhesus Rhadinovirus Is Similar to ORF74 of Kaposi's Sarcoma-Associated Herpesvirus. Journal of Virology. 2003 Feb 1;77(3):1738–46.

117. Jacobs SR, Damania B. The Viral Interferon Regulatory Factors of KSHV: Immunosuppressors or Oncogenes? Frontiers in Immunology. 2011;2:1–11.

118. Robinson BA, Estep RD, Messaoudi I, Rogers KS, Wong SW. Viral interferon regulatory factors decrease the induction of type I and type II interferon during rhesus macaque rhadinovirus infection. Journal of Virology. 2012 Feb;86(4):2197–211.

119. Langlais CL, Jones JM, Estep RD, Wong SW. Rhesus rhadinovirus R15 encodes a functional homologue of human CD200. Journal of Virology. 2006 Mar;80(6):3098–103.

120. Estep RD, Rawlings SD, Li H, Manoharan M, Blaine ET, O'Connor MA, et al. The rhesus rhadinovirus CD200 homologue affects immune responses and viral loads during in vivo infection. Journal of Virology. 2014 Sep;88(18):10635–54.

121. Umbach JL, Strelow LI, Wong SW, Cullen BR. Analysis of rhesus rhadinovirus microRNAs expressed in virus-induced tumors from infected rhesus macaques. Virology. 2010 Sep;405(2):592–9.

122. Estep RD, Powers MF, Yen BK, Li H, Wong SW. Construction of an infectious rhesus rhadinovirus bacterial artificial chromosome for the analysis of Kaposi's sarcoma-associated herpesvirus-related disease development. Journal of Virology. 2007 Mar;81(6):2957–69.

123. Simas JP, Efstathiou S. Murine gammaherpesvirus 68: a model for the study of gammaherpesvirus pathogenesis. Trends in Microbiology. 1998 Jul;6(7):276–82.

124. Moore PS, Chang Y. Kaposi's sarcoma-associated herpesvirus immunoevasion and tumorigenesis: two sides of the same coin? Annu Rev Microbiol. USA; 2003;57(1):609–39.

125. Wakeling MN, Roy DJ, Nash AA, Stewart JP. Characterization of the murine gammaherpesvirus 68 ORF74 product: a novel oncogenic G protein-coupled receptor. Journal of General Virology. 2001 May;82(Pt 5):1187–97.

126. Martinez-Guzman D, Rickabaugh T, Wu T-T, Brown H, Cole S, Song MJ, et al. Transcription program of murine gammaherpesvirus 68. Journal of Virology. 2003 Oct;77(19):10488–503.

127. Hughes DJ, Kipar A, Sample JT, Stewart JP. Pathogenesis of a model

gammaherpesvirus in a natural host. Journal of Virology. 2010 Apr;84(8):3949–61.

128. Barton E, Mandal P, Speck SH. Pathogenesis and host control of gammaherpesviruses: lessons from the mouse. Annu Rev Immunol. 2011;29(1):351–97.

129. Ambros V. The functions of animal microRNAs. Nature. 2004 Sep 16;431(7006):350–5.

130. Bartel DP. MicroRNAs: genomics, biogenesis, mechanism, and function. Cell. 2004 Jan 23;116(2):281–97.

131. Plaisance-Bonstaff K, Renne R. Viral miRNAs. Methods Mol Biol. Totowa, NJ: Humana Press; 2011;721(Chapter 3):43–66.

132. Grey F, Hook L, Nelson J. The functions of herpesvirus-encoded microRNAs. Med Microbiol Immunol. Springer-Verlag; 2008 Jun;197(2):261–7.

133. Zhu Y, Haecker I, Yang Y, Gao S-J, Renne R. γ-Herpesvirus-encoded miRNAs and their roles in viral biology and pathogenesis. Current Opinion in Virology. 2013 Jun 1;3(3):266–75.

134. Kincaid RP, Sullivan CS. Virus-encoded microRNAs: an overview and a look to the future. Hobman TC, editor. PLoS Pathog. 2012 Dec;8(12):e1003018.

135. Tsuda Y, Parkins CJ, Caposio P, Feldmann F, Botto S, Ball S, et al. A cytomegalovirus-based vaccine provides long-lasting protection against lethal Ebola virus challenge after a single dose. Vaccine. 2015 May 5;33(19):2261–6.

136. Cullen BR. Viruses and microRNAs. Nat Genet. 2006 Jun;38 Suppl(6s):S25–30.

137. Lee Y, Ahn C, Han J, Choi H, Kim J, Yim J, et al. The nuclear RNase III Drosha initiates microRNA processing. Nature. 2003 Sep 25;425(6956):415–9.

138. Bartel DP. MicroRNAs: target recognition and regulatory functions. Cell. Elsevier; 2009 Jan 23;136(2):215–33.

139. Faller M, Guo F. MicroRNA biogenesis: there's more than one way to skin a cat. Biochim Biophys Acta. 2008 Nov;1779(11):663–7.

140. Ziegelbauer JM. Functions of Kaposi's sarcoma-associated herpesvirus microRNAs. BBA - Gene Regulatory Mechanisms. Elsevier B.V; 2011 Nov 12;1809(11-12):623–30.

141. Qin Z, Peruzzi F, Reiss K, Dai L. Role of Host MicroRNAs in Kaposi's Sarcoma-Associated Herpesvirus Pathogenesis. Viruses. 2014

Nov;6(11):4571–80.

142. Samols MA, Hu J, Skalsky RL, Renne R. Cloning and Identification of a MicroRNA Cluster within the Latency-Associated Region of Kaposi's Sarcoma-Associated Herpesvirus. Journal of Virology. 2005 Jun 30;79(14):9301–5.

143. Gottwein E. Kaposi's sarcoma-associated herpesvirus microRNAs. Front Microbiol. 2012 Apr 30;3:165–178.

144. Haecker I, Gay L, Morse A, McCrory M, Yang Y, Hu J, et al. Comprehensive analysis of the KSHV MiRNA targetome bBioMed Central Ltd; 2012 Apr 19;7(Suppl 1):O4.

145. Liang D, Lin X, Lan K. Looking at Kaposi's Sarcoma-Associated Herpesvirus-Host Interactions from a microRNA Viewpoint. Front Microbiol. 2011;2:271.

146. Chugh PE, Sin S-H, Ozgur S, Henry DH, Menezes P, Griffith J, et al. Systemically Circulating Viral and Tumor-Derived MicroRNAs in KSHV-Associated Malignancies. Gao S-J, editor. PLoS Pathog. 2013 Jul 18;9(7):e1003484–22.

147. Skalsky RL, Samols MA, Plaisance KB, Boss IW, Riva A, Lopez MC, et al. Kaposi's Sarcoma-Associated Herpesvirus Encodes an Ortholog of miR-155. Journal of Virology. 2007 Nov 9;81(23):12836–45.

148. Gottwein E, Mukherjee N, Sachse C, Frenzel C, Majoros WH, Chi J-TA, et al. A viral microRNA functions as an orthologue of cellular miR-155. Nature. 2007 Dec 13;450(7172):1096–9.

149. McClure LV, Sullivan CS. Kaposi's sarcoma herpes virus taps into a host microRNA regulatory network. Cell Host and Microbe. 2008 Jan 17;3(1):1–3.

150. Zhao Y, Xu H, Yao Y, Smith LP, Kgosana L, Green J, et al. Critical role of the virus-encoded microRNA-155 ortholog in the induction of Marek's disease lymphomas. Cullen BR, editor. PLoS Pathog. 2011 Feb;7(2):e1001305.

151. Motsch N, Pfuhl T, Mrazek J, Barth S, Grässer FA. Epstein-Barr virus-encoded latent membrane protein 1 (LMP1) induces the expression of the cellular microRNA miR-146a. RNA Biol. 2007 Nov;4(3):131–7.

152. Gatto G, Rossi A, Rossi D, Kroening S, Bonatti S, Mallardo M. Epstein-Barr virus latent membrane protein 1 trans-activates miR-155 transcription through the NF-kappaB pathway. Nucleic Acids Research. Oxford University Press; 2008 Nov;36(20):6608–19.

153. McAllister SC, Hansen SG, Ruhl RA, Raggo CM, DeFilippis VR, Greenspan D, et al. Kaposi sarcoma-associated herpesvirus (KSHV) induces heme oxygenase-1 expression and activity in KSHV-infected endothelial cells.

Blood. American Society of Hematology; 2004 May 1;103(9):3465–73.

154. Botto S, Totonchy JE, Gustin JK, Moses AV. Kaposi Sarcoma Herpesvirus Induces HO-1 during De Novo Infection of Endothelial Cells via Viral miRNA-Dependent and -Independent Mechanisms. mBio. 2015;6(3):e00668.

155. Boss IW, Nadeau PE, Abbott JR, Yang Y, Mergia A, Renne R. A Kaposi's Sarcoma-Associated Herpesvirus-Encoded Ortholog of MicroRNA miR-155 Induces Human Splenic B-Cell Expansion in NOD/LtSz-scid IL2R null Mice. Journal of Virology. 2011 Sep 9;85(19):9877–86.

156. Liang D, Gao Y, Lin X, He Z, Zhao Q, Deng Q, et al. A human herpesvirus miRNA attenuates interferon signaling and contributes to maintenance of viral latency by targeting IKKε. Cell Res. Nature Publishing Group; 2011 May;21(5):793–806.

157. Liu Y, Sun R, Lin X, Liang D, Deng Q, Lan K. Kaposi's sarcoma-associated herpesvirus-encoded microRNA miR-K12-11 attenuates transforming growth factor beta signaling through suppression of SMAD5. Journal of Virology. American Society for Microbiology; 2012 Feb;86(3):1372–81.

158. Dempsey PW, Vaidya SA, Cheng G. The art of war: Innate and adaptive immune responses. Cell Mol Life Sci. Birkhäuser-Verlag; 2003 Dec;60(12):2604–21.

159. Litman GW, Rast JP, Fugmann SD. The origins of vertebrate adaptive immunity. Nat Rev Immunol. Nature Publishing Group; 2010 Aug;10(8):543–53.

160. Litman GW, Cannon JP, Dishaw LJ. Reconstructing immune phylogeny: new perspectives. Nat Rev Immunol. Nature Publishing Group; 2005 Nov;5(11):866–79.

161. Yan N, Chen ZJ. Intrinsic antiviral immunity. Nat Immunol. Nature Publishing Group; 2012 Mar;13(3):214–22.

162. Guasparri I, Keller SA, Cesarman E. KSHV vFLIP is essential for the survival of infected lymphoma cells. Journal of Experimental Medicine. Rockefeller Univ Press; 2004 Apr 5;199(7):993–1003.

163. Bellows DS, Chau BN, Lee P, Lazebnik Y, Burns WH, Hardwick JM. Antiapoptotic herpesvirus Bcl-2 homologs escape caspase-mediated conversion to proapoptotic proteins. Journal of Virology. American Society for Microbiology (ASM); 2000 Jun;74(11):5024–31.

164. Zhang X, Dawson CW, He Z, Huang P. Immune evasion strategies of the human gamma-herpesviruses: Implications for viral tumorigenesis. J Med Virol. 2011 Dec 14;84(2):272–81.

165. O'Neill LAJ, Golenbock D, Bowie AG. The history of Toll-like receptors - redefining innate immunity. Nat Rev Immunol. Nature Publishing Group;

2013 Jun;13(6):453–60.

166. Kawai T, Akira S. The role of pattern-recognition receptors in innate immunity: update on Toll-like receptors. Nat Immunol. 2010 May;11(5):373–84.

167. Takeda K, Akira S. Toll-like receptors. Curr Protoc Immunol. Hoboken, NJ, USA: John Wiley & Sons, Inc; 2015;109:14.12.1–14.12.10.

168. Paludan SR, Bowie AG, Horan KA, Fitzgerald KA. Recognition of herpesviruses by the innate immune system. Nat Rev Immunol. 2011 Feb;11(2):143–54.

169. Unterholzner L. The interferon response to intracellular DNA: why so many receptors? Immunobiology. 2013 Nov;218(11):1312–21.

170. Li T, Diner BA, Chen J, Cristea IM. Acetylation modulates cellular distribution and DNA sensing ability of interferon-inducible protein IFI16. Proc Natl Acad Sci USA. National Acad Sciences; 2012 Jun 26;109(26):10558–63.

171. Unterholzner L, Keating SE, Baran M, Horan KA, Jensen SB, Sharma S, et al. IFI16 is an innate immune sensor for intracellular DNA. Nat Immunol. 2010 Nov;11(11):997–1004.

172. Kerur N, Veettil MV, Sharma-Walia N, Bottero V, Sadagopan S, Otageri P, et al. IFI16 acts as a nuclear pathogen sensor to induce the inflammasome in response to Kaposi Sarcoma-associated herpesvirus infection. Cell Host and Microbe. Elsevier; 2011 May 19;9(5):363–75.

173. Unterholzner L, Bowie AG. Innate DNA sensing moves to the nucleus. Cell Host and Microbe. Elsevier; 2011 May 19;9(5):351–3.

174. Brulois K, Jung JU. Interplay between Kaposi's sarcoma-associated herpesvirus and the innate immune system. Cytokine and Growth Factor Reviews. Elsevier Ltd; 2014 Jul 15;:1–13.

175. Lagos D, Vart RJ, Gratrix F, Westrop SJ, Emuss V, Wong P-P, et al. Toll-like receptor 4 mediates innate immunity to Kaposi sarcoma herpesvirus. Cell Host and Microbe. Elsevier; 2008 Nov 13;4(5):470–83.

176. Gack MU, Shin YC, Joo C-H, Urano T, Liang C, Sun L, et al. TRIM25 RING-finger E3 ubiquitin ligase is essential for RIG-I-mediated antiviral activity. Nature. 2007 Apr 19;446(7138):916–20.

177. West JA, Wicks M, Gregory SM, Chugh P, Jacobs SR, Zhang Z, et al. An important role for mitochondrial antiviral signaling protein in the Kaposi's sarcoma-associated herpesvirus life cycle. Journal of Virology. American Society for Microbiology; 2014 May;88(10):5778–87.

178. Inn K-S, Lee SH, Rathbun JY, Wong L-Y, Toth Z, Machida K, et al. Inhibition of RIG-I-mediated signaling by Kaposi's sarcoma-associated herpesvirus-

encoded deubiquitinase ORF64. Journal of Virology. American Society for Microbiology; 2011 Oct;85(20):10899–904.

179. Kurt-Jones EA, Popova L, Kwinn L, Haynes LM, Jones LP, Tripp RA, et al. Pattern recognition receptors TLR4 and CD14 mediate response to respiratory syncytial virus. Nat Immunol. 2000 Nov;1(5):398–401.

180. Tal G, Mandelberg A, Dalal I, Cesar K, Somekh E, Tal A, et al. Association between common Toll-like receptor 4 mutations and severe respiratory syncytial virus disease. Journal of Infectious Diseases. Oxford University Press; 2004 Jun 1;189(11):2057–63.

181. Perry ST, Compton T. Kaposi's sarcoma-associated herpesvirus virions inhibit interferon responses induced by envelope glycoprotein gpK8.1. Journal of Virology. American Society for Microbiology; 2006 Nov;80(22):11105–14.

182. Zhu FX, Sathish N, Yuan Y. Antagonism of host antiviral responses by Kaposi's sarcoma-associated herpesvirus tegument protein ORF45. Lindenbach B, editor. PLoS ONE. Public Library of Science; 2010;5(5):e10573.

183. Gregory SM, Damania B. Inhibition of the inflammasome response by a viral protein that interacts with NLRs. Commun Integr Biol. 2011 Jul;4(4):416–8.

184. Franchi L, Muñoz-Planillo R, Núñez G. Sensing and reacting to microbes through the inflammasomes. Nat Immunol. Nature Publishing Group; 2012 Apr;13(4):325–32.

185. Franchi L, Kamada N, Nakamura Y, Burberry A, Kuffa P, Suzuki S, et al. NLRC4-driven production of IL-1β discriminates between pathogenic and commensal bacteria and promotes host intestinal defense. Nat Immunol. 2012 Apr 8;13(5):449–56.

186. Lee H-R, Toth Z, Shin YC, Lee J-S, Chang H, Gu W, et al. Kaposi's sarcoma-associated herpesvirus viral interferon regulatory factor 4 targets MDM2 to deregulate the p53 tumor suppressor pathway. Journal of Virology. American Society for Microbiology; 2009 Jul;83(13):6739–47.

187. Lefort S, Soucy-Faulkner A, Grandvaux N, Flamand L. Binding of Kaposi's Sarcoma-Associated Herpesvirus K-bZIP to Interferon-Responsive Factor 3 Elements Modulates Antiviral Gene Expression. Journal of Virology. 2007 Sep 26;81(20):10950–60.

188. Zhu FX, Yuan Y. The ORF45 protein of Kaposi's sarcoma-associated herpesvirus is associated with purified virions. Journal of Virology. American Society for Microbiology (ASM); 2003 Apr;77(7):4221–30.

189. Zhu FX, King SM, Smith EJ, Levy DE, Yuan Y. A Kaposi's sarcoma-associated herpesviral protein inhibits virus-mediated induction of type I interferon by blocking IRF-7 phosphorylation and nuclear accumulation.

Proceedings of the National Academy of Sciences. National Acad Sciences; 2002 Apr 16;99(8):5573–8.

190. Zhu FX, Li X, Zhou F, Gao S-J, Yuan Y. Functional characterization of Kaposi's sarcoma-associated herpesvirus ORF45 by bacterial artificial chromosome-based mutagenesis. Journal of Virology. American Society for Microbiology; 2006 Dec;80(24):12187–96.

191. Schwarz KB. Oxidative stress during viral infection: a review. Free Radical Biology and Medicine. 1996;21(5):641–9.

192. McGuire KA, Barlan AU, Griffin TM, Wiethoff CM. Adenovirus type 5 rupture of lysosomes leads to cathepsin B-dependent mitochondrial stress and production of reactive oxygen species. Journal of Virology. American Society for Microbiology; 2011 Oct;85(20):10806–13.

193. Tung W-H, Hsieh H-L, Lee I-T, Yang C-M. Enterovirus 71 induces integrin β1/EGFR-Rac1-dependent oxidative stress in SK-N-SH cells: role of HO-1/CO in viral replication. J Cell Physiol. Wiley Subscription Services, Inc., A Wiley Company; 2011 Dec;226(12):3316–29.

194. Kavouras JH, Prandovszky E, Valyi-Nagy K, Kovacs SK, Tiwari V, Kovacs M, et al. Herpes simplex virus type 1 infection induces oxidative stress and the release of bioactive lipid peroxidation by-products in mouse P19N neural cell cultures. J Neurovirol. Springer-Verlag; 2007 Oct;13(5):416–25.

195. Hu S, Sheng WS, Schachtele SJ, Lokensgard JR. Reactive oxygen species drive herpes simplex virus (HSV)-1-induced proinflammatory cytokine production by murine microglia. Journal of Neuroinflammation. BioMed Central Ltd; 2011;8(1):123.

196. Gonzalez-Dosal R, Horan KA, Rahbek SH, Ichijo H, Chen ZJ, Mieyal JJ, et al. HSV infection induces production of ROS, which potentiate signaling from pattern recognition receptors: role for S-glutathionylation of TRAF3 and 6. Britt WJ, editor. PLoS Pathog. Public Library of Science; 2011 Sep;7(9):e1002250.

197. Lassoued S, Ben Ameur R, Ayadi W, Gargouri B, Ben Mansour R, Attia H. Epstein-Barr virus induces an oxidative stress during the early stages of infection in B lymphocytes, epithelial, and lymphoblastoid cell lines. Molecular and Cellular Biochemistry. Springer US; 2008 Jun;313(1-2):179–86.

198. Bottero V, Chakraborty S, Chandran B. Reactive oxygen species are induced by Kaposi's sarcoma-associated herpesvirus early during primary infection of endothelial cells to promote virus entry. Journal of Virology. 2013 Feb;87(3):1733–49.

199. Tenhunen R, Marver HS, Schmid R. Microsomal heme oxygenase. Characterization of the enzyme. Journal of Biological Chemistry. 1969 Dec 10;244(23):6388–94.

200. Trakshel GM, Ewing JF, Maines MD. Heterogeneity of haem oxygenase 1 and 2 isoenzymes. Rat and primate transcripts for isoenzyme 2 differ in number and size. Biochem J. Portland Press Ltd; 1991 Apr 1;275 (Pt 1)(Pt 1):159–64.

201. Ryter SW, Choi AMK. Heme oxygenase-1/carbon monoxide: from metabolism to molecular therapy. Am J Respir Cell Mol Biol. American Thoracic Society; 2009 Sep;41(3):251–60.

202. Ryter SW, Alam J, Choi AMK. Heme Oxygenase-1/Carbon Monoxide: From Basic Science to Therapeutic Applications. Physiol Rev. 2006 Mar 20;:1–68.

203. Kanezaki R, Toki T, Yokoyama M, Yomogida K, Sugiyama K, Yamamoto M, et al. Transcription Factor BACH1 Is Recruited to the Nucleus by Its Novel Alternative Spliced Isoform. Journal of Biological Chemistry. 2001 Mar 9;276(10):7278–84.

204. Zhang J, Ohta T, Maruyama A, Hosoya T, Nishikawa K, Maher JM, et al. BRG1 Interacts with Nrf2 To Selectively Mediate HO-1 Induction in Response to Oxidative Stress. Molecular and Cellular Biology. 2006 Oct 17;26(21):7942–52.

205. Dhakshinamoorthy S, Jain AK, Bloom DA, Jaiswal AK. Bach1 Competes with Nrf2 Leading to Negative Regulation of the Antioxidant Response Element (ARE)-mediated NAD(P)H:Quinone Oxidoreductase 1 Gene Expression and Induction in Response to Antioxidants. Journal of Biological Chemistry. 2005 Apr 22;280(17):16891–900.

206. Subjeck JR, Shyy TT. Stress protein systems of mammalian cells. Am J Physiol. 1986 Jan;250(1 Pt 1):C1–17.

207. Shibahara S, Müller RM, Taguchi H. Transcriptional control of rat heme oxygenase by heat shock. Journal of Biological Chemistry. 1987 Sep 25;262(27):12889–92.

208. Yoshida T, Biro P, Cohen T, Müller RM, Shibahara S. Human heme oxygenase cDNA and induction of its mRNA by hemin. Eur J Biochem. 1988 Feb 1;171(3):457–61.

209. Ryter SW, Choi AMK. Targeting heme oxygenase-1 and carbon monoxide for therapeutic modulation of inflammation. Translational Research. Elsevier Inc; 2015 Jul 16;:1–28.

210. Ryter SW, Tyrrell RM. The heme synthesis and degradation pathways: role in oxidant sensitivity. Heme oxygenase has both pro- and antioxidant properties. Free Radical Biology and Medicine. 2000 Jan 15;28(2):289–309.

211. Lanceta L, Mattingly JM, Li C, Eaton JW. How Heme Oxygenase-1 Prevents Heme-Induced Cell Death. Tsuji Y, editor. PLoS ONE. 2015 Aug 13;10(8):e0134144–15.

212. Stevens B, Small RD. The photoperoxidation of unsaturated organic molecules--XV. O21Delta g quenching by bilirubin and biliverdin. Photochem Photobiol. 1976 Jan;23(1):33–6.

213. Robertson P, Fridovich I. A reaction of the superoxide radical with tetrapyrroles. Arch Biochem Biophys. 1982 Feb;213(2):353–7.

214. Liu X-M, Chapman GB, Peyton KJ, Schafer AI, Durante W. Carbon monoxide inhibits apoptosis in vascular smooth muscle cells. Cardiovascular Research. 2002 Aug 1;55(2):396–405.

215. Fang J, Akaike T, Maeda H. Antiapoptotic role of heme oxygenase (HO) and the potential of HO as a target in anticancer treatment. Apoptosis. Kluwer Academic Publishers; 2004 Jan;9(1):27–35.

216. Peterson SJ, Frishman WH. Targeting Heme Oxygenase. Cardiology in Review. 2009 May;17(3):99–111.

217. Richardson DR, Ponka P. The molecular mechanisms of the metabolism and transport of iron in normal and neoplastic cells. Biochim Biophys Acta. 1997 Mar 14;1331(1):1–40.

218. Vile GF, Basu-Modak S, Waltner C, Tyrrell RM. Heme oxygenase 1 mediates an adaptive response to oxidative stress in human skin fibroblasts. Proceedings of the National Academy of Sciences. National Academy of Sciences; 1994 Mar 29;91(7):2607–10.

219. Vlahakis JZ, Kinobe RT, Bowers RJ, Brien JF, Nakatsu K, Szarek WA. Imidazole-dioxolane compounds as isozyme-selective heme oxygenase inhibitors. J Med Chem. American Chemical Society; 2006 Jul 13;49(14):4437–41.

220. Morisawa T, Wong RJ, Bhutani VK, Vreman HJ, Stevenson DK. Inhibition of heme oxygenase activity in newborn mice by azalanstat. Can J Physiol Pharmacol. 2008 Oct;86(10):651–9.

221. Alaoui-Jamali MA, Bismar TA, Gupta A, Szarek WA, Su J, Song W, et al. A novel experimental heme oxygenase-1-targeted therapy for hormone-refractory prostate cancer. Cancer Research. American Association for Cancer Research; 2009 Oct 15;69(20):8017–24.

222. Kinobe RT, Dercho RA, Nakatsu K. Inhibitors of the heme oxygenase - carbon monoxide system: on the doorstep of the clinic? Can J Physiol Pharmacol. 2008 Sep;86(9):577–99.

223. Yadav B. Selective inhibition of hemeoxygenase-1 as a novel therapeutic target for anticancer treatment. J Nanomedic Nanotechnol. 2011;s4(01):1–8.

224. Choi AM, Knobil K, Otterbein SL, Eastman DA, Jacoby DB. Oxidant stress responses in influenza virus pneumonia: gene expression and transcription factor activation. Am J Physiol. 1996 Sep;271(3 Pt 1):L383–91.

225. Renton KW. Depression of hepatic cytochrome P-450-dependent mixed function oxidases during infection with encephalomyocarditis virus. Biochem Pharmacol. 1981 Aug 15;30(16):2333–6.

226. Azri S, Renton KW. Factors involved in the depression of hepatic mixed function oxidase during infections with Listeria monocytogenes. Int J Immunopharmacol. 1991;13(2-3):197–204.

227. Rydkina E, Sahni A, Silverman DJ, Sahni SK. Rickettsia rickettsii infection of cultured human endothelial cells induces heme oxygenase 1 expression. Infect Immun. American Society for Microbiology (ASM); 2002 Aug;70(8):4045–52.

228. Schmidt WN. Heme and HO-1 inhibition of HCV, HBV, and HIV. 2012 Oct 1;:1–13.

229. Hill-Batorski L, Halfmann P, Neumann G, Kawaoka Y. The cytoprotective enzyme heme oxygenase-1 suppresses Ebola virus replication. Journal of Virology. American Society for Microbiology; 2013 Dec;87(24):13795–802.

230. Fukunaga M, Silverberg SG. Hyaline globules in Kaposi's sarcoma: a light microscopic and immunohistochemical study. Mod Pathol. 1991 Mar;4(2):187–90.

231. Schenk P. Erythrophagocytosis in Kaposi's sarcoma in acquired immune deficiency syndrome. ORL J Otorhinolaryngol Relat Spec. 1986;48(3):167–73.

232. Schenk P, Konrad K. Ultrastructure of Kaposi's sarcoma in acquired immune deficiency syndrome (AIDS). Arch Otorhinolaryngol. 1985;242(3):305–13.

233. Kao GF, Johnson FB, Sulica VI. The nature of hyaline (eosinophilic) globules and vascular slits of Kaposi's sarcoma. Am J Dermatopathol. 1990 Jun;12(3):256–67.

234. Raggo C, Ruhl R, McAllister S, Koon H, Dezube BJ, Früh K, et al. Novel cellular genes essential for transformation of endothelial cells by Kaposi's sarcoma-associated herpesvirus. Cancer Research. American Association for Cancer Research; 2005 Jun 15;65(12):5084–95.

235. Abraham NG, Kappas A. Pharmacological and clinical aspects of heme oxygenase. Pharmacol Rev. American Society for Pharmacology and Experimental Therapeutics; 2008 Mar;60(1):79–127.

236. Banerjee P, Basu A, Wegiel B, Otterbein LE, Mizumura K, Gasser M, et al. Heme oxygenase-1 promotes survival of renal cancer cells through modulation of apoptosis- and autophagy-regulating molecules. J Biol Chem. American Society for Biochemistry and Molecular Biology; 2012 Sep 14;287(38):32113–23.

237. Gozzelino R, Jeney V, Soares MP. Mechanisms of Cell Protection by Heme

Oxygenase-1. Annu Rev Pharmacol Toxicol. 2010 Feb;50(1):323–54.

238. Miyazaki T, Kirino Y, Takeno M, Samukawa S, Hama M, Tanaka M, et al. Expression of heme oxygenase-1 in human leukemic cells and its regulation by transcriptional repressor Bach1. Cancer Science. 2010 Mar 2;101(6):1409–16.

239. Do MT, Kim HG, Khanal T, Choi JH, Kim DH, Jeong TC, et al. Metformin inhibits heme oxygenase-1 expression in cancer cells through inactivation of Raf-ERK-Nrf2 signaling and AMPK-independent pathways. Toxicology and Applied Pharmacology. Elsevier B.V; 2013 May 26;:1–10.

240. Lin P-H, Lan W-M, CHAU LY. TRC8 suppresses tumorigenesis through targeting heme oxygenase-1 for ubiquitination and degradation. Nature Publishing Group; 2012 Jun 11;:1–10.

241. Ferrándiz ML, Devesa I. Inducers of heme oxygenase-1. Curr Pharm Des. 2008;14(5):473–86.

242. Paine A, Eiz-Vesper B, Blasczyk R, Immenschuh S. Signaling to heme oxygenase-1 and its anti-inflammatory therapeutic potential. Biochem Pharmacol. 2010 Dec 15;80(12):1895–903.

243. Sun J, Hoshino H, Takaku K, Nakajima O, Muto A, Suzuki H, et al. Hemoprotein Bach1 regulates enhancer availability of heme oxygenase-1 gene. The EMBO Journal. European Molecular Biology Organization; 2002 Oct 1;21(19):5216–24.

244. Malhotra D, Portales-Casamar E, Singh A, Srivastava S, Arenillas D, Happel C, et al. Global mapping of binding sites for Nrf2 identifies novel targets in cell survival response through ChIP-Seq profiling and network analysis. Nucleic Acids Research. Oxford University Press; 2010 Sep;38(17):5718–34.

245. Shan Y, Lambrecht RW, Donohue SE, Bonkovsky HL. Role of Bach1 and Nrf2 in up-regulation of the heme oxygenase-1 gene by cobalt protoporphyrin. FASEB J. Federation of American Societies for Experimental Biology; 2006 Dec;20(14):2651–3.

246. Warnatz H-J, Schmidt D, Manke T, Piccini I, Sultan M, Borodina T, et al. The BTB and CNC homology 1 (BACH1) target genes are involved in the oxidative stress response and in control of the cell cycle. J Biol Chem. American Society for Biochemistry and Molecular Biology; 2011 Jul 1;286(26):23521–32.

247. Elton TS, Selemon H, Elton SM, Parinandi NL. Regulation of the MIR155 host gene in physiological and pathological processes. Gene. Elsevier B.V; 2013 Dec 10;532(1):1–12.

248. Qin Z, Freitas E, Sullivan R, Mohan S, Bacelieri R, Branch D, et al. Upregulation of xCT by KSHV-encoded microRNAs facilitates KSHV

dissemination and persistence in an environment of oxidative stress. Mesri EA, editor. PLoS Pathog. Public Library of Science; 2010 Jan;6(1):e1000742.

249. Brulois KF, Chang H, Lee AS-Y, Ensser A, Wong L-Y, Toth Z, et al. Construction and manipulation of a new Kaposi's sarcoma-associated herpesvirus bacterial artificial chromosome clone. Journal of Virology. American Society for Microbiology; 2012 Sep;86(18):9708–20.

250. Chang HH, Ganem D. A Unique Herpesviral Transcriptional Program in KSHV-Infected Lymphatic Endothelial Cells Leads to mTORC1 Activation and Rapamycin Sensitivity. Cell Host and Microbe. Elsevier Inc; 2013 Apr 17;13(4):429–40.

251. Gallaher AM, Das S, Xiao Z, Andresson T, Kieffer-Kwon P, Happel C, et al. Proteomic Screening of Human Targets of Viral microRNAs Reveals Functions Associated with Immune Evasion and Angiogenesis. Dittmer DP, editor. PLoS Pathog. 2013 Sep 5;9(9):e1003584–14.

252. Plaisance-Bonstaff K, Choi H, Beals T, Krueger B, Boss I, Gay L, et al. KSHV miRNAs Decrease Expression of Lytic Genes in Latently Infected PEL and Endothelial Cells by Targeting Host Transcription Factors. Viruses. 2014 Oct;6(10):4005–23.

253. Skalsky RL, Cullen BR. Viruses, microRNAs, and Host Interactions. Annu Rev Microbiol. 2010 Oct 13;64(1):123–41.

254. Hardy S, Kitamura M, Harris-Stansil T, Dai Y, Phipps ML. Construction of adenovirus vectors through Cre-lox recombination. Journal of Virology. American Society for Microbiology (ASM); 1997 Mar;71(3):1842–9.

255. Lin X, Li X, Liang D, Lan K. MicroRNAs and unusual small RNAs discovered in Kaposi's sarcoma-associated herpesvirus virions. Journal of Virology. American Society for Microbiology; 2012 Dec;86(23):12717–30.

256. Lee Y-M, Auh Q-S, Lee D-W, Kim J-Y, Jung H-J, Lee S-H, et al. Involvement of Nrf2-Mediated Upregulation of Heme Oxygenase-1 in Mollugin-Induced Growth Inhibition and Apoptosis in Human Oral Cancer Cells. BioMed Research International. 2013;2013(4):1–14.

257. Gjyshi O, Bottero V, Veettil MV, Dutta S, Singh VV, Chikoti L, et al. Kaposi's sarcoma-associated herpesvirus induces Nrf2 during de novo infection of endothelial cells to create a microenvironment conducive to infection. Swaminathan S, editor. PLoS Pathog. Public Library of Science; 2014 Oct;10(10):e1004460.

258. Coen N, Duraffour S, Topalis D, Snoeck R, Andrei G. Spectrum of activity and mechanisms of resistance of various nucleoside derivatives against gammaherpesviruses. Antimicrobial Agents and Chemotherapy. American Society for Microbiology; 2014 Dec;58(12):7312–23.

259. Dittmer DP, Krown SE. Targeted therapy for Kaposi“s sarcoma and Kaposi”s sarcoma-associated herpesvirus. Curr Opin Oncol. 2007 Sep;19(5):452–7.

260. Dittmer DP, Damania B. Kaposi sarcoma associated herpesvirus pathogenesis (KSHV)--an update. Current Opinion in Virology. 2013 Jun;3(3):238–44.

261. Wang L, Damania B. Kaposi's sarcoma-associated herpesvirus confers a survival advantage to endothelial cells. Cancer Research. American Association for Cancer Research; 2008 Jun 15;68(12):4640–8.

262. Myoung J, Ganem D. Generation of a doxycycline-inducible KSHV producer cell line of endothelial origin: Maintenance of tight latency with efficient reactivation upon induction. Journal of Virological Methods. 2011 Jun;174(1-2):12–21.

263. Vieira J, O'Hearn PM. Use of the red fluorescent protein as a marker of Kaposi's sarcoma-associated herpesvirus lytic gene expression. Virology. 2004 Aug 1;325(2):225–40.

264. Jeffery HC, Wheat RL, Blackbourn DJ, Nash GB, Butler LM. Infection and transmission dynamics of rKSHV.219 in primary endothelial cells. Journal of Virological Methods. 2013 Oct;193(1):251–9.

265. Ellison TJ, Kedes DH. Variable episomal silencing of a recombinant herpesvirus renders its encoded GFP an unreliable marker of infection in primary cells. Gao S-J, editor. PLoS ONE. Public Library of Science; 2014;9(11):e111502.

266. Altschuler Y, Barbas SM, Terlecky LJ, Tang K, Hardy S, Mostov KE, et al. Redundant and distinct functions for dynamin-1 and dynamin-2 isoforms. J Cell Biol. The Rockefeller University Press; 1998 Dec 28;143(7):1871–81.

267. Kramer MF. Stem-Loop RT-qPCR for miRNAs. Hoboken, NJ, USA: John Wiley & Sons, Inc; 2001.

268. Feng P, Moses A, Früh K. Evasion of adaptive and innate immune response mechanisms by γ-herpesviruses. Current Opinion in Virology. 2013 Jun;3(3):285–95.

269. Boehme KW, Compton T. Innate Sensing of Viruses by Toll-Like Receptors. Journal of Virology. 2004 Jul 14;78(15):7867–73.

270. West JA, Gregory SM, Sivaraman V, Su L, Damania B. Activation of plasmacytoid dendritic cells by Kaposi's sarcoma-associated herpesvirus. Journal of Virology. 2011 Jan;85(2):895–904.

271. West J, Damania B. Upregulation of the TLR3 pathway by Kaposi's sarcoma-associated herpesvirus during primary infection. Journal of Virology. 2008 Jun;82(11):5440–9.

272. Ahmad H, Gubbels R, Ehlers E, Meyer F, Waterbury T, Lin R, et al. Kaposi Sarcoma-associated Herpesvirus Degrades Cellular Toll-Interleukin-1 Receptor Domain-containing Adaptor-inducing -Interferon (TRIF). Journal of Biological Chemistry. 2011 Mar 4;286(10):7865–72.

273. Bellare P, Ganem D. Regulation of KSHV lytic switch protein expression by a virus-encoded microRNA: an evolutionary adaptation that fine-tunes lytic reactivation. Cell Host and Microbe. 2009 Dec 17;6(6):570–5.

274. Gjyshi O, Flaherty S, Veettil MV, Johnson KE, Chandran B, Bottero V. Kaposi's Sarcoma-Associated Herpesvirus Induces Nrf2 Activation in Latently Infected Endothelial Cells through SQSTM1 Phosphorylation and Interaction with Polyubiquitinated Keap1. Hutt-Fletcher L, editor. Journal of Virology. 2015 Jan 26;89(4):2268–86.

275. Bak I. Heme oxygenase-1 related carbon monoxide production and ventricular fibrillation in isolated ischemic/reperfused mouse myocardium. The FASEB Journal. 2003 Sep 18;:1–3.

276. Xue J, Habtezion A. Carbon monoxide-based therapy ameliorates acute pancreatitis via TLR4 inhibition. J Clin Invest. 2014 Jan;124(1):437–47.

277. Nakahira K, Kim HP, Geng XH, Nakao A, Wang X, Murase N, et al. Carbon monoxide differentially inhibits TLR signaling pathways by regulating ROS-induced trafficking of TLRs to lipid rafts. Journal of Experimental Medicine. 2006 Oct 2;203(10):2377–89.

278. Riquelme SA, Bueno SM, Kalergis AM. Carbon monoxide down-modulates Toll-like receptor 4/MD2 expression on innate immune cells and reduces endotoxic shock susceptibility. Immunology. 2015 Feb;144(2):321–32.

279. Wang XM, Kim HP, Nakahira K, Ryter SW, Choi AMK. The heme oxygenase-1/carbon monoxide pathway suppresses TLR4 signaling by regulating the interaction of TLR4 with caveolin-1. J Immunol. 2009 Mar 15;182(6):3809–18.

280. Song Y, Shi Y, Ao L-H, Harken AH, Meng X-Z. TLR4 mediates LPS-induced HO-1 expression in mouse liver: role of TNF-alpha and IL-1beta. World J Gastroenterol. 2003 Aug;9(8):1799–803.

281. Yang Y-C, Huang Y-T, Hsieh C-W, Yang P-M, Wung B-S. Carbon monoxide induces heme oxygenase-1 to modulate STAT3 activation in endothelial cells via S-glutathionylation. Ushio-Fukai M, editor. PLoS ONE. 2014;9(7):e100677.

282. Abate A, Zhao H, Wong RJ, Stevenson DK. The role of Bach1 in the induction of heme oxygenase by tin mesoporphyrin. Biochemical And Biophysical Research Communications. 2007 Mar 16;354(3):757–63.

283. Schoggins JW, Rice CM. Interferon-stimulated genes and their antiviral effector functions. Current Opinion in Virology. 2011 Dec;1(6):519–25.

284. Schneider WM, Chevillotte MD, Rice CM. Interferon-stimulated genes: a complex web of host defenses. Annu Rev Immunol. 2014;32(1):513–45.

285. Hong Y-K, Foreman K, Shin JW, Hirakawa S, Curry CL, Sage DR, et al. Lymphatic reprogramming of blood vascular endothelium by Kaposi sarcoma-associated herpesvirus. Nat Genet. 2004 Jul;36(7):683–5.

286. Marinissen MJ, Tanos T, Bolós M, de Sagarra MR, Coso OA, Cuadrado A. Inhibition of heme oxygenase-1 interferes with the transforming activity of the Kaposi sarcoma herpesvirus-encoded G protein-coupled receptor. Journal of Biological Chemistry. 2006 Apr 21;281(16):11332–46.

287. Martin MJ, Tanos T, Garcia AB, Martin D, Gutkind JS, Coso OA, et al. The G 12/13 Family of Heterotrimeric G Proteins and the Small GTPase RhoA Link the Kaposi Sarcoma-associated Herpes Virus G Protein-coupled Receptor to Heme Oxygenase-1 Expression and Tumorigenesis. Journal of Biological Chemistry. 2007 Oct 1;282(47):34510–24.

288. Lu M, Suen J, Frias C, Pfeiffer R, Tsai MH, Chuang E, et al. Dissection of the Kaposi's Sarcoma-Associated Herpesvirus Gene Expression Program by Using the Viral DNA Replication Inhibitor Cidofovir. Journal of Virology. 2004 Nov 24;78(24):13637–52.

289. Lei X, Zhu Y, Jones T, Bai Z, Huang Y, Gao SJ. A Kaposi's Sarcoma-Associated Herpesvirus MicroRNA and Its Variants Target the Transforming Growth Factor Pathway To Promote Cell Survival. Journal of Virology. 2012 Oct 6;86(21):11698–711.

290. Ramalingam D, Happel C, Ziegelbauer JM. Kaposi's sarcoma-associated herpesvirus microRNAs repress breakpoint cluster region protein expression, enhance Rac1 activity, and increase in vitro angiogenesis. Journal of Virology. 2015 Apr;89(8):4249–61.

291. Samols MA, Skalsky RL, Maldonado AM, Riva A, Lopez MC, Baker HV, et al. Identification of Cellular Genes Targeted by KSHV-Encoded MicroRNAs. PLoS Pathog. 2007;3(5):e65–8.

292. Lo M, Wang Y-Z, Gout PW. The x(c)- cystine/glutamate antiporter: a potential target for therapy of cancer and other diseases. J Cell Physiol. 2008 Jun;215(3):593–602.

293. Dai L, Cao Y, Chen Y, Parsons C, Qin Z. Targeting xCT, a cystine-glutamate transporter induces apoptosis and tumor regression for KSHV/HIV-associated lymphoma. Journal of Hematology & Oncology. 2014 Apr 4;7(1):1–12.

294. Veettil MV, Sadagopan S, Sharma-Walia N, Wang F-Z, Raghu H, Varga L, et al. Kaposi's sarcoma-associated herpesvirus forms a multimolecular complex of integrins (alphaVbeta5, alphaVbeta3, and alpha3beta1) and CD98-xCT during infection of human dermal microvascular endothelial cells, and CD98-xCT is essential for the postentry stage of infection. Journal of

Virology. 2008 Dec;82(24):12126–44.

295. Babu SG, Ponia SS, Kumar D, Saxena S. Cellular oncomiR orthologue in EBV oncogenesis. 2011 Oct;41(10):891–8.

296. Linnstaedt SD, Gottwein E, Skalsky RL, Luftig MA, Cullen BR. Virally induced cellular microRNA miR-155 plays a key role in B-cell immortalization by Epstein-Barr virus. Journal of Virology. 2010 Nov;84(22):11670–8.

297. Carroll PA, Brazeau E, Lagunoff M. Kaposi's sarcoma-associated herpesvirus infection of blood endothelial cells induces lymphatic differentiation. Virology. 2004 Oct 10;328(1):7–18.

298. Wu Y-H, Hu T-F, Chen Y-C, Tsai Y-N, Tsai Y-H, Cheng C-C, et al. The manipulation of miRNA-gene regulatory networks by KSHV induces endothelial cell motility. Blood. American Society of Hematology; 2011 Sep 8;118(10):2896–905.

299. Kim T-H, Hur E-G, Kang S-J, Kim J-A, Thapa D, Lee YM, et al. NRF2 blockade suppresses colon tumor angiogenesis by inhibiting hypoxia-induced activation of HIF-1α. Cancer Research. 2011 Mar 15;71(6):2260–75.

300. Pan H, Wang H, Zhu L, Mao L, Qiao L, Su X. The role of Nrf2 in migration and invasion of human glioma cell U251. World Neurosurg. 2013 Sep;80(3-4):363–70.

301. Mitsuishi Y, Taguchi K, Kawatani Y, Shibata T, Nukiwa T, Aburatani H, et al. Nrf2 redirects glucose and glutamine into anabolic pathways in metabolic reprogramming. Cancer Cell. 2012 Jul 10;22(1):66–79.

302. Hayashi A, Suzuki H, Itoh K, Yamamoto M, Sugiyama Y. Transcription factor Nrf2 is required for the constitutive and inducible expression of multidrug resistance-associated protein 1 in mouse embryo fibroblasts. Biochemical And Biophysical Research Communications. 2003 Oct 24;310(3):824–9.

303. Maher JM, Dieter MZ, Aleksunes LM, Slitt AL, Guo G, Tanaka Y, et al. Oxidative and electrophilic stress induces multidrug resistance-associated protein transporters via the nuclear factor-E2-related factor-2 transcriptional pathway. Hepatology. 2007 Nov;46(5):1597–610.

304. Dai L, Qiao J, Nguyen D, Struckhoff AP, Doyle L, Bonstaff K, et al. Role of heme oxygenase-1 in the pathogenesis and tumorigenicity of Kaposi's sarcoma-associated herpesvirus. Oncotarget. 2016 Feb 7;5(0).

305. Speck SH, Ganem D. Viral Latency and Its Regulation: Lessons from the γ-Herpesviruses. Cell Host and Microbe. 2010 Jul;8(1):100–15.

306. Ye F, Zhou F, Bedolla RG, Jones T, Lei X, Kang T, et al. Reactive oxygen species hydrogen peroxide mediates Kaposi's sarcoma-associated herpesvirus reactivation from latency. Früh K, editor. PLoS Pathog. 2011

May;7(5):e1002054.

307. Li X, Feng J, Sun R. Oxidative stress induces reactivation of Kaposi's sarcoma-associated herpesvirus and death of primary effusion lymphoma cells. Journal of Virology. 2011 Jan;85(2):715–24.

308. Ruan Y, Wang L, Zhao Y, Yao Y, Chen S, Li J, et al. Carbon monoxide potently prevents ischemia-induced high-mobility group box 1 translocation and release and protects against lethal renal ischemia-reperfusion injury. Kidney Int. 2014 Sep;86(3):525–37.

309. Shih R-H, Yang C-M. Induction of heme oxygenase-1 attenuates lipopolysaccharide-induced cyclooxygenase-2 expression in mouse brain endothelial cells. Journal of Neuroinflammation. 2010;7(1):86.

310. Koliaraki V, Kollias G. A New Role for Myeloid HO-1 in the Innate to Adaptive Crosstalk and Immune Homeostasis. In: Crossroads between Innate and Adaptive Immunity III. New York, NY: Springer New York; 2011. pp. 101–11.

311. Rémy S, Blancou P, Tesson L, Tardif V, Brion R, Royer PJ, et al. Carbon monoxide inhibits TLR-induced dendritic cell immunogenicity. J Immunol. 2009 Feb 15;182(4):1877–84.

312. Vivot K, Langlois A, Bietiger W, Dal S, Seyfritz E, Pinget M, et al. Pro-inflammatory and pro-oxidant status of pancreatic islet in vitro is controlled by TLR-4 and HO-1 pathways. Bozza PT, editor. PLoS ONE. 2014;9(10):e107656.

313. Sato M, Suemori H, Hata N, Asagiri M, Ogasawara K, Nakao K, et al. Distinct and essential roles of transcription factors IRF-3 and IRF-7 in response to viruses for IFN-alpha/beta gene induction. Immunity. 2000 Oct;13(4):539–48.

314. Hiscott J. Triggering the innate antiviral response through IRF-3 activation. Journal of Biological Chemistry. American Society for Biochemistry and Molecular Biology; 2007 May 25;282(21):15325–9.

315. Pae H-O, Oh G-S, Choi B-M, Chae S-C, Kim Y-M, Chung K-R, et al. Carbon monoxide produced by heme oxygenase-1 suppresses T cell proliferation via inhibition of IL-2 production. The Journal of Immunology. 2004 Apr 15;172(8):4744–51.

316. Tilton C, Clippinger AJ, Maguire T, Alwine JC. Human Cytomegalovirus Induces Multiple Means To Combat Reactive Oxygen Species. Journal of Virology. 2011 Nov 3;85(23):12585–93.

317. Lee J, Koh K, Kim Y-E, Ahn J-H, Kim S. Upregulation of Nrf2 expression by human cytomegalovirus infection protects host cells from oxidative stress. J Gen Virol. 2013 Jul;94(Pt 7):1658–68.

318. Browne EP, Wing B, Coleman D, Shenk T. Altered cellular mRNA levels in human cytomegalovirus-infected fibroblasts: viral block to the accumulation of antiviral mRNAs. Journal of Virology. 2001 Dec;75(24):12319–30.

319. Sinzger C, Hahn G, Digel M, Katona R, Sampaio KL, Messerle M, et al. Cloning and sequencing of a highly productive, endotheliotropic virus strain derived from human cytomegalovirus TB40/E. Journal of General Virology. 2008 Feb;89(Pt 2):359–68.

320. Hargett D, Shenk TE. Experimental human cytomegalovirus latency in CD14+ monocytes. Proc Natl Acad Sci USA. National Acad Sciences; 2010 Nov 16;107(46):20039–44.

321. Arvin A, Campadelli-Fiume G, Mocarski E, Moore PS, Roizman B, Whitley R, et al. Comparative virion structures of human herpesviruses. Cambridge: Cambridge University Press; 2007.

322. Deng B, O'Connor CM, Kedes DH, Zhou ZH. Cryo-electron tomography of Kaposi's sarcoma-associated herpesvirus capsids reveals dynamic scaffolding structures essential to capsid assembly and maturation. Journal of Structural Biology. 2008 Mar;161(3):419–27.